EFFICIENT AND FAIR SCHEDULING FOR WIRELESS NETWORKS

BY

ATİLLA ERYILMAZ

B.S., Boğaziçi University, 1999
M. S., University of Illinois at Urbana-Champaign, 2001

DISSERTATION

Submitted in partial fulfillment of the requirements
for the degree of Doctor of Philosophy in Electrical Engineering
in the Graduate College of the
University of Illinois at Urbana-Champaign, 2005

Urbana, Illinois

Efficient and Fair Scheduling for Wireless Networks

Approved by
Prof. Bruce Hajek
Prof. P. R. Kumar
Prof. R. Srikant (Chairman)
Prof. Pramod Viswanath

_____

_____

_____

_____

_____

ABSTRACT

This dissertation addresses the problem of scheduling inelastic and elastic flows in multi-hop wireless networks. Schedulers, by setting the rules for transmission strategies, play a critical role in determining the performance of the network. Thus, a good understanding of schedulers is vital for the design of high performance networks.

Towards this goal, we start by studying the problem of stable scheduling for a class of cellular wireless networks. The goal is to stabilize the queues holding information to be transmitted over a fading channel. Few assumptions are made on the arrival process statistics other than the assumption that their mean values lie within the capacity region and that they satisfy a version of the law of large numbers. We prove that, for any mean arrival rate that lies in the capacity region, the queues are stable under the policy we propose. Moreover, we show that it is easy to incorporate imperfect queue length information and other approximations that simplify the implementation of our policy.

Next, we focus on the performance of well-known schedulers for serving delay-constrained traffic. In particular, we provide analytical as well as numerical analysis of *Opportunistic* and *Time-Division-Multiplexing* schedulers. We demonstrate that the behavior of the throughputs supportable by these schedulers are quite different when delay constraints are imposed.

We then consider the problem of fair end-to-end resource allocation in wireless networks. First, we consider the problem of allocating resources (time slots, frequency, power, etc.) at a base station to many competing flows, where each flow is intended for a different receiver. The channel conditions may be time-varying and different for different receivers. It is well-known that appropriately chosen queue-length based policies are throughput-optimal while other policies based on the estimation of channel statistics can be used to allocate resources

fairly among competing users. We show that a combination of queue-length-based scheduling at the base station and congestion control implemented either at the base station or at the end users can lead to fair resource allocation and queue-length stability. These results are then generalized to multi-hop wireless networks. However, for general multi-hop networks, we require a centralized scheduling policy. For a simple interference model, we study distributed and asynchronous versions of the mechanisms that we proposed, and prove their convergence properties.

To İrem,

my parents, Melek and Halit,

and my brothers, Erol and Ertuğrul.

ACKNOWLEDGMENTS

I am sincerely grateful to my advisor, Professor Srikant, for his guidance and support throughout my graduate studies. Getting to know him both at the professional and personal level has been a privilege. His example will no doubt have a great positive impact on my future endeavors.

I would like to express my gratitude to Professors B. Hajek, P. R. Kumar and P. Viswanath for serving on my dissertation committee. Their insightful comments and suggestions have significantly improved the content of this thesis.

I am deeply indebted to İrem Köprülü, for this thesis would not be complete without her help and support. Her care and understanding allowed me to tackle obstacles with greater confidence.

I would like to thank my family for believing in me throughout my life. Their love and encouragement have given me the courage to pursue my dreams.

I would like to acknowledge my friends Murat, Yıldırım, Cenk, Serdar, Barış, Yeşim, Mustafa (and all others who are escaping my memory now) who have always been there to share the load and joy of life. I am indebted to all my friends at the Coordinated Science Laboratory - Xinzhou, Sujay, Ashvin, Grace, Serdar, Lei, Loc, Akshay, Srinivas, Niranjan, Vignesh, Aleks, Çagrı, Kivanç and Tansu- with whom I had many fruitful conversations on technical and non-technical subjects. Also, I would like to thank the group secretary, Terri, for her patient and helpful attitude in answering my numerous questions.

TABLE OF CONTENTS

LIST OF TABLES

Table **Page**

LIST OF FIGURES

Figure **Page**

CHAPTER 1

INTRODUCTION

A wireless network is composed of a set of nodes that share a common medium. Compared to its wireline counterparts, wireless networks have unique characteristics such as interference amongst concurrent transmissions, time-variations in the channel conditions, power limitations and mobility of the nodes.

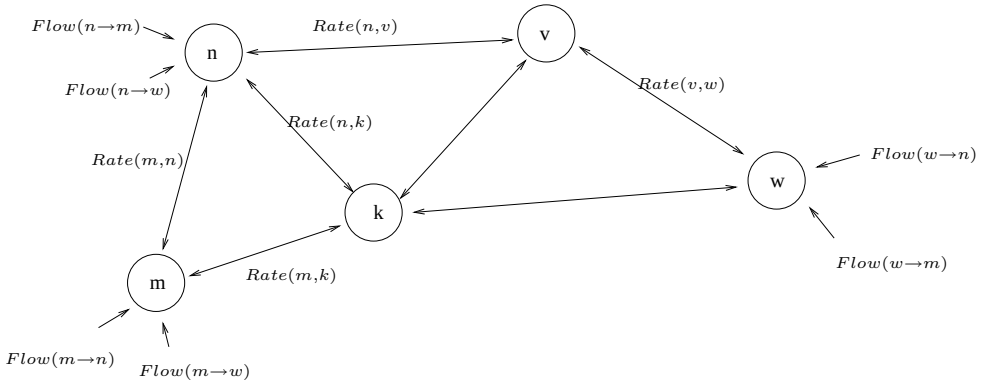

Figure 1.1 Wireless Network Model

There are typically a number of end-to-end flows that compete for the available resources of a wireless network. These flows are either *inelastic* or *elastic* in nature. Inelastic flows have intrinsic rate characteristics that cannot be modified by the application. Examples of such flows include real-time voice and video conferencing calls. On the other hand, an elastic flow's rate

can be adjusted in response to congestion feedback from the network. Data traffic that do not have strict delay constraints are examples of such flows.

The nodes in the network share the traffic load by relaying data from different sources towards their destinations. Each node maintains a buffer that contains the packets of the flows that traverse it. It is critical that these buffers are kept stable to ensure that all the input data reach their respective destination eventually.

Throughout this dissertation, it is assumed that the node locations are fixed and there is a common synchronized clock at every node of the network. This assumption enables a time-slotted model for the system, where we can design algorithms that operate at discrete time instants.

Our goal is to develop and analyze algorithms that guarantee stability of the buffers and have optimality characteristics in terms of the achieved throughput of the flows and fair allocation of the resources. Furthermore, we also address practical considerations such as imperfections in the feedback, computational complexity, and delays.

1.1 Main Contributions and Outline of the Dissertation

1.1.1 Throughput-optimal Scheduling

In Chapter 2, we consider a wireless network shared by inelastic flows, where data collected in N separate queues are to be transmitted over a common medium that is time-varying. Several well-known models fit into this definition. Two such examples would be the downlink and the uplink scenarios of a cellular network.

A *scheduling policy* is an allocation of service rates to the various queues, under the constraint that, at each time instant and each channel state, the set of allocated rates lies within a pre-specified set of allowable rates. The set of allowable rates for each channel state is assumed to be a convex region. A scheduling policy is said to be *throughput-optimal* if it stabilizes the queues for any set of flows that are stabilizable by any other policy.

We present a general class of throughput-optimal scheduling policies which stabilizes the system using only queue length information and the current channel state (i.e., without knowing channel or arrival statistics). We show that this class contains a variety of policies that use probabilistic, periodic or otherwise scheduled queue length updates, policies that result in computational reduction and policies that use head-of-the-line waiting times.

1.1.2 Scheduling for Delay Constrained Traffic over Fading Channels

In Chapter 3, we consider the problem of scheduling delay-constrained-packets, generated by multiple users that share a common fading wireless channel. We focus on schedulers that provide flow isolation in the long run, that is, each flow essentially sees the system as a Single-Input-Single-Output queue. Such schedulers, as opposed to schedulers that use queue length information, may be more fair to flows with low throughputs and more misbehavior by other users. Using large deviations to characterize the probability that the QoS constraint (an upper bound on delay) is violated, we provide analytical expressions for the throughput levels achievable as a function of a given scheduler. We study two widely-used examples of schedulers that provide flow isolation, namely *Opportunistic* and *Time Division Multiplexing (TDM)* schedulers. Recently, there has been much interest in opportunistic scheduling, i.e., scheduling packets from a user who has the largest SNR (signal-to-noise ratio), to maximize the network's throughput. In this chapter, we compare the throughput achievable for delay constrained traffic under fair opportunistic scheduling (i.e., a modification of opportunistic scheduling to ensure fair resource allocation) with the throughput under TDM scheduling. We numerically compare the performance of the two scheduling algorithms under various channel conditions. We show that the opportunistic scheduler outperforms the TDM scheduler when the number of users is small but the TDM scheduler performs better when the number of users exceeds a threshold which depends on the channel parameters. We further present simulation results that compare these schedulers to queue length based schedulers.

1.1.3 Fair Resource Allocation

In Chapter 4, we turn our attention to scheduling elastic traffic. We provide a cross-layer mechanism that comprises of a queue-length-based scheduler operating at the Medium Access Control (MAC) Layer, and a congestion control mechanism operating at the Network Layer.

We show that the interaction between the end-to-end congestion controller and the local queue-length-based scheduler interestingly results in a fair allocation of the resources, where we define a fair allocation as the one that maximizes a certain function of the mean rates over the set of supportable rates. Furthermore, using virtual queues, the buffer levels are kept low and hence the delays experienced by the flows are also low. We also provide a characterization of the point of operation for the queue-length and service rate levels for each of the flows.

1.1.4 Generalizations to Multi-hop Wireless Networks

Chapter 5 extends the results of the previous chapter to the multi-hop wireless networks setting. This extension allows us to draw an interesting connection between the Lagrange multipliers of a certain optimization problem and the equilibrium point of the buffer occupancy levels. In particular, we show that the difference between the queue-lengths at the two ends of each link converges to the optimal Lagrange multiplier associated with the constraint of that link. This Lagrange multiplier has been interpreted as the "price" of the link in earlier works [1–4]. Thus, our result shows that the queue lengths have a direct correspondence with the prices.

1.1.5 Asynchronous Congestion Control

The resource allocation mechanism in Chapter 5 is centralized. In Chapter 6, we consider a congestion control mechanism that operates in conjunction with a distributed scheduler in a wireless network with a simple interference model. The key contribution of this chapter is to allow delays in the rate-congestion price communication between the nodes. The updates are required to happen infinitely often, but the delays are allowed to be potentially unbounded. Such a mechanism is referred to as being *totally asynchronous* in literature [5]. We prove

that under the proposed mechanism, the flow rates converge to the fair allocation point in an appropriate fashion.

Finally, we provide conclusions and directions for future research in Chapter 7. Also, some of the proofs are moved to the Appendix.

CHAPTER 2

THROUGHPUT-OPTIMAL SCHEDULING IN CELLULAR NETWORKS

2.1 Overview

Stable scheduling policies for wireless systems without time-varying channels were first studied in [6]. In fact the model in [6] can also be thought of as a model for a high-speed input-queued switch. Systems with time-varying channels, but limited to the case of ON and OFF channels were studied in [7]. More general channel models have been studied by others recently [8–11]. We generalize the class of scheduling policies considered in [7–9, 12]. Further, we allow imperfect queue length information and prove the stability of policies that reduce computational complexity. These class of policies for wireless networks are natural extensions of those studied in [13, 14] for high-speed switches. Our proof uses a Lyapunov function argument along the lines of the proofs in [6, 15]. We also refer the reader to [16, 17] for a geometric approach to scheduling problems.

In the context of time-varying wireless channels with many users, our work is an example of exploiting multiuser diversity to maximize the capacity of the system. Here, we try to maximize the throughput of the system without the knowledge of system statistics. Alternatively, one can formulate a fair resource allocation problem where each user is allocated a certain fraction of the system resources according to some criterion [18, 19]. The approaches in [18, 19] are not throughput optimal, but are *fair* according to some appropriate notion of fairness. Our work

and other related work assume that the channel is time-varying and attempt to exploit this feature. In [20], an interesting technique to induce time variations in channels which may not be inherently time-varying is discussed.

The rest of the chapter is organized as follows. Section 2.2 describes the system model and presents a statement of the problem we consider in this chapter, the scheduling policy and assumption on the arrival and channel processes. We state the main theorem, which establishes the stability of the system, in Section 2.3. Section 2.4 gives several useful applications of the policy operating both in uplink and downlink scenarios. Several properties of the set of scheduling policies are illustrated through simulations in Section 2.5. The proofs of the theorems are collected in the Appendix.

2.2 System model

Consider a wireless network where N data streams are to be transmitted over a single fading channel. An example of such a network can be a single transmitter sending data to N receivers (the downlink in a cellular system) as depicted in Figure 2.1 or N transmitters sending data to a single receiver (the uplink) as shown in Figure 2.2. We assume that the arriving bits are stored in N separate queues, one for each data stream. Assuming that time is slotted, the evolution of the i^{th} queue is described by the following equation:

$$q_i[t+1] = (q_i[t] + a_i[t] - \eta_i[t])^+, \tag{2.1}$$

where $a_i[t]$ is the number of bits arriving to Queue i at time t and $\eta_i[t]$ is the number of bits from Queue i that are served at time t. One can also ensure that $q_i[t]$ takes on only discrete values in our model. This would be more realistic when transmission can take place only in units of packets, for example. In such a case, there may be wasted service even when $q_i[t] > 0$. To allow for this, we can rewrite the evolution of the queue lengths given by (2.1) as

$$q_i[t+1] = q_i[t] + a_i[t] - \eta_i[t] + u_i[t],$$

where $u_i[t]$ is a positive quantity, which denotes the wasted service provided to the i^{th} queue during slot t.

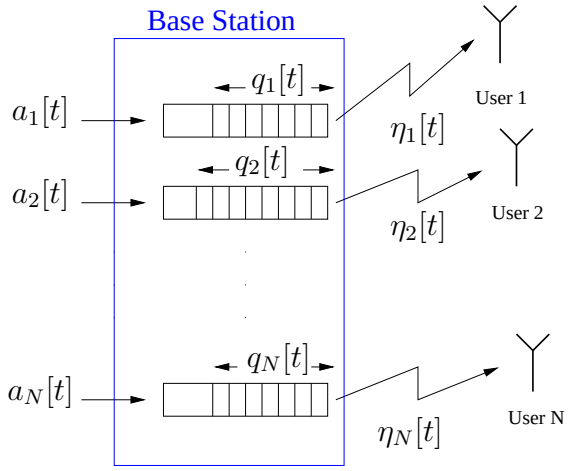

Figure 2.1 Downlink model

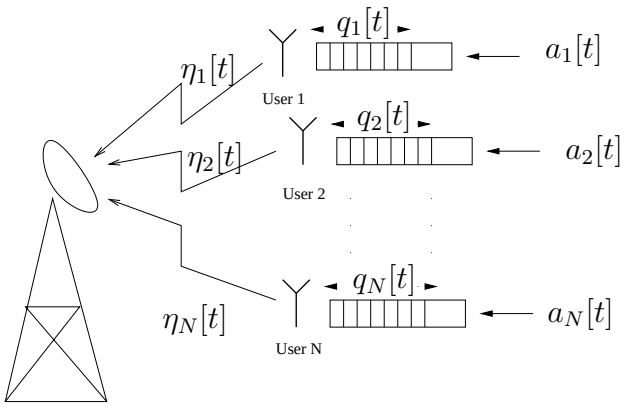

Figure 2.2 Uplink model

The state of the channel is assumed to be fixed within a time slot, but is allowed to vary from one slot to the next. Let J be the number of possible channel states. Suppose that the channel is in State j at time t, then $\{\eta_i[t]\}$ is constrained to be in some region $\mathcal{C}_j$. Thus, $\mathcal{C}_j$ identifies the allowable set of rates at which the queues can be drained when the channel is in State j. For now, we can simply visualize $\mathcal{C}_j$ to be a bounded, convex region such as the broadcast channel capacity region [21]. Precise conditions on the allowable set of rates, the channel state process and arrival processes will be given later.

In this chapter, we consider the following class of scheduling policies: at any time t, given the current channel state $s[t]$, the scheduler chooses a service rate vector $\mu = (\mu_1, \cdots, \mu_N)' \in \mathcal{C}_{s[t]}$ that maximizes a certain objective function. More precisely, μ satisfies:

$$\mu \in \arg\max_{\eta \in \mathcal{C}_{s[t]}} \quad \sum_{i=1}^{N} f_i(q_i[t])\eta_i, \tag{2.2}$$

where $f_i : [0, \infty) \to [0, \infty)$ are functions that satisfy the following conditions:

- $f_i(q)$ is a nondecreasing, continuous function with $\lim_{q\to\infty} f_i(q) = \infty$.
- Given any $M_1 > 0$, $M_2 > 0$ and $0 < \epsilon < 1$, there exists an $\mathcal{X} < \infty$, such that for all $q > \mathcal{X}$, we have

$$(1-\epsilon)f_i(q) \le f_i(q - M_1) \le f_i(q + M_2) \le (1+\epsilon)f_i(q), \qquad \forall i. \tag{2.3}$$

Examples of the the functions $f_i(\cdot)$ that satisfy (2.3) are $f_i(q) = (K_i q)^\alpha$ for any $K_i \in [0, \infty)$ and $\alpha \in [0, \infty)$, or $f_i(q) = e^{\sqrt{q}} - 1$. Note that the exponential function $f_i(q) = e^{\alpha q} - 1$ for any fixed $\alpha > 0$ does not satisfy (2.3).

As we will see later, for various reasons, it may be difficult to implement the policy (2.2). For example, the queue length information may be delayed, the maximization involved may be too complex or one may wish to use waiting times, instead of queue lengths, to choose the service rates. We will show later that, in all such cases, the scheduling policy will satisfy the following property.

Property 2.1. *Given any ρ and ζ such that $0 \leq \rho, \zeta < 1$, there exists a $B > 0$ such that the scheduling policy satisfies the following condition: at any time t, with probability greater than $(1 - \rho)$, the scheduler chooses a service rate vector $\mu = (\mu_1, \cdots, \mu_N)' \in \mathcal{C}_{s[t]}$ that satisfies:*

$$\sum_{i=1}^{N} f_i(q_i[t])\mu_i \quad \geq \quad (1-\zeta) \max_{\eta \in \mathcal{C}_{s[t]}} \quad \sum_{i=1}^{N} f_i(q_i[t])\eta_i \tag{2.4}$$

whenever $\|\mathbf{q}[t]\| > B$, where $\mathbf{q}[t] := (q_1[t], \cdots, q_N[t])'$, and $s[t] \in \{1, \cdots, J\}$ is the channel state in time slot t. $\diamond$

This property relaxes the set of scheduling policies satisfying (2.2) to those that yield an objective function, which can be made arbitrarily close to the maximum for large enough queue lengths. Hence, this relaxation requires tight allocation for large queue lengths, but allows approximately optimal values for small values. In Section 2.3, for the purpose of establishing stability, we will consider scheduling policies that satisfy the above property. And in Section 2.4 we will see that inaccurate queue length information, or computational complexity issues can be resolved by fitting them into this relaxed model.

In the following subsections, we state the various assumptions that we make on the arrival and channel processes, the admissible rate regions, and state a fact about the scheduling policy which will be useful for later proofs.

2.2.1 The channel state process

1) The channel state process has a stationary distribution, where the stationary probability of being in state j, $j \in \{1, \cdots, J\}$, is denoted by π_j. Further, we assume $\pi_j > 0 \; \forall j$.

2) Let us denote the state of the channel at time n by $s[n]$. Note that $s[n]$ can take any one of the J possible values. Given any $\epsilon > 0$, there exists a positive integer $\bar{M}$ such that $\forall M > \bar{M}$

$$E\left[\left|\pi_j - \frac{1}{M}\sum_{n=t}^{t+M-1} I_{s[n]=j}\right|\right] < \epsilon, \tag{2.5}$$

for any $t > 0$ and $j = 1, 2, \ldots, J$.

2.2.2 The achievable rate regions $\{\mathcal{C}_j\}$

1) Consider any region $\mathcal{C}_j$ and any $\eta \in \mathcal{C}_j$. There exists an $\hat{\eta}$ such that $\eta_i \leq \hat{\eta}$. In other words, each of the regions $\mathcal{C}_j$ is bounded.

2) Each of the regions $\mathcal{C}_j$, $j = 1, 2, \ldots, J$ is convex.

3) For each $j = 1, 2, \ldots, J$, the following is true: if $\{\eta_1, \eta_2, \ldots, \eta_i, \ldots, \eta_N\} \in \mathcal{C}_j$, then $\{\eta_1, \eta_2, \ldots, 0, \ldots, \eta_N\} \in \mathcal{C}_j$ for all $i = 1, 2, \ldots, N$.

4) Fix a channel state j. Given any fixed $A \in \Re^+$, $\forall \epsilon > 0$, $\exists R < \infty$ such that, for any $\mathbf{q} \in \left(\Re^N\right)^+$, $\mathbf{y} \in \left(\Re^N\right)^+$ satisfying $|q_i - y_i| < A, \; i = 1, \cdots, N$ and $\|\mathbf{q}\|, \|\mathbf{y}\| > R$, we have

$$\left|\sum_{i=1}^{N} f_i(q_i)\mu_i(j, \mathbf{q}) - \sum_{i=1}^{N} f_i(y_i)\mu_i(j, \mathbf{y})\right| < \epsilon \sum_{i=1}^{N} f_i(q_i)\mu_i(j, \mathbf{q}),$$

where μ is determined according to our scheduling policy. (We use the notation $\mu(j, \mathbf{q})$ to denote the vector of service rates when the current channel state is j and the current queue length vector is $\mathbf{q}$). This assumption simply states that for large enough queue lengths, the optimum objective functions for two queue length vectors within a bounded distance from each other must be approximately equal. Note that, this is not an additional property that the scheduling policy should satisfy, but a property of the boundary of the achievable rate region. Moreover, this assumption is satisfied for any achievable region with a smooth boundary, hence it is not restrictive.

2.2.3 The arrival processes

1) The arrivals to each Queue i form a stationary process, with a mean denoted by $\lambda_i := E[a_i[1]]$.

2) Define

$$\bar{\mathcal{C}} = \{\eta : \eta = \sum_{j=1}^{J} \pi_j \eta^{(j)} \text{ and } \eta^{(j)} \in \mathcal{C}_j, \forall j\}.$$

The vector of mean arrival rates λ is such that there exists $\nu \in \bar{\mathcal{C}}$ satisfying $\nu_i > \lambda_i \; \forall i$.

3) Given any $\epsilon > 0$, there exists a positive integer $\bar{M}$ such that $\forall M > \bar{M}$

$$E\left[\left|\frac{1}{M}\sum_{n=t}^{t+M-1} a_i[n] - \lambda_i\right|\right] < \epsilon, \qquad \forall i. \tag{2.6}$$

4) Finally, f_i and $a_i[t]$ should satisfy

$$\lim_{A\to\infty} \sum_{i=1}^{N} A f_i(A) P(a_i[1] > A) \;\; = \;\; 0.$$

This assumption states that the tail of the arrival distribution should decay fast enough compared to the functions $\{f_i(\cdot)\}$. This assumption is needed since we do not want a single arrival to move the queue length vector outside a bounded region around the previous point. This assumption implicitly states a condition on $\{f_i(\cdot)\}$ as a function of the tail distribution of the arrival process.

2.2.4 Observation on the Scheduling Policy

Claim 2.1. *If the scheduling policy satisfies Property 2.1, then with probability greater than* $(1-\rho)$, $\bar{\mu} := \sum_{j=1}^{J} \pi_j \mu(j, \mathbf{q})$ *satisfies*

$$\sum_{i=1}^{N} f_i(q_i)\bar{\mu}_i \geq (1-\zeta) \max_{\eta\in\bar{\mathcal{C}}} \sum_{i=1}^{N} f_i(q_i)\eta_i \tag{2.7}$$

for all $\|\mathbf{q}\| > B$.

Proof: See Section A.1 of the Appendix for the proof. ◇

2.3 Stability of the stochastic model

We state the main result of the chapter in the following theorem.

Theorem 2.1. *For sufficiently small values of $\zeta, \rho \geq 0$, the system is stable in the mean under the policy described in Section 2.2, i.e.,*

$$\limsup_{p\to\infty} \frac{1}{p} \sum_{t=0}^{p-1} E\left[||\mathbf{f}(\mathbf{q}[t])||_2\right] < \infty, \tag{2.8}$$

where $||\mathbf{f}(\mathbf{q})||_2 := \left(\sum_{i=1}^{N} f_i^2(q_i)\right)^{1/2}$.

Proof: The proof of the theorem is in Appendix A.2. ◇

In addition to the assumptions presented in Section 2.2, if we further assume that the queue lengths $\{q_i[t]\}$ can only take values in $\{0, 1, 2, \ldots\}$, and that the arrival and channel state processes make the queueing system an aperiodic Markov chain with a single communicating class, then the stability-in-the-mean property further implies that the Markov chain is *positive recurrent* [15].

An example of a system that is positive recurrent is one where the arrival and channel state processes satisfy the following conditions:

- *The arrival process to each queue is a Markov-modulated Poisson process.* In other words, the arrival process is in one of many states, the stochastic process describing the evolution of these states is a countable state, aperiodic Markov chain with a single communicating class. Further, in each arrival state, the number of arrivals generated is a Poisson random variable. The mean of the Poisson random variable can be state dependent.

- *The channel state process is a countable state, aperiodic Markov chain with a single communicating class.*

Under the above conditions, if we enlarge the definition of the state to be

$$(\text{channel state, states of the arrival processes, queue lengths}),$$

then the state transition process is a Markov chain. Further, due to the Poisson nature of the arrivals, it is easy to see that the queue lengths can empty from any initial state with non-zero probability, and that from any state with empty queues, it is possible to reach any other state with non-zero probability. Thus, the Markov chain has a single communicating class. Further, it is also easy to see that the system can remain in any state with empty queues for more than one time instant with non-zero probability. Thus, the Markov chain is also aperiodic. Finally, we note that the arrival and channel state processes are short-range dependent and, thus, satisfy the law-of-large-number type conditions (2.5) and (2.6) in Section 2.2.

2.3.1 Instability

If the mean arrival rate vector λ lies outside the average achievable rate region $\bar{\mathcal{C}}$, then the system will be unstable. To prove this, we make use of the *Strict Separation Theorem,* [22, Proposition B. 14] which states that since λ is a point that does not belong to the convex set $\bar{\mathcal{C}}$, there exists a vector β such that

$$\sum_{i=1}^{N} \beta_i \mu_i \leq \sum_{i=1}^{N} \beta_i \lambda_i - \delta,$$

for some $\delta > 0$. Further, due to the fact that $\lambda_i \geq 0, \ \forall i$, and Assumption (3) in Section 2.2.2, a little thought shows that β_i can be chosen to be non-negative, with at least one β_i positive. Given this β, we define the Lyapunov function,

$$W(\mathbf{q}) := \sum_{i=1}^{N} \beta_i q_i.$$

Then, from a drift analysis, we have

$$\begin{aligned} E\left(W(\mathbf{q}[t+1]) - W(\mathbf{q}[t]) \quad |\mathbf{q}[t]\right) &= \sum_{i=1}^{N} \beta_i E\left(q_i[t+1] - q_i[t] \,|\, \mathbf{q}[t]\right) \\ &= \sum_{i=1}^{N} \beta_i E\left(a_i[t] - \eta_i[t] + u_i[t] \,|\, \mathbf{q}[t]\right) \\ &\geq \sum_{i=1}^{N} \beta_i \left(\lambda_i - E(\eta_i[t] \,|\, \mathbf{q}[t])\right) \\ &\geq \delta, \end{aligned}$$

which implies that $E(W(\mathbf{q}[t])) \to \infty$ as $t \to \infty$ and therefore, the system is not stable-in-the-mean.

2.3.2 Non-convex set of allowable rates

There are many practical systems where the set of rate vectors that can be used by the scheduler may not be convex. An example is a cellular downlink with a TDMA protocol, where at each time instant only one of many users can be served. We will refer to the set of rate vectors that can actually be implemented by the scheduler as the *set of allowable rates*. Then we define the *achievable rate region* to be the convex hull of the set of allowable rates for each channel state j. Now suppose we use a policy of the form

$$\mu[t] \in \arg \max_{\eta[t] \in \mathcal{C}_{s[t]}} \sum_{i=1}^{N} f_i(q_i[t])\eta_i[t], \tag{2.9}$$

where $\mathcal{C}_{s[t]}$ denotes the achievable rate region for channel state $s[t]$. We claim that this policy will yield a set of optimal rate vectors, at least one element of which is in the set of allowable rate vectors. That is, at least one of the rate vectors satisfying (2.9) must be allowable.

To see that this claim is true, we first note that, from the definition of a convex hull, any rate, ν, which belongs to the convex hull can be written as a convex combination of some allowable rate vectors, $\{\mathbf{c}^n\}$, i.e.,

$$\nu \;=\; \sum_{n=1}^{L} \alpha_n \mathbf{c}^n,$$

where $L > 0$ is an integer and $\sum_{n=1}^{L} \alpha_n = 1$ with $\alpha_n > 0 \, \forall n$. If for any state j, and some queue length vector $\mathbf{q}$, the set of rates which maximizes (2.9) does not contain any of the allowable rate vectors, then we must have at least one achievable rate vector, ν, such that it satisfies

$$\sum_{i=1}^{N} f_i(q_i)\nu_i \;>\; \sum_{i=1}^{N} f_i(q_i)c_i^n \qquad \forall n \in \{1, \ldots, L\},$$

which in turn implies

$$\sum_{n=1}^{L} \alpha_n \sum_{i=1}^{N} f_i(q_i)c_i^n \;>\; \sum_{i=1}^{N} f_i(q_i)c_i^n \qquad \forall n \in \{1, \ldots, L\}.$$

However, the last equation cannot be true since the convex combination of a set of positive numbers cannot be strictly larger than each of them. Hence, by contradiction, it follows that at least one solution to the maximization problem in (2.9) must belong to the set of allowable rates.

2.4 Applications

The scheduling policy given in (2.2) is a generalization of the policy examined in [6, 8, 12]. In a later section, we show through simulations that general functions of the form $f_i(\cdot)$ can be very useful in controlling queue lengths. In this section, we show that the introduction of the parameters, ρ, ζ, enables the application of the policy to scenarios where instantaneous queue length information is not available or the scheduler has computational limitations.

2.4.1 Infrequent or Delayed Queue Length Updates

Consider the multiple access uplink scenario, where each of the N users maintains an infinite length queue, holding information to be transmitted to the base station over a fading multiple access channel. This scenario is depicted in Figure 2.2. In this case, it may not be reasonable to expect the queue length to be updated at each time slot. To reduce the amount of information transferred between the transmitters and the base station, suppose that each transmitter updates the queue length only once every T time slots. Let $\hat{q}_i[t]$ denote the estimate of the queue length of the i^{th} queue at time t. In other words, $\hat{q}_i[t]$ is the last update of the queue length, prior to time t, received by the base station from Transmitter i. Further, suppose that at each time slot t, the base station allocates a service rate vector that satisfies

$$\arg \max_{\eta[t] \in \mathcal{C}_{s[t]}} \sum_{i=1}^{N} f_i(\hat{q}_i[t])\eta_i[t]. \tag{2.10}$$

In the following theorem, we show that this policy satisfies Property 1 in Section 2.2.

Theorem 2.2. *Suppose that the scheduler is only allowed to sample the queue length information once every T slots (i.e. $\hat{q}_i[nT + l] = q_i[nT]$ for $l = 0, 1, \ldots, T - 1$ and $n = 0, 1, \ldots$), and*

it uses this sampled value as the current queue length to determine the service rates according to (2.10), then the system is stable-in-the-mean.

Proof: Since the mean arrival rate to each of the queues is finite, given any $\rho \in (0,1)$, we can find $A < \infty$ such that

$$Prob\{a_i[t] \leq A \, \forall i\} > (1-\rho).$$

Let us consider two sampling instants t and $t+T$. Consider any $n \in \{0, \cdots, T-1\}$, and define the following quantities for each channel state j :

$$\mu^*(j, \mathbf{q}[t+n]) \in \arg\max_{\mu \in \mathcal{C}_j} \sum_{i=1}^{N} f_i(q_i[t+n])\mu_i(j, \mathbf{q}[t+n])$$

$$\hat{\mu}(j, \hat{\mathbf{q}}[t+n]) = \hat{\mu}(j, \mathbf{q}[t]) \in \arg\max_{\mu \in \mathcal{C}_j} \sum_{i=1}^{N} f_i(q_i[t])\mu_i(j, \mathbf{q}[t]).$$

Observe that for any $i \in \{1, 2, \ldots, N\}$, and $n \in \{0, 1, \ldots, T-1\}$, we have

$$q_i[t+n] - TA \leq \hat{q}_i[t+n] = q_i[t] \leq q_i[t+n] + T\hat{\eta} \qquad \text{w.p. } (1-\rho)^T.$$

Then, due to (2.3), for any $\epsilon_1 > 0$, we can find a bounded region around the origin outside of which we have,

$$\sum_{i=1}^{N} f_i(\hat{q}_i[t+n])\hat{\mu}_i(j, \hat{\mathbf{q}}[t+n]) \;\; \leq \;\; (1+\epsilon_1) \sum_{i=1}^{N} f_i(q_i[t+n])\hat{\mu}_i(j, \hat{\mathbf{q}}[t+n]). \quad (2.11)$$

Moreover, due to Assumption (4) of Section 2.2.2, given any $\zeta_1 \in (0,1)$, we can find a bounded region around the origin, outside of which the following inequality holds

$$\begin{aligned} \sum_{i=1}^{N} f_i(\hat{q}_i[t+n])\hat{\mu}_i(j, \hat{\mathbf{q}}[t+n]) &= \sum_{i=1}^{N} f_i(q_i[t])\hat{\mu}_i(j, \mathbf{q}[t]) \\ &\geq (1-\zeta_1) \sum_{i=1}^{N} f_i(q_i[t+n])\mu_i^*(j, \mathbf{q}[t+n]) \qquad \text{w.p. } (1-\rho)^T. \end{aligned}$$

Combining this result with (2.11), we can state that given any $\zeta \in (0,1)$, the following inequality holds outside a bounded region around the origin.

$$\sum_{i=1}^{N} f_i(q_i[t+n])\hat{\mu}_i(j, \hat{\mathbf{q}}[t+n]) \;\; \geq \;\; (1-\zeta) \sum_{i=1}^{N} f_i(q_i[t+n])\mu_i^*(j, \mathbf{q}[t+n]) \qquad \text{w.p. } (1-\rho)^T.$$

Therefore, this policy satisfies Property 1. $\diamond$

There are alternative ways to update the queue length information instead of periodic sampling. For example, the scheduler may sample each queue with some probability at each time instant. In this case, given any $\epsilon > 0$, we can find a T such that the probability that all queues have been updated at least once in the past T slots is greater than $1 - \epsilon$. By making ϵ arbitrarily small and following the lines of the proof of previous theorem, we can again prove the stability of the system.

While periodic sampling and random sampling would ensure stability, they may result in poor delay performance. An alternative sampling technique which may be particularly useful with bursty arrivals, is to update the queue length information for each queue whenever the absolute value of the difference between the current length and the last update exceeds some threshold. Along the lines of the proof of the previous theorem, we can again show that this policy is stable. However, we will show through simulations later that this update mechanism reduces the mean queueing delay as compared to random or periodic sampling.

Finally, we note that delayed queue length updates can also be cast in the same framework as above.

2.4.2 Reducing computational complexity

Typically, the allowed set of power levels at a mobile or a base station is a finite set. Consequently, the set of allowable rates will be finite for each channel state. In this case, as discussed earlier, the achievable rate region in each state is the convex hull of the set of allowable rates in the state. The convex hull would be a convex polyhedron and a policy of the form

$$\arg \max_{\eta[t] \in \mathcal{C}_{s[t]}} \sum_{i=1}^{N} f_i(q_i[t]) \eta_i[t]$$

would involve an optimization over the vertices of the convex polygon. The complexity issues arising due to this has been addressed in the context of high-speed switches in [13, 14].

In this section, we show that the solutions proposed in [13, 14] for high-speed switches are also applicable to wireless networks with time-varying connectivity and more general functions $f_i(q_i)$ than the ones considered in [13, 14]. The basic idea behind the solution in [14] is to

perform a Hamiltonian walk over the set of allowable rates (or more simply, over the vertices of the convex polygon of allowable rates) for each state, and store in memory, the *best* schedule so far in each channel state. (In our context, performing a Hamiltonian walk corresponds to maintaining a list of allowable rates and visiting each possible rate vector in a fixed order. Once all the rate vectors are visited, the list is again scanned from the beginning.) This way, at each step we only need to compare two values, which is a significant reduction of complexity. In the following, we present the algorithm and prove its stability.

Algorithm A: Assume that the current channel state is $s[t] = j$ and let $t^{(j)}_{[-d]}$ denote the d^{th} time slot before t when the channel was in State j. Let $\mathcal{L}^{(j)}$ denote the number of available rate vectors we need to choose from when the channel state is j, and $\eta[t^{(j)}_{[-d]}]$ denote the rate vector at time $t^{(j)}_{[-d]}$. (Note that $t^{(j)}_{[-1]}$ denotes the last time before t when the channel state was j. In the following, we will omit the subscript $[-d]$ when $d = 1$.) Then the algorithm is comprised of the repetition of the following steps:

(I) $\mathbf{h}[t] =$ next rate vector visited by the Hamiltonian walk in the current channel state $s[t] = j$.

(II)

$$\eta[t] = \arg \max_{\nu \in \{\eta[t^{(j)}], \mathbf{h}[t]\}} \sum_{i=1}^{N} f_i(q_i[t])\nu_i.$$

Remark: Even if Step (I) of the algorithm is modified to choosing a rate vector *randomly* from the set of possible rate vectors as in [13], the following theorem will continue to hold. Since the proof is essentially the same, only *Algorithm A* is considered here.

An example Hamiltonian walk is provided in Figure 2.3 for a two user scenario. The dots represent the set of feasible rate allocations and the arrows show a possible Hamiltonian walk within the set.

Theorem 2.3. *The policy defined by* Algorithm A *satisfies Property 1 of Section 2.2 and hence Theorem 2.1 continues to hold.*

Proof: For any $\rho_1 > 0$, we can find an $A < \infty$ such that $Prob\{a_i[t] \leq A \, \forall i\} > (1 - \rho_1)$. Then, note that for any $t, n \geq 0$, we have

$$q_i[t] - n\hat{\eta} \leq q_i[t+n] \leq q_i[t] + nA \qquad \forall i, \qquad \text{w.p.} \quad (1-\rho_1)^n,$$

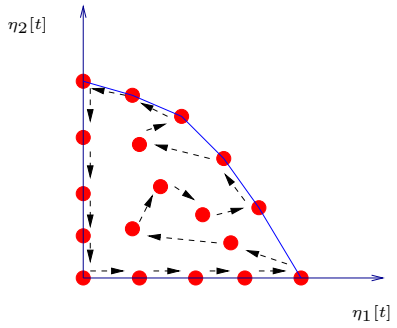

Figure 2.3 Finite set of rates and Hamiltonian walk

which in turn implies that $\forall \epsilon_1 > 0$ and any allowable rate vector ν, we can find a large enough bounded region, outside of which, the following holds:

$$\left| \sum_{i=1}^{N} f_i(q_i[t+n])\nu_i - \sum_{i=1}^{N} f_i(q_i[t])\nu_i \right| \leq \epsilon_1 \sum_{i=1}^{N} f_i(q_i[t])\nu_i, \qquad \text{w.p.} \quad (1-\rho_1)^n. \tag{2.12}$$

The assumptions on the channel state process imply that the probability of not visiting a state j within M slots goes to zero as M tends to infinity. Therefore, for any $\rho_2 > 0$, we can find a finite M, such that the probability of not visiting a state j is less than ρ_2, and this is true for any $j \in \{1, \cdots, J\}$.

Consider any slot m and, without loss of generality, assume that the channel state at that slot is j. Also let us define $\mathcal{L} := \max_j \mathcal{L}^{(j)} < \infty$. Let $\eta^*[m]$ be a rate vector that satisfies the following at time m :

$$\eta^*[m] \in \arg \max_{\eta[t] \in \mathcal{C}_j} \sum_{i=1}^{N} f_i(q_i[m])\eta_i[m].$$

Then, as observed in [14], due to the nature of the Hamiltonian walk, there exists a time slot $m' \in [m^{(j)}_{[-\mathcal{L}]}, m]$ for which the channel state satisfies $s[m'] = j$, and the rate vector visited by the Hamiltonian walk at that time is $\mathbf{h}[m'] = \eta^*[m]$. In other words, we can write $m' = m^{(j)}_{[-t]}$ for some $t \in \{0, \ldots, \mathcal{L}\}$.

Moreover, repeating the argument that the channel state process visits state j at least once in M slots with probability $(1-\rho_2)$, we have

$$m - M\mathcal{L} \leq m^{(j)}_{[-\mathcal{L}]} \leq m \qquad \text{w.p.}(1-\rho_2)^{\mathcal{L}}. \tag{2.13}$$

Combining this observation with the properties of m' we have $m' \in [m - M\mathcal{L}, m]$ with probability $(1-\rho_2)^{\mathcal{L}}$. Then, Step (II) of the algorithm enables us to write

$$\sum_{i=1}^{N} \eta_i[m'] f_i(q_i[m']) \geq \sum_{i=1}^{N} \eta_i^*[m] f_i(q_i[m']) \tag{2.14}$$

$$\geq (1-\epsilon_1) \sum_{i=1}^{N} \eta_i^*[m] f_i(q_i[m]) \text{ w.p. } (1-\rho_2)^{\mathcal{L}}(1-\rho_1)^{M\mathcal{L}}, \tag{2.15}$$

where the last inequality follows from (2.12) and (2.13).

Also note that, for any n and any $\epsilon_2 > 0$, we can find a bounded region around the origin, outside of which we have: with probability $(1-\rho_1)^M(1-\rho_2)$,

$$(1-\epsilon_2) \sum_{i=1}^{N} f_i(q_i[n^{(s[n])}]) \eta_i[n^{(s[n])}] \leq \sum_{i=1}^{N} f_i(q_i[n]) \eta_i[n^{(s[n])}] \leq \sum_{i=1}^{N} f_i(q_i[n]) \eta_i[n], \tag{2.16}$$

where the first inequality follows from (2.12), and the second inequality is due to Step (II) of Algorithm A. We continue as follows:

$$\sum_{i=1}^{N} f_i(q_i[m]) \eta_i[m]$$

$$\geq (1-\epsilon_2)^t \sum_{i=1}^{N} f_i(q_i[m']) \eta_i[m'] \qquad \text{w.p. } (1-\rho_1)^{tM}(1-\rho_2)^t \tag{2.17}$$

$$\geq (1-\epsilon_1)(1-\epsilon_2)^{\mathcal{L}} \sum_{i=1}^{N} f_i(q_i[m]) \eta_i^*[m] \qquad \text{w.p. } (1-\rho_1)^{2M\mathcal{L}}(1-\rho_2)^{2\mathcal{L}}. \tag{2.18}$$

In the previous steps, (2.17) follows from (2.16), and step (2.18) follows from (2.15) and the fact that $|t| \leq \mathcal{L}$. Hence, given any $\zeta > 0$, and $\rho > 0$, we can find $\rho_1, \rho_2 > 0$ satisfying $(1-\rho_1)^{M\mathcal{L}}(1-\rho_2)^{2\mathcal{L}} \geq (1-\rho)$ and find parameters $\epsilon_1, \epsilon_2 > 0$ satisfying $(1-\epsilon_1)(1-\epsilon_2)^{\mathcal{L}} \geq (1-\zeta)$, which in turn yields

$$\sum_{i=1}^{N} f_i(q_i[m]) \eta_i[m] \geq (1-\zeta) \sum_{i=1}^{N} f_i(q_i[m]) \eta_i^*[m] \qquad \forall m, \qquad \text{w.p. } (1-\rho),$$

outside a closed, bounded region around the origin. Therefore, we have proved that Algorithm A satisfies Property 1. ◇

We note that, while *Algorithm A* lowers the computational complexity considerably, it adds a memory requirement non-existent previously. To see this, first observe that the algorithm

keeps track the rate vectors for each fading state. Since the number of fading states increases exponentially with the number of users, so will the memory requirement. Evidently such a memory requirement is necessary to assure stability if computational complexity is an issue. Alternatively, one can tradeoff between memory and computational complexity requirements, by using Algorithm A only in some channel states and performing exact computations in other channel states. For example, in some channel states, the SNR may be too low so that a packet cannot be transmitted unless the transmit power is above some threshold. This may limit the number of candidate optimal solutions, thus automatically reducing the computation required. For these states, one can use exact computation, whereas, for other states, reduced complexity algorithms could be used.

2.4.3 Downlink

In the downlink scenario, a single transmitter maintains N infinite length queues, one for each receiver and sends this information over a fading channel as depicted in Figure 2.1. Hence, the scheduler at the transmitter has immediate access to the queue length values at any time, and we assume that it knows the current channel state. Then at the beginning of each time slot, say t, it chooses the service rate vector $\mu[t]$, such that

$$\mu[t] \in \arg \max_{\eta[t] \in \mathcal{C}_{s[t]}} \sum_{i=1}^{N} f_i(q_i[t])\eta_i[t], \tag{2.19}$$

whenever $\|\mathbf{q}\| > B$ for any fixed value $B < \infty$. Then the results of Section 2.3 hold for this system. This is a generalization of the result in [8] where the result has been proved for the case $f_i(q)$ of the form $(K_i q)_i^{\alpha}$. As we will see through simulations later, our generalization allows for better queue length performance.

2.4.4 Waiting Times

Instead of the current queue length information, the scheduler may alternatively use the delay experienced by the packets within the queues as its input. To incorporate this into our model, we first let $w_i[t]$ denote the waiting time of the head of the line (H.O.L.) packet in the

i^{th} queue at time t. In the following, we consider a policy that chooses the service rate vector $\mu[t]$, such that

$$\mu[t] \in \arg \max_{\eta[t] \in \mathcal{C}_{s[t]}} \sum_{i=1}^{N} h_i(w_i[t])\eta_i[t], \tag{2.20}$$

for continuous, non-decreasing functions $\{h_i(\cdot)\}$, satisfying $h_i(0) = 0$ and $\lim_{x\to\infty} h_i(x) = \infty$.

Observe that given any $\mathcal{W} < \infty$ and $\epsilon \in (0, 1)$, we can find a value $\mathcal{X}$ such that for all $q_i[t] > \mathcal{X}$, we have $w_i[t] \geq \mathcal{W}$ with probability greater than or equal to $(1 - \epsilon)$. In this subsection alone, we make stronger assumptions on the arrival process than we had previously used. Let us assume that given any $\delta > 0$, we can find a $\Gamma < \infty$ so that, with probability greater than $(1 - \delta)$, we have

$$\lambda_i w_i[t] - \Gamma\sqrt{w_i[t]} \leq q_i[t] \leq \lambda_i w_i[t] + \Gamma\sqrt{w_i[t]} \qquad \forall i, t.$$

Thus, we assume that the arrival process obeys a central limit theorem (CLT). Conditions on the arrival process under which it obeys a CLT are given, for example, in [23].

From the CLT assumption, it is easy to see that $w_i[t]$ can be upper and lower bounded as follows:

$$\alpha_i q_i[t] - K\sqrt{q_i[t]} \leq w_i[t] \leq \alpha_i q_i[t] + K\sqrt{q_i[t]} \qquad \forall i, t,$$

for appropriate values of $\{\alpha_i\}$ and K. Then, we have

$$h_i(\alpha_i q_i[t] - K\sqrt{q_i[t]}) \leq h_i(w_i[t]) \leq h_i(\alpha_i q_i[t] + K\sqrt{q_i[t]}) \qquad \forall i, t.$$

We assume that, given any $\epsilon > 0$ and a finite K, we can find a bounded region around the origin, outside of which the following holds:

$$(1 - \epsilon)h_i(\alpha_i q_i) \leq h_i(\alpha_i q_i - K\sqrt{q_i}) \leq h_i(\alpha_i q_i + K\sqrt{q_i}) \leq (1 + \epsilon)h_i(\alpha_i q_i), \qquad \forall i. \tag{2.21}$$

Now, if we define $f_i(q_i[t]) := h_i(\alpha_i q_i[t])$, then (2.21) implies that outside a bounded region around the origin,

$$(1 - \epsilon)f_i(q_i[t]) \leq h_i(w_i[t]) \leq (1 + \epsilon)f_i(q_i[t]) \qquad \forall i.$$

This property enables us to bound (2.20) as follows

$$\max_{\eta[t]\in\mathcal{C}_{s[t]}} \sum_{i=1}^{N} h_i(w_i[t])\eta_i[t] \;\;\geq\;\; (1-\epsilon) \max_{\eta[t]\in\mathcal{C}_{s[t]}} \sum_{i=1}^{N} f_i(q_i[t])\eta_i[t],$$

which shows that (2.4) is satisfied.

An example of $h_i(\cdot)$ that satisfy (2.21) is $h_i(w) := K_i w^{\alpha_i}\ \forall \alpha_i > 0$. To see that this is in fact the case, we can write

$$\begin{aligned} h_i(q_i \pm K\sqrt{q_i}) &= K_i(q_i \pm K\sqrt{q_i})^{\alpha_i} \\ &= K_i q_i^{\alpha_i}\left(1 \pm \frac{K}{\sqrt{q_i}}\right)^{\alpha_i}, \end{aligned}$$

where the term in the parenthesis can be made arbitrarily close to 1 by choosing q_i large enough. Hence, (2.21) holds.

Another example of $h_i(\cdot)$ that satisfies (2.21) is $h_i(w) := \exp(w^{\alpha_i})\ \forall \alpha_i \in (0, 0.5)$. To justify this, we proceed as follows:

$$\begin{aligned} h_i(q_i \pm K\sqrt{q_i}) &= \exp((q_i \pm K\sqrt{q_i})^{\alpha_i}) \\ &= \exp(q_i^{\alpha_i}(1 \pm \frac{K}{\sqrt{q_i}})^{\alpha_i}) \\ &\approx \exp(q_i^{\alpha_i}(1 \pm \frac{K\alpha_i}{\sqrt{q_i}})) \\ &= \exp(q_i^{\alpha_i})\exp(\pm K\alpha_i q_i^{(\alpha_i - 0.5)}), \end{aligned}$$

where the second exponent can be made arbitrarily small by choosing q_i large enough if $\alpha_i \in (0, 0.5)$.

In the previous example of $h_i(\cdot)$, if $\alpha_i \in [0.5, 1)$, then the system described above is not necessarily stable in the mean. To guarantee stability, we have to strengthen the conditions on the arrival process. Suppose that we consider leaky bucket type of arrivals, i.e., the number of arrivals between time s and t, denoted by $A(s,t)$, satisfies $A(s,t) \leq \rho(t-s) + \sigma\ \forall\ 0 \leq s < t$ with positive constants ρ, σ. There are many examples of stationary stochastic processes that satisfy such a constraint when the arrival process is further peak-rate constrained. We refer the reader to [24] for one such example. The leaky-bucket constraint limits the burstiness of the

arrivals, which in turn enables us to upper-bound the difference between q_i and $\lambda_i w_i$, with high probability, by a large enough constant. Hence, with probability greater than $(1-\delta)$, we have

$$\beta_i q_i[t] - K \leq w_i[t] \leq \beta_i q_i[t] + K \qquad \forall i, t,$$

for appropriate values of $\{\beta_i\}$ and K. Then, we have

$$h_i(\beta_i q_i[t] - K) \leq h_i(w_i[t]) \leq h_i(\beta_i q_i[t] + K) \qquad \forall i, t.$$

If we define $f_i(q) := h_i(\beta_i q)$, and assume that $\{f_i(\cdot)\}$ satisfies (2.3), then the previous set of inequalities holds. Then it is easy to see that $\{h_i(\cdot)\}$ of the form $h_i(w) := \exp(w^{\alpha_i})\ \forall \alpha_i \in [0.5, 1)$ satisfies (2.21).

2.5 Simulations

In this section, the performance of the class of scheduling policies described in Section 2.2 is illustrated through simulations. For ease of exposition, most of the simulations consider the case of two users.

2.5.1 Experiment 1: Stability and Queue-length Evolution

In this experiment, we illustrate the effect of using different sets of functions $\{f_i(q)\}$ on the queue length evolution of the system. The average arrival rates to the two queues are $\lambda_1 = 50$ and $\lambda_2 = 50$. The channel is in one of five states and the achievable rates η_{1s} and η_{2s} for the two queues when the channel is in State s satisfy the following equation:

$$\eta_{1s}^2 + \eta_{2s}^2 \leq r_s \sqrt{\lambda_1^2 + \lambda_2^2}.$$

The values for r_s were chosen to be 0.3, 0.7, 1, 1.3 and 1.7. The channel state process is a discrete-time Markov chain, such that, given that the Markov chain is in a particular state, the probability of a transition to any other state (including itself) is 0.2. The number of arrivals to each queue in each time slot has a Poisson distribution. The arrivals to the two queues are

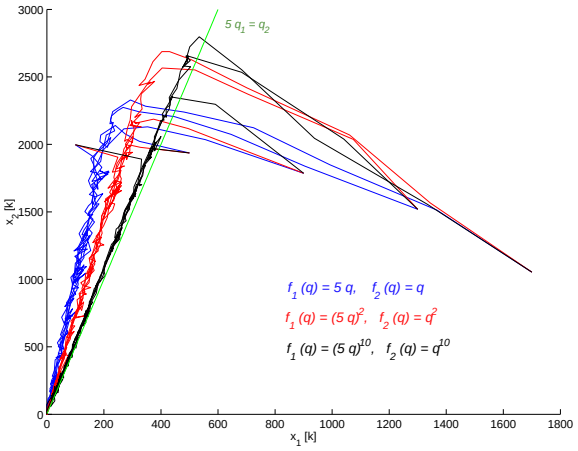

Figure 2.4 Queue length evolutions in the stochastic model.

independent from time slot to slot, and are independent of each other and of the channel state process.

The functions we used in the simulations are of the form $f_i(q_i) = (K_i q_i)^\alpha$. Using functions of this form, the queue length evolutions are illustrated in Figure 2.4. Observe that as α increases, the queue length vector gets closer to the line $K_1 q_1 = K_2 q_2$ from any initial condition, after which it stays around it and moves toward the origin. Such a behavior empirically shows that we can choose the functions $\{f_i(\cdot)\}$ so that priorities may be assigned to different queues without sacrificing stability. Moreover, this analysis justifies the fairness property inherent in the policy, again through empirical methods. We note that the rule in [9] drives the system to the line where the $K_i q_i$ for all the users are equal and is shown to be path-wise optimal in [10].

2.5.2 Experiment 2: Delay Characteristics

In this experiment, the channel setting is kept the same as in Experiment 1, but the arrivals to both of the queues are chosen to be independent, Bernoulli distributed random variables having mean λ_i for Queue i with a peak value of 500 packets per slot. In the case of such bursty arrivals, this experiment compares the performance of two queue length update mechanisms:

- periodically updating the queue length information (we refer to this policy as the *Periodic Update Policy*) and

- updating it either when the number of arrivals exceeds a certain limit since the last update or if the time since the last update has exceeded a threshold (we refer to this policy as the *Enhanced Update Policy*).

The stability analysis of such systems was done in Section 2.4.1.

In the Periodic update policy, the values of the queue lengths are updated once in every 200 slots in our simulations. When the arrivals are bursty, such a strategy does not track the queue length values very closely. Even though, we have proved that the system will be stable in the mean, the packets might experience large delays.

On the other hand, if we instead use the Enhanced update strategy, which guarantees that the queue length information is updated at least once in every 200 slots and also whenever current queue length differs from the most recent update by more than a certain threshold (50 in our example), then we get better performance under a bursty traffic, since we can track the actual queue length values more closely.

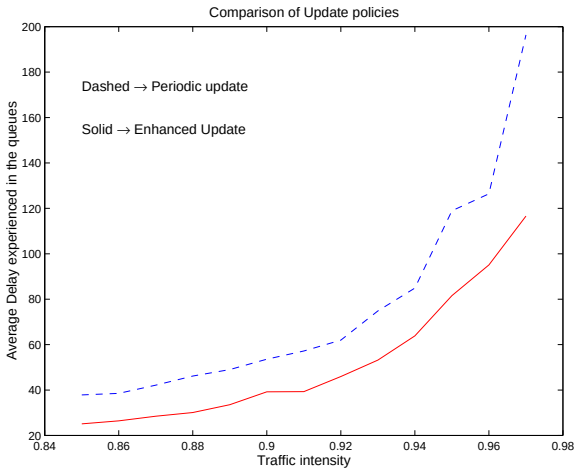

Figure 2.5 Delay characteristics of the two queue length update strategies defined in Experiment 2, with varying load.

We note that the average achievable rate region is a quarter circle of radius 50. We define *traffic intensity* to be the ratio $\sqrt{\lambda_1^2 + \lambda_2^2}/50$. Figure 2.5 examines the effect of varying the traffic intensity for the two update policies, where the sampling time for the periodic update policy and the bound for the threshold update policy are both taken to be 50. It is seen that under heavy load, the Enhanced update policy yields much better average delay performance.

2.5.3 Experiment 3: Buffer Overflow Performance

In this experiment, our goal is to study the ability of our class of policies to minimize buffer overflow. For this purpose, we consider the following measure of performance:

$$P(q_1 > B_1) + P(q_2 > B_2),$$

where B_1 and B_2 are both taken to be 5000. In other words, the objective is the sum of the overflow probabilities in the two queues. We wish to study the impact of the choice of $\{f_i(\cdot)\}$ on the above performance measure.

We use the following heuristic to choose $\{f_i(\cdot)\}$. From Markov's inequality, we have $P(q_i > B_i) \leq \frac{g_i(q_i/B_i)}{g_i(1)}$ for any positive, increasing function $g_i(\cdot)$. Since we do not have expressions for the overflow probability, we choose functions $\{f_i(\cdot)\}$ that we expect would minimize the above upper bounds on the overflow probability. To do this, we choose $f_i(q_i) = g_i'(q_i)$. The heuristic behind this is that, in the fluid model (see proof of Theorem 2.1 in the Appendix), at each instant, we attempt to minimize the time derivative of $\sum_i g_i(q_i)$. Thus, it is natural to choose $\{f_i(\cdot)\}$ to be the derivatives of the upper bound expressions.

1. The first policy chooses μ such that

   $$\sum_{i=1}^{n} \mu_i \frac{q_i}{B_i^2}$$

   is maximized over all μ within the current achievable rate region. This corresponds to $g_i(q_i) = (q_i/B_i)^2$.

2. The second policy chooses μ such that

   $$\sum_{i=1}^{n} \mu_i \exp(\frac{q_i}{B_i})^{0.5}$$

   is maximized. This corresponds to

   $$g_i(q_i) = \frac{1}{B_i} \int_0^{q_i} e^{\sqrt{y}} dy.$$

3. For comparison, we also study the performance of the $EXP-Q$ rule which was shown to be throughput-optimal in [9], and has recently been shown to be path-wise optimal in the heavy traffic regime [10]. This policy chooses μ such that

$$\sum_{i=1}^{n} \mu_i e^{\left(\frac{\frac{q_i}{B_i}}{1+\sqrt{\frac{1}{n}\left(\frac{q_1}{B_1}+\frac{q_2}{B_2}+\ldots+\frac{q_n}{B_n}\right)}} \right)}$$

is maximized over all μ within the current achievable rate region.

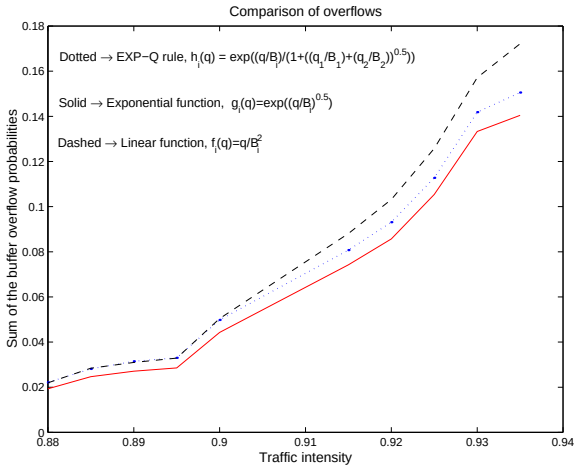

Figure 2.6 Comparison of the policies with increasing traffic intensity.

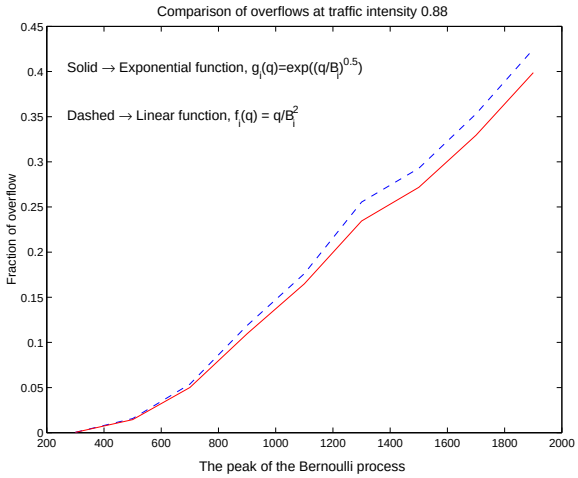

Figure 2.7 Comparison of the policies with increasing burstiness of the Bernoulli arrivals.

The channel state process is allowed to vary among five equiprobable states as in Experiments 1 and 2. The initial queue length values are chosen as $(q_1[0], q_2[0]) = (1000, 1000)$. Note that this choice is arbitrary and we ran the simulations for 10 million iterations so that the transient effects will be negligible. The arrival rates are chosen as $(\lambda_1, \lambda_2) = (50, 50)$. In Figure 2.6, the performance of the three policies are compared as a function of traffic intensity. The range of traffic intensities for which the fraction of overflow duration is on the order of 10^{-3} to 10^{-2} is shown in the figure. It can be seen that with increasing traffic intensity, the second policy, which uses an exponential function to determine the rates, enables a 10% to 20% reduction in the overflow probability compared to the first policy. Somewhat surprisingly, the second policy has a 5% to 10% smaller overflow probability compared to the EXP-Q rule.

Even though the EXP-Q has been proved to be path-wise optimal in [10], it is an asymptotic result in the heavy-traffic regime and so it is quite possible that another scheme could perform slightly better at traffic intensities within the boundary of the capacity region. This illustrates the fact that by suitably choosing of functions $f_i(q_i)$, system performance can be improved. However, we do not have a theoretical handle on how these $f_i(q_i)$ should be chosen given a requirement on the overflow probability. This is a subject of future research.

Figure 2.7 shows the effect of increasing the burstiness of the arrivals on the overflows of the two policies. We increase the burstiness by increasing the peak value, M, of the Bernoulli arrivals while keeping the mean unchanged. Although the figure is plotted for the traffic intensity of 0.88, it is representative of other traffic intensities. Again, the exponential function gives a better performance than the linear function.

2.5.4 Experiment 4: Effect of Number of Users

In this final experiment, we repeat Experiments 2 and 3 for more than two users. For this purpose, we increase the number of queues to five and change the average achievable rate region to a sphere in the $5-$dimensional Euclidean space with radius 50. We keep the remaining settings of the earlier experiments unchanged for comparison.

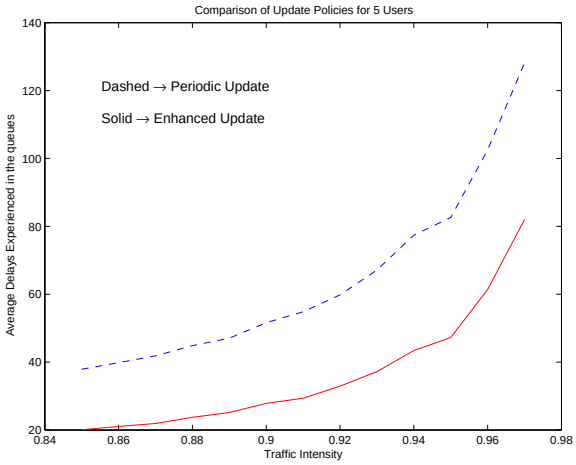

Figure 2.8 Delay characteristics of the two queue length update strategies for five users, with varying load.

Figure 2.8 depicts the performance of the Periodic and Enhanced Update policies for the new model. Compared to Figure 2.5, we can see that the increase in the number of users had no significant impact on the performances of the two policies.

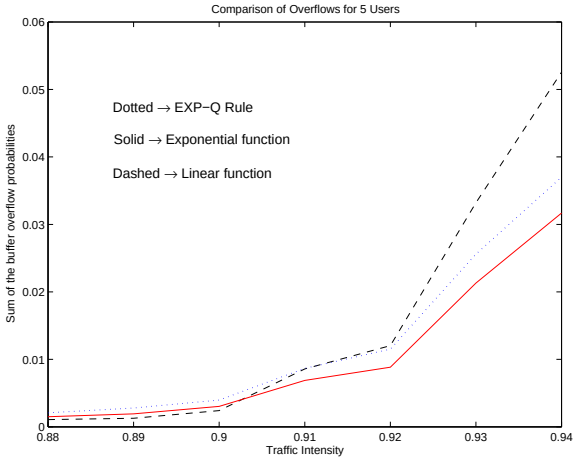

Figure 2.9 Comparison of the policies with increasing traffic intensity for five users.

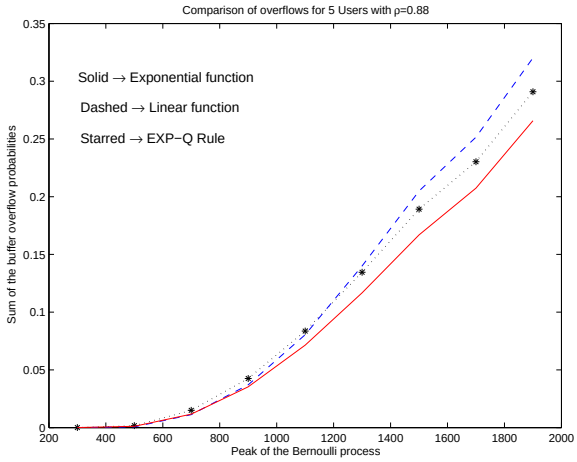

Figure 2.10 Comparison of the policies with increasing arrival burstiness for five users.

Figures 2.9 and 2.10 depict the overflow performances of the three policies described in Experiment 2 with varying ρ and M, respectively. We can again see the same characteristics with Figures 2.6 and 2.7. However, the buffer overflow probability averaged over the five users yields lower values for the same load as compared to the case of two users. We believe that this is due to a form of "statistical multiplexing" with a larger number of users.

CHAPTER 3

SCHEDULING WITH QoS CONSTRAINTS OVER FADING CHANNELS

3.1 Problem Statement and Main Contributions

A number of schedulers have been proposed to serve N flows that share a common wireless channel with independent fading conditions for each flow [7, 8, 10, 19, 20, 25–28]. Among these, [7, 10, 25, 26] use queue length as well as channel state information in scheduling the transmissions. Here, the basic idea is to give priority to the flows that have longer backlogs and that have good enough channel conditions. It is shown that these policies are *throughput optimal* in the sense that any mean throughput that can possibly be achieved under stability can be achieved by these policies. Moreover, since buffer occupancy levels are involved in the decision process, these schedulers are expected to provide low delay levels for the flows. However, they may be unfair to flows with low rates since the buffer occupancies of high rate flows will dominate the system. Also, the implementation of these policies require a separate feedback channel to convey the channel state and buffer occupancy levels to a central controller, which may be impractical. Furthermore, these policies may be vulnerable to adversary attacks that provide incorrect queue length information to drain the system resources. Due to these reasons, in this chapter we are interested in the performance of a more robust class of schedulers: ones that provide flow isolation in the sense that when looked over long intervals the network can be decomposed into N separate Single-Input-Single-Output queues with independent service rate

processes that depend on the particular type of scheduler and N, Prominent examples of such schedulers are the TDM scheduler and Opportunistic scheduler, which will be the focus of this chapter.

A TDM scheduler is a resource allocation scheme where each user is guaranteed a fixed fraction of the time slots periodically. An Opportunistic scheduler [19, 20, 27, 28], on the other hand, exploits the channel gain fluctuations by serving the flow that has the best channel state. When there are several users in the network and the channel state for each of them fades independently of the others, it is likely that at least one of them has a good channel state, and the gain in throughput using this type of scheduling is called the *multi-user diversity gain*. Systems such as HDR over CDMA [29], and EDGE over GSM have been developed that take advantage of the channel fluctuations in the multi-user context. Even if the the wireless channel does not fluctuate fast enough, channel fluctuations can be artificially induced in order to improve the overall performance [20, 30]. However, large fluctuations result in large mean delay levels, hence the Quality of Service (QoS) constraints becomes more and more difficult to satisfy with increasing number of users.

There are two issues with opportunistic scheduling: *fairness* and *Quality-of-Service (QoS) degradation* caused by flows having to wait till their channel becomes sufficiently good for them to receive service. The fairness problem has been studied extensively in [19,20,27], where instead of serving the user with the best channel state, the instantaneous bit-rate is weighted by some factor to achieve to achieve *proportional fairness* or some other fairness criterion. However, the latency experienced by the flows might still be bad under a fair allocation, for the service given to a flow is subject to random fluctuations. Hence, there is a trade-off between the multi-user diversity gain exploited in opportunistic scheduling and the delay experienced by the flows. We study this tradeoff between throughput gain and QoS degradation in this chapter. Specifically, we compare the performance of fair opportunistic scheduling with the performance of TDM scheduling.

The main advantage of opportunistic scheduling is the gain in throughput that is achieved when the number of users increases. On the other hand, when the number of users is large, the amount of service given to a user is highly variable, which may cause a deterioration in the de-

lay experienced by the packets of the user. Thus, one might expect a tradeoff between throughput and QoS guarantees. We will show that this is indeed true and numerically characterize a threshold on the number of users, below which opportunistic scheduling is advantageous and above which TDM is preferable.

It is often argued that opportunistic scheduling increases the overall network throughput when the number of users increases. A key contribution of the chapter is to point out an analytical formulation that characterizes how the overall network throughput behaves for delay-constrained-traffic. In particular, we show that the supportable throughput increases initially and then decreases and goes to zero when the number of users becomes large. For reasonable channel parameters, our numerical computations show that when the number is as small as ten, the total supportable throughput of the network under a QoS constraint can become zero. The number of users that can be supported with some reasonable throughput level, such as 100 Kbps per user, will be even smaller than this. Thus, our chapter provides a methodology for evaluating the tradeoff between the long-term throughput increase due to opportunistic scheduling versus the short-term throughput guarantee that can be provided using TDM.

We assume that the delay constraint of each flow is in the form of a small tail probability of the steady state delay being larger than, say d slots. The arrival rate that can be supported under such a delay constraint will be called the *supportable* rate. The above delay constraint may arise either due to real-time applications or to ensure efficient operation of non-real-time applications that use TCP. The latter is due to the fact that TCP's throughput suffers if the RTT is large [31]. In both cases, the QoS constraint can be expressed as a constraint on the maximum delay experienced at the base station.

In this chapter, we evaluate the probability of QoS violation using large deviations theory [32] and perform numerical computations as well as simulations using typical values for the system parameters. We observe that the opportunistic scheduler takes advantage of the multi-user diversity for small enough N and supports much higher total throughput levels compared to the TDM scheduler. The optimum (in the sense of maximizing the total supportable throughput) number of users that can be supported as well as the threshold up to which opportunistic scheduler supersedes the TDM scheduler can be clearly identified in our results.

Simulation results, which turn out to be in exact agreement with the theoretical results, are presented afterwards.

In a related work [33, 34], QoS constrained scheduling is considered for the case where the channel conditions and arrival rates are i.i.d. among the users. The author concentrates on the MaxQueue rule for ON-OFF channels in detail. This rule gives service to the flow with the maximum backlog over all flows whose channel state is ON. The *effective capacity* of this rule is derived and compared with the greedy rule, which serves the user with the best channel in each slot. It is shown that there is a non-negligible difference between the effective capacity of the two rules as the QoS constraint (total queue length tail distribution) gets more strict. However, in our chapter we consider more realistic fading channels with delay constraints and study the characteristics of the supportable throughput of schedulers that provide flow isolation as function of the number of users.

The chapter is organized as follows: Section 3.2 introduces the system model and the large deviations result that will be used to evaluate the QoS provided to the users of the wireless network. In Section 3.3, opportunistic and TDM schedulers are described and analyzed for the case where the channel state processes for all the users are i.i.d. The effect of channel spectrum splitting is considered in Section 3.4. Section 3.5 generalizes the analysis of the opportunistic scheduler to the case where the channel state processes of the different users are independent, but not identical. Simulation results are presented in Section 3.6.

3.2 Assumptions and Channel Model

Consider a system that consists of N flows sharing a common time-varying medium. A typical example of such a system, depicted in Figure 3.1 is the *downlink* in cellular wireless communication. Let the time be slotted, with each *slot* being of size T_c sec. The bandwidth available for communication is W Hz. The number of arrivals to each flow is assumed to be a constant and equal to λ packets per time slot. The case with random arrivals can be analyzed using large deviations theory in a similar fashion to the constant arrival model. By studying the performance for large enough d, the stochastic nature of the arrivals can be approximated by the

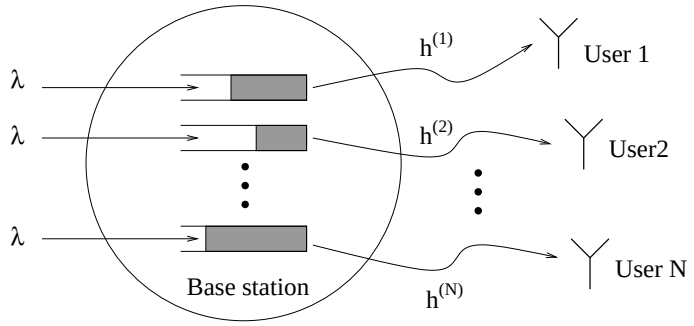

Figure 3.1 Downlink scenario in cellular communication with a single base station and N users.

mean behavior using the law of large numbers. Since such an analysis adds unnecessary technical details to the analysis without affecting the general behavior of the performance curves, we do not include them in our presentation. However, we provide simulations in Section 3.6 where we observe the effect of randomness in the arrivals for reasonable system parameters. It should also be noted that the assumption of symmetric arrivals to each queue is made for the purposes of presentation. All of the analysis holds for the case when each flow has a different arrival rate as well as a different delay constraint.

We define each *packet* to be of size $W \times T_c$ nats for convenience. We have introduced the notion of packet for notational convenience; however, the network is allowed to serve a fraction of a packet in a time slot. In fact, in HDR and other real wireless systems, the amount served in each time slot is quantized in a manner that is independent of the size of the arriving packets. As will become clear later, here we assume that each user who is chosen for service in a time slot is given an amount of service (in bits) equal to the information-theoretic capacity of the channel under the channel condition at that time instant. We simply measure this amount of service in units of packets which has been defined above.

Next, we focus on a single flow among N and describe the queueing-theoretic model that we will use to evaluate the QoS violation for that flow. Since we are considering the packets as being infinitely divisible, i.e., as a fluid, we define the delay experienced in a time slot t to be the maximum delay in terms of number of slots, experienced by any bit served in the time slot. Let D_t denote this delay in slot t. We assume that if a bit is served within the same slot that it entered the queue, it has experienced a delay of zero. Let $A(t)$ and $S(t)$ be the total number

of arrivals and departures in $[1, t]$, respectively. Obviously, due to the deterministic nature of arrivals, we have $A(t) = \lambda t$. Assuming empty queues initially, the event $D_t \geq d$, is equivalent to the event $S(t) - A(t-d) \leq 0$. Hence we can write the following

$$P(D_t \geq d) = P(S(t) - A(t-d) \leq 0) = P(S(t) - \lambda(k-d) \leq 0) = P(A(t) - S(t) \geq \lambda d).$$

But notice that $A(t) - S(t)$ is nothing but the length of a queue at time t, given that the queue was empty at the beginning of time slot 1. Let us denote this queue length at time t as $Q[t]$. Figure 3.2 depicts the defined parameters for a typical operation of the queue.

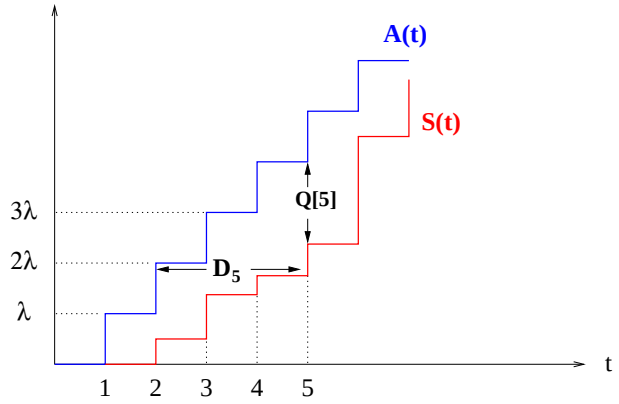

Figure 3.2 Typical arrival and service pattern along with parameters of interest.

If we define QoS violation to be the event that the delay exceeds some threshold d, then the steady-state probability of QoS violation can be described as

$$\lim_{t\to\infty} P(D_t \geq d) \quad = \quad \lim_{t\to\infty} P(Q[t] \geq \lambda d).$$

Recall that we denote the (random) amount of offered service at time slot k by $\mu[k]$. Therefore, the total offered service up to time t is given by $M(t) = \sum_{k=1}^{t} \mu[k]$. For ease of representation, let us define $X(t) = A(t) - M(t) = \sum_{k=1}^{t} x[k]$, where $x[k] = \lambda - \mu[k]$. Then we can utilize a well-known upper bound of large deviations which is also known to be asymptotically tight [32]:

$$P(Q[\infty] \geq \lambda d) \quad \leq \quad e^{-\lambda d \inf\limits_{y\geq 0} \left\{ \frac{\mathfrak{I}_x(y)}{y} \right\}}, \tag{3.1}$$

where $\mathfrak{I}_x(\theta) := \theta x - \Lambda_x(\theta)$ and $\Lambda_x(\theta)$ is defined as $\Lambda_x(\theta) = \lim_{t\to\infty} \frac{1}{t} \sum_{k=1}^{t} \ln E\left(e^{\theta x[k]}\right)$. Precise conditions on the process $\{x[k]\}$ for the above result to hold are given in [32].

Suppose that the QoS constraint is of the form $\lim_{t\to\infty} P(D_t \geq d) \leq 10^{-\zeta}$, for some fixed $\zeta > 0$. Then, from (3.1), the QoS constraint can also be expressed as

$$\lambda \inf_{y\geq 0} \left\{ \frac{\mathfrak{I}_x(y)}{y} \right\} \geq \delta, \tag{3.2}$$

where $\delta := \frac{\zeta}{d} \ln(10)$. The following fact is also established in [32].

Fact 3.1. *The condition (3.2) is equivalent to* $\Lambda_x\left(\frac{\delta}{\lambda}\right) \leq 0.$ ◇

Using Fact 3.1 and the fact that the arrival process is deterministic, (3.2) can be equivalently written as

$$\Lambda_\mu\left(-\frac{\delta}{\lambda}\right) \leq -\delta, \tag{3.3}$$

where $\Lambda_\mu(\theta) = \lim_{t\to\infty} \frac{1}{t} \sum_{k=1}^{t} \ln E\left(e^{\theta\mu[k]}\right)$. This inequality provides a relationship among the service rate distribution, the delay constraint of the flows and the supportable throughput level. Given the scheduler and the delay constraint parameters d and ζ, any λ that satisfies this inequality is supportable. Next, we use this model to analyze the opportunistic and TDM scheduling policies.

3.2.1 Channel Model

Throughout the chapter, we assume that the channel realization is available to both the base station and the users. This can be accomplished by maintaining a fast control channel between the two parties to communicate the measured channel characteristics at the time. Also, based on the channel realization, the transmitter is allowed to adjust its transmission rate accordingly. Due to significant performance improvements provided by channel state information (CSI) and rate adjustment based on channel quality, the proposed 3G technologies, such as HDR [29], suggest such features.

The baseband channel model we employ in this section can be represented as

$$y^{(i)}[t] = h^{(i)}[t]x[t] + \omega^{(i)}[t], \qquad i = 1, \cdots, n, \tag{3.4}$$

where $x[t] \in \mathcal{C}$ is the transmitted signal in slot t, $y^{(i)}[t] \in \mathcal{C}$ is the received signal by user i in slot t, $h^{(i)}[t] \in \mathcal{C}$ is the complex channel state between the transmitter and the i^{th} user, and $\omega^{(i)}[t] \in \mathcal{C}$ is a zero mean symmetric complex Gaussian random variable with two-sided power spectral density N_0. It is assumed that the channel gains are identically and independently distributed both across users and across time slots. These are reasonable assumptions provided that the length of each time slot, T_c, is chosen to be the coherence time of the system, and the users see sufficiently different channels. Moreover, it is assumed that the transmission power level is fixed at P for all time-slots. The sufficiency of a single channel realization in describing the received signal, implies that the channel is frequency non-selective. That is to say, the transmission bandwidth is smaller than the coherence bandwidth of the system.

We use $\mu^{(i)}[k]$ to denote the available service to user i in slot k, and assume that it is given by Shannon's formula

$$\mu^{(i)}[k] \;=\; WT_c \ln\left(1 + \frac{P}{WN_0}|h^{(i)}[k]|^2\right) \quad nats \;=\; \ln\left(1 + SNR \cdot |h^{(i)}[k]|^2\right) \quad packets,$$

where $SNR := \frac{P}{WN_0}$.

In the following sections, we will analyze the maximum supportable total throughput as a function of the number of flows, N, over non-selective fading channels for different scheduling policies under various fading distributions.

3.3 Scheduling in Time

In this section, we provide descriptions and analysis of two popular schedulers: Opportunistic and Time-Division-Multiplexing (TDM) schedulers. Furthermore, we perform numerical computations for typical channel parameters to understand the behavior and compare the performance of these schedulers. Here, we will assume that the channel distributions experienced by different flows are the same. We will remove this assumption in Section 3.5.

3.3.1 Analysis of Opportunistic Scheduling

Since the channel gains are i.i.d. and assuming that all flows have to be treated equally, fairness considerations such as proportional fairness do not enter into the picture and thus, we can use the following rule to describe the opportunistic scheduler we will consider.

OPPORTUNISTIC SCHEDULER: At each time slot, choose the flow that has the best channel gain for transmission. In other words, if $|h^{(i)}[k]|$ denotes the channel gain for flow $i \in \{1, \cdots, n\}$ in slot k, then only flow $i^*[k]$ is allowed transmit in slot k, where $i^* := \arg\max_i |h^{(i)}[k]|$. $\diamond$

The sum capacity of the system described by (3.4) is achieved by this opportunistic scheduler under the given conditions [27]. The following proposition describes the service distribution provided by this scheduler.

Proposition 3.1. *The service distribution of any given flow, say i, at slot k, operating under the Opportunistic Scheduling Policy is given by*

$$P(\mu^{(i)}[k] \leq r) \;=\; \frac{1}{n}(P(Z^{(i)}[k] \leq r))^n + 1 - \frac{1}{n} \qquad \forall r \geq 0,$$

where $Z^{(i)}[k] = \ln\left(1 + SNR \cdot |h^{(i)}[k]|^2\right)$.

Proof. The result trivially follows from the i.i.d assumption on the channel processes. $\square$

We can write the c.d.f. of $Z^{(i)}[k]$ easily as $F_{Z^{(i)}[k]}(r) = F_{|h^{(i)}[k]|^2}\left(\frac{e^r-1}{SNR}\right)$, which is only dependent on the fading channel distribution we are considering. For example, if we consider Rayleigh fading scenario, $|h^{(i)}[k]|^2$ is exponentially distributed with unit mean.

Now that we have an expression for the service distribution, the computation of $\Lambda_\mu(\cdot)$ is straight forward. Due to the difficulties in getting a closed-form expression, we will numerically solve (3.3) and obtain the total supportable throughput for the network as a function of the number of users under the opportunistic scheduling policy. These results will be demonstrated in Section 3.3.3.

3.3.2 Analysis of TDM Scheduling

In this section, we will study the following TDM scheduler, which is also a Round-Robin scheduler for our scenario.

TDM SCHEDULER: Each flow is periodically scheduled to transmit once every N slots, regardless of the channel gain realizations. ◇

One way of approach is to assume that the system started at time 1 and a flow assigned to that slot is uniformly and randomly chosen among the N flows. Once this choice is known the rest of the assignments are periodically done according to the TDM scheduler described above. Equivalently, given that we are interested in the moment generating function of flow j, it is equally possible that the first time slot to which flow j is assigned can be one of $1, 2, \cdots, n$.

We are interested in $\Lambda_{\mu^{(j)}}(\theta)$, which is defined as

$$\Lambda_{\mu^{(j)}}(\theta) = \lim_{t\to\infty} \frac{1}{t} \ln \left(\frac{1}{n} \sum_{i=1}^{n} E \left[\exp\left(\theta \sum_{k=1}^{t} \mu^{(j)}[k] \right) \mid \text{Serve flow j at time i} \right] \right)$$

where $\mu^{(j)}[k]$ denotes the amount of service offered to the flow j at time slot k. The log-moment generating function of $\{\mu^{(j)}[k]\}$ under the TDM scheduling policy is given by the following proposition.

Proposition 3.2. *For the TDM scheduler $\Lambda_{\mu^{(j)}}(\theta) = \frac{1}{n}\Lambda_Z(\theta)$, where $\Lambda_Z(\theta)$ is the log moment generating function of $Z^{(1)} := \ln\left(1 + SNR \cdot |h^{(1)}|^2\right)$.*

Proof. Due to the nature of the scheduler, given that flow j is first served at time i implies that only $\mu^{(j)}[i], \mu^{(j)}[i+N], \mu^{(j)}[i+2N], \cdots$ can take positive values, while the service at the rest of the time slots must be zero.

This observation enables us to write $\Lambda_{\mu^{(j)}}(\theta)$ as

$$\Lambda_{\mu^{(j)}}(\theta) = \lim_{t\to\infty} \frac{1}{t} \ln \left(\frac{1}{n} \sum_{i=1}^{n} \left(E\left[e^{\theta Z^{(1)}} \right] \right)^{\lfloor \frac{t-i}{n} \rfloor + 1} \right). \tag{3.5}$$

It is not difficult to see that the following upper and lower bounds can be applied to the floor function: for $i \in \{1, 2, \cdots, n\}, \quad t \geq 1$:

$$\frac{t}{n} - 2 \leq \lfloor \frac{t}{n} \rfloor - 1 \leq \lfloor \frac{t-i}{n} \rfloor \leq \lfloor \frac{t}{n} \rfloor \leq \frac{t}{n}.$$

If we use these bounds on (3.5), we get for each $j \in \{1, \cdots, n\}$:

$$\lim_{t\to\infty}\left(\frac{1}{n}-\frac{1}{t}\right)\Lambda_Z(\theta) \leq \quad \Lambda_{\mu^{(j)}}(\theta) \quad \leq \lim_{t\to\infty}\left(\frac{1}{n}+\frac{1}{t}\right)\Lambda_Z(\theta)$$

which gives the desired result. □

3.3.3 Numerical computations and Comparison

In this section, we numerically compare the performance of the two scheduling policies using reasonable values for the channel parameters (such as the SNR value, coherence time, delay constraint, etc.). We let $T_c = 1$ msec and $W = 1.25$ MHz, which are reasonable values for the coherence time and bandwidth. For many applications, typically the delay experienced by each flow should not be not more than 100 msec. Examples applications include TCP where excessive delays can cause frequent time-outs, transmission of streaming video where excessive jitter should be avoided while a small amount of jitter can be tolerated by an appropriately designed play-out buffer. Hence, in all the simulations in this chapter, we take $d = 100$ and the QoS constraint is always assumed to be as follows: we require that the probability that the delay exceeds d is constrained to be less than or equal to 10^{-5}[1].

Under Rayleigh fading scenario, Figure 3.3 depicts the total supportable throughput versus number of users curve for different levels of SNR. In the figure, the solid lines represent the opportunistic scheduler case, whereas the dashed lines are for the TDM scheduler. For each SNR level, we have drawn a dotted line whose slope indicates a threshold throughput per user such that for any rate above this threshold, the opportunistic scheduler can admit more users with that guaranteed rate per user compared to the TDM scheduler. For any rate below the threshold, the TDM scheduler performs better. We make the following observations:

- The total throughput is larger under opportunistic scheduling when the number of users is small. On the other hand, the TDM scheduler performs better when the number of users is large. This is due to the fact that, under opportunistic scheduling, the initial increase in the number of users improves the multi-user diversity gain more than it hurts the

[1]Modifying this threshold to a less stringent level will not change the curves significantly.

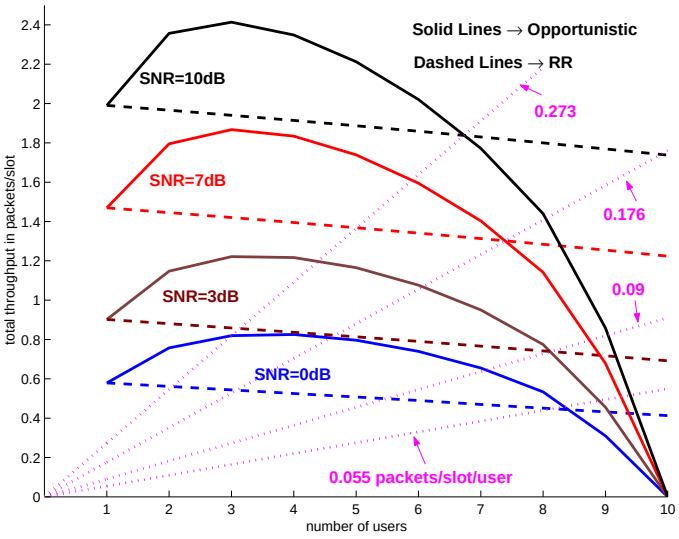

Figure 3.3 Total throughput as a function of the number of users N, for the two schedulers with various SNR levels.

delay constraint. However, as N get larger, the fluctuations in the offered service under opportunistic scheduling affect the performance much more severely and supportable throughput drops sharply. Such a phenomenon does not occur in the TDM scheduler because it does not exploit the multi-user diversity gain.

- Whether one should use opportunistic scheduling or not depends upon the throughput that the wireless service provider expects to provide to the users of the network. When the SNR is 0 dB, from Figure 3.3, when the required throughput per user is 0.055 packets-per-slot (which is approximately equal to 100 Kbps), the network is indifferent between using opportunistic scheduling or TDM scheduling. Thus, if the required throughput is smaller than this, then the network should use opportunistic scheduling if the number of users is below eight and it should use TDM when the number of users is larger. On the other hand, if the required throughput is larger than 0.055 packets per slot, then the network should use opportunistic scheduling and use admission control to restrict the number of users to be at a supportable level. Similar conclusions can be drawn for other SNR levels from the figure.

3.3.3.1 Ricean Fading

In this section, we study the performance of the schedulers under Ricean fading while varying the strength of the line-of-sight component. We let the channel gain of user i, which we recall is denoted by $|h^{(i)}[k]|^2$, be equal to a factor κ plus an exponential random variable with unit mean. Thus, κ indicates the relative strength of the line-of-sight component. The SNR level is taken to be zero dB in all cases. Increasing κ while keeping the mean of $|h|^2$ fixed at 1 results in decreasing variance of the distribution. The comparison of Rayleigh and Ricean fading channels in terms of total supportable rates (i.e., the sum of the supportable rates for all users in the network) under opportunistic as well as TDM schedulers is provided in Figure 3.4. In the figure, only the cases of $\kappa = 0$ and $\kappa = 5$ are plotted since the observations are similar

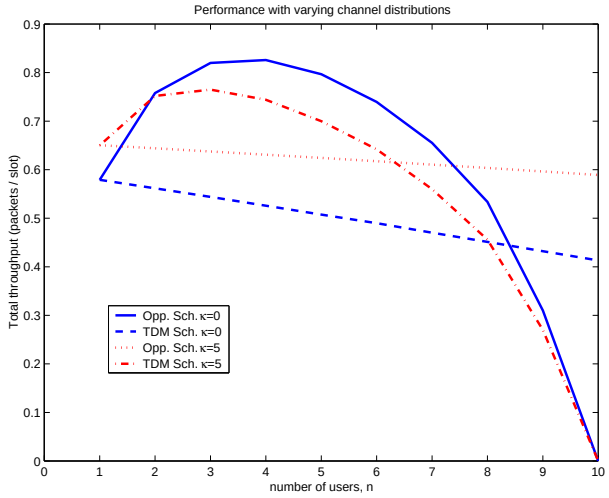

Figure 3.4 Performance of the schedulers under differing channel distributions.

for other values of κ. We can make several observations regarding Figure 3.4:

- As N gets larger, the multi-user diversity effect kicks in for the opportunistic scheduler and the improvement is higher for service distributions with larger variance. This is to be expected, because the main idea underlying the opportunistic scheduler is the ability to find a favorable channel condition over a large set of independent realizations.

- As the variance of the service distribution decreases, the rate of decrease (as a function of the number of users) in the TDM scheduler's total throughput decreases. Thus, a less-variable channel is more advantageous for TDM as is to be expected.

- As a result of the above remarks, as the κ factor increases, the advantage of the opportunistic scheduler over the TDM scheduler is further reduced. The threshold level for the number of users, above which the TDM scheduler exhibits better performance, decreases as κ increases. However, the general behavior of the opportunistic scheduler relative to the TDM scheduler remains the same.

The above discussion points out that if the channel has a strong line-of-sight component, then TDM will perform better and opportunistic scheduling will perform worse. However, the above discussion also indicates that the general shape of the performance curve (number of users versus total throughput) remains the same. Therefore, in the remainder of the chapter, we will carry out the numerical computations only for the Rayleigh fading scenario as a representative case.

3.4 Scheduling in Time and Frequency

In actual systems, more than one frequency band may exist, each of which is of size W Hz. We refer to each band of size W Hz as a *channel*. Then the question is how to distribute the services among the users over these channels.

Suppose there are M non-overlapping channels available for transmission. Furthermore, we assume that the channel gains for each user over different channels are identically and independently distributed as exponential random variables with unit mean. Then we can extend the formulation in (3.4) as

$$y_m^{(i)}[t] = h_m^{(i)}[t]x_m[t] + \omega_m^{(i)}[t], \qquad i = 1, \cdots, n, \quad m = 1, \cdots, M, \tag{3.6}$$

where the subscript m indicates that the corresponding parameter is associated with the m^{th} channel.

In this section, we will study modified versions of the opportunistic and the TDM scheduler of Section 3.3. Also, we will compare the results for opportunistic scheduling over a single band of MW Hz as opposed to M channels of size W Hz each. We will see the advantage of the latter approach.

3.4.1 Analysis of the Modified Opportunistic Scheduler

The user assignments to channels for a given slot is given by

MODIFIED OPPORTUNISTIC SCHEDULER: For a given time slot, and over a given channel, say m, serve the user that satisfies $\arg\max_j |h_m^{(j)}|$. $\diamond$

Then it is easy to see that the service offered to queue i in a given slot is given by $\mu^{(i)} = \sum_{m=1}^{M} \mu_m^{(i)}$, where $\mu_m^{(i)}$ denotes the service offered to queue i over channel m. Therefore, we have

$$\Lambda_{\mu^{(i)}}(\theta) := \ln E\left[e^{\theta\mu^{(i)}}\right] = \ln\left(E\left[e^{\theta\mu_m^{(i)}}\right]\right)^M = M\Lambda_{\mu_m^{(i)}}(\theta).$$

The distribution of $\mu_m^{(i)}$ is exactly in the same form as the distribution of $\mu^{(i)}$ of Section 3.3.1. Here, it should be noted that we assume that the SNR is the same over the different channels. Such an assumption is reasonable since the carrier would spend the same power per bandwidth.

Hence, we can utilize the derivation of Section 3.3.1 to compute $\Lambda_{\mu^{(i)}}(\theta)$. The numerical computation of the corresponding supportable rates will be provided in Section 3.4.3, along with comparisons with earlier schedulers as well as new schedulers.

3.4.2 Analysis of Modified TDM Scheduling

A natural modification of the TDM Scheduler studied in Section 3.3.2 is given below.

MODIFIED TDM SCHEDULER: Suppose the users are numbered from 1 to N, and the channels are numbered from 1 to M. Then, in time slot 1, the scheduler starts from user 1 and assigns the first available channel to it (then that channel is no longer available to other users in that time slot), and continues to assign users to channels sequentially until either all the N users are scheduled, or the available channels in the current slot is exhausted. In the former case, the scheduler wraps around and continues the same assignment procedure starting from user 1.

In the latter case, no other assignment is made and in the next time slot the same assignment procedure continues starting from the user that was blocked due to unavailability of channels in the current slot. $\diamond$

The following two examples will clarify the scheduling policy:

- Take $N = 5$ and $M = 3$. In time slot 1, user i is assigned to channel i, while in time slot 2, user 4 is assigned to channel 1, user 5 is assigned to channel 2 and user 1 is assigned to channel 3.

- Take $N = 3$ and $M = 5$. In this case, in the first time slot, channel 1 is allocated to user 1, channel 2 to user 2, channel 3 to user 3, channel 4 to user 1 again and channel 5 to user 2. In the next time slot, channel 1 is assigned to user 3, channel 2 to user 1 and so on.

A closer look into the operation of the above scheduler reveals the fact that, each user will be (roughly) periodically assigned to a channel once every $\frac{n}{M}$ slots. This is similar to the situation in Section 3.3.2 and similar calculations yield $\Lambda_{\mu^{(i)}}(\theta) = \frac{M}{n} \ln E(e^{\theta Z^{(1)}})$, where $Z^{(1)}$ was defined earlier.

3.4.3 Numerical Computations of the Modified Schedulers

Figure 3.5 depicts the cases $M = 2, 3$ for the Rayleigh fading scenario. We observe the following:

- The increase in M enhances the total throughput performance and allows more users into the system for a given rate.

- If the expected rate per user is larger than 0.09 packets/slot (which is approximately equal to 162 Kbps), then the opportunistic scheduler is better, whereas for any lower rate, the TDM scheduler performs better.

- The opportunistic scheduler can be better exploited for large M. Compared to the case when there was only a single channel available, when there are two or more channels, TDM scheduling outperforms opportunistic scheduling only for a much larger number of users.

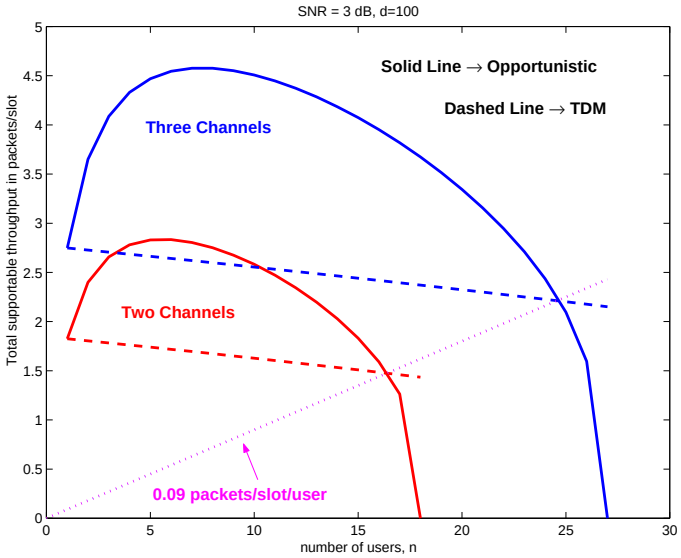

Figure 3.5 Performance of the modified schedulers with varying number of channels

In order to exhibit the advantage of implementing the opportunistic scheduler over multiple independently varying channels instead of a single frequency band of the same total size, we consider a frequency band of size W Hz and partition it into K *sub-bands* of equal size with $K \in \{1, 2, 3\}$. Here, we assume that the total power is split equally among the sub-bands. Then, we implement the modified scheduler for different values of K. Figure 3.6 depicts the results as well as the threshold on the expected throughput level per user, above which the opportunistic scheduler is more advantageous compared to TDM. Our first observation is that the threshold level decreases with increasing K. Also, we can clearly see that as K increases the opportunistic scheduler performs significantly better even for smaller levels of throughput per user, whereas the TDM scheduler changes only slightly. Hence, if possible, it is more advantageous in terms of total throughput to split the available frequency band into independently varying sub-bands and then use opportunistic scheduling.

3.5 Fair Scheduling

In the previous sections, we have assumed that mean signal-to-noise ratio is the same (equal to 1) for all users. However, this is not very realistic and in this section, we study the situation

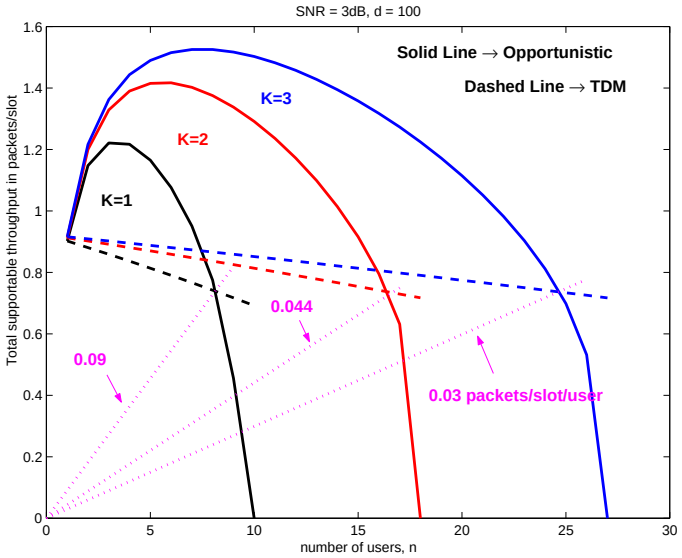

Figure 3.6 Performance of the modified schedulers with varying number of sub-bands

where the mean SNR could be different for different users. Here, we will only study the single channel case, while the extension to M channels can be carried in a straightforward manner along the same lines.

In a wireless medium, the channel conditions of different users need not be identically distributed, because different users may be at different distances from the base station. In order to provide some measure of fairness to compensate for different mean SNR levels, we add weighting factors to the scheduling decisions as in [19, 27].

FAIR OPPORTUNISTIC SCHEDULER: At each time slot, the service is given to the user that satisfies

$$\arg \max_{1 \leq j \leq n} \left\{ \beta^{(j)} \mu^{(j)} + \nu^{(j)} \right\},$$

where $\{\beta^{(j)}, \nu^{(j)}\}$ is a set of non-negative constants associated with different users. ◇

Here, it should be noted that proportional fairness [27] or other forms of fairness can be achieved using this model if these parameters are chosen appropriately [19]. The following proposition provides an expression for the probability that user i is chosen among the N users in a given slot. This expression will be used in the next proposition to compute the service distribution for user i.

Proposition 3.3. *For the opportunistic scheduler, in a given slot, the probability that user i is served is given by*

$$\alpha^{(i)} := \int_0^\infty f_{|h^{(i)}|^2}(x) \prod_{j=1, j\neq i}^{n} F_{|h^{(j)}|^2}(g_j^{(i)}(x))dx,$$

where $f_{|h^{(i)}|^2}(x)$ is the p.d.f. of $|h^{(j)}|^2$ and $g_j^{(i)}(x) := \frac{1}{SNR}\left[\exp\left(\frac{\beta^{(i)}\ln(1+xSNR)+\nu^{(i)}-\nu^{(j)}}{\beta^{(j)}} - 1\right)\right]$. For the special case of Rayleigh fading and when both $\beta^{(j)}$ and $\nu^{(j)}$ are equal for all j, the expression simplifies to

$$\alpha^{(i)} = 1 + \sum_{k=1}^{n-1}\left(\sum_{(\gamma^1,\cdots,\gamma^k)\in\Gamma(k)} \frac{(-1)^k m_i}{m_i + m_{\gamma^1} + \cdots + m_{\gamma^k}}\right),$$

where $\Gamma(k)$ contains all $k-$tuples of the set $\{1,\cdots,n\}\backslash\{i\}$, and $m_j = \frac{1}{E\left[|h^{(j)}[k]|^2\right]}$.

Proof. The proof follows from a conditioning argument as follows.

$$\begin{aligned} P\left(i \text{ is chosen}\right) &= P\left(\beta^{(i)}\mu^{(i)} + \nu^{(i)} = \max_{1\leq j\leq n} \beta^{(j)}\mu^{(j)} + \nu^{(j)}\right) \\ &= \int_0^\infty f_{|h(i)|^2}(x) \prod_{j=1, j\neq i}^{n} P\left(|h^{(j)}|^2 \leq g_j^{(i)}(x)\right) dx, \end{aligned}$$

which, under Rayleigh fading, equals

$$\int_0^\infty m_i e^{-m_i x} \prod_{j=1, j\neq i}^{n} \left(1 - e^{-m_j g_j^{(i)}(x)}\right) dx,$$

and for the special case of all $\{\beta^{(j)}\}$ and $\{\nu^{(j)}\}$ equal, we have $g_j^{(i)}(x) = x,\ \forall i, j$. Computing the previous equation gives the desired result. □

Proposition 3.4. *For the opportunistic scheduling, the probability density function of the service process for user i, denoted as $f_{\mu^{(i)}}(r)$, is given by*

$$f_{\mu^{(i)}}(r) = \mathfrak{I}_{\{r\geq 0\}}\left[\frac{e^r}{SNR} f_{|h^{(i)}|^2}\left(\frac{e^r-1}{SNR}\right) \prod_{j=1, j\neq i}^{n} F_{|h^{(j)}|^2}\left(g_j^{(i)}\left(\frac{e^r-1}{SNR}\right)\right) + (1-\alpha^{(i)})\delta(r)\right],$$

where $\alpha^{(i)}$ and $g_j^{(i)}(x)$ are defined in Proposition 3.3, $\mathfrak{I}_A$ is the indicator function for event A, and $\delta(r)$ is the Kronecker delta function.

Proof. Consider the cumulative distribution function of $\mu^{(i)}$:

$$\begin{aligned} P(\mu^{(i)} \leq r) &= P\left(i \text{ is chosen}\right) P(\mu^{(i)} \leq r \mid i \text{ is chosen}) \\ &\quad + \underbrace{P\left(i \text{ is not chosen}\right)}_{=1-\alpha^{(i)}} \underbrace{P(\mu^{(i)} \leq r \mid i \text{ is not chosen})}_{=1 \quad \forall r \geq 0}. \end{aligned}$$

But we also observe that

$$\begin{aligned} P\left(i \text{ is chosen}\right) P(\mu^{(i)} \leq r \mid i \text{ is chosen}) &= P(|h^{(i)}|^2 \leq \frac{e^r - 1}{SNR} \text{ and } h^{(j)} \leq h^{(i)} \; \forall j \neq i) \\ &= \int_0^{\frac{e^r-1}{SNR}} f_{|h^{(i)}|^2}(x) \prod_{j=1, j\neq i}^{n} F_{|h^{(j)}|^2}(g_j^{(i)}(x)) dx. \end{aligned}$$

Substituting this expression into the CDF of $\mu^{(i)}$ and taking the derivative with respect to r yields the result. □

3.5.1 Numerical computations of the Fair Scheduler

Suppose there are two classes of users, one having an exponentially distributed $|h_1|^2$ with mean 1, and the other having an independently and exponentially distributed $|h_2|^2$ with mean 2. We let N_i denote the number of users in the i^{th} class, $i \in \{1, 2\}$. We take $\frac{P}{WN_0}$ to be 3 dB. In the numerical computations we consider the case when the additive constants $\nu^{(j)}$ are zero. We assume that the delay constraint for all users is equal to $d^{(i)} = 100$, the rest of the parameters are unmodified. We assume that the arrival rates to the users within the same class are equal, but they may be different for different classes. We use λ_i to denote the arrival rate to a single user in class $i \in \{1, 2\}$.

To demonstrate the effect of the fair scheduler, we consider the following scenario. We assume that the base station aims to guarantee a rate of 100 Kbps per user for each of the users, regardless of whether it is in class 1 or class 2. Then, we ask which pairs of (n_1, n_2) are supportable with different choices of $\{\beta^{(1)}, \beta^{(2)}\}$ parameters.

Initially, we consider the scheduler that takes $\beta^{(1)} = \beta^{(2)} = 1$, i.e. that does not attempt to reduce the unfairness experienced by class 1 users. Recall that such a policy aims to maximize the total throughput. Figure 3.7 depicts the region of supportable users at the guaranteed rate of 100 Kbps per user. We observe the following:

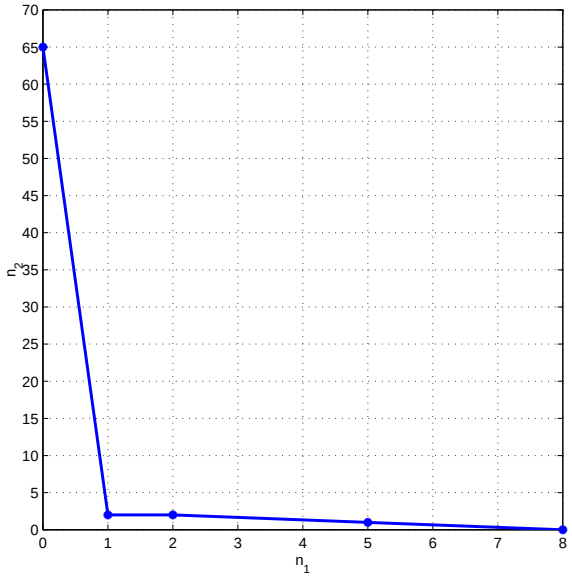

Figure 3.7 Supportable region of users at rate 100 Kpbs/user, when $\beta^{(1)} = \beta^{(2)} = 1$. All points below the curve are supportable.

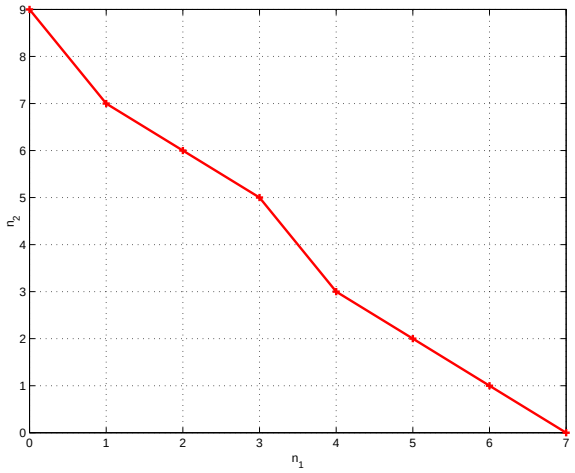

Figure 3.8 Supportable region of users at rate 100 Kpbs/user, when $\beta^{(1)}/\beta^{(2)} = 3/2$. All points below the curve are supportable.

- The existence of only a few class 2 users in the system drops the number of supportable class 1 users significantly. We observe that even with allowing a single class 2 user to share the system, the number of class 1 users must drop to 5 from 8. Two class 2 users will further drop this number to 2, and eventually the existence of three class 2 users does not allow even a single class 1 user in the system. These effects are because class 2 users will capture the system resources due to their more favorable channel conditions.

- We can also observe that with fair scheduling the bad channel conditions of class 1 users limit the scheduler from successfully exploiting the class 2 users' good conditions. Without the existence of any class 1 users, 65 class 2 users can be supported at 100 Kbps/user. However, the inclusion of even a single class 1 user drops this number drastically to 2. Therefore, the class with the bad channel conditions becomes a bottleneck.

In order to compensate for the bad channel conditions of users of class 1, we use a fair allocation as in [20, 27]. In [20, 27], the decision on which user to serve in a given slot is both a function of the channel conditions and the amount of service that each user has received. In steady state, this corresponds to an appropriate choice of the set $\{\beta^{(j)}\}$. To illustrate this

effect, we apply the fair opportunistic scheduler to the scenario we studied above by setting $\beta^{(1)}/\beta^{(2)} = 3/2$. With this modification, we assign priorities to class 1 users and make the allocation more fair. Again, we plot the pairs (n_1, n_2) that are supportable at a guaranteed rate of 100 Kbps per user in Figure 3.8. We observe that both classes of users are now supported much more fairly. Moreover, except for the case when $N_1 = 0$, the region in Figure 3.7 is strictly dominated by the region in Figure 3.8. This is due to the fact that the new set of weighting factors improves the performance of the class 1 users.

3.6 Simulations

In this section, we compare the numerical results obtained in the previous sections using large deviations with simulation results. Figures 3.9 and 3.10, respectively, compare the numerical results of Figures 3.3 and 3.6 with simulation results. It can be seen from the figures that the simulation results are almost identical with the numerical results. Hence, our formulation captures the actual system dynamics quite accurately even for reasonable parameter values.

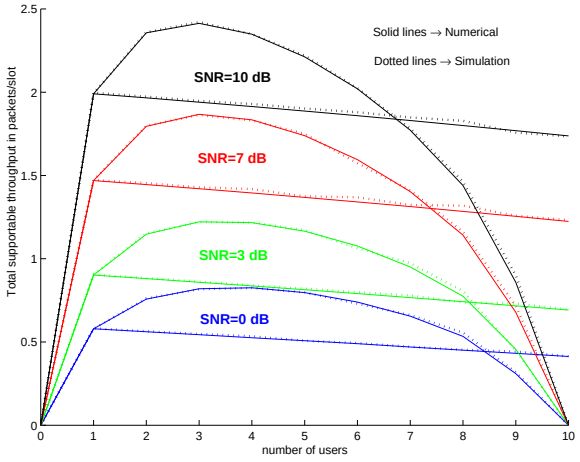

Figure 3.9 Simulations versus numerical computations for single channel system with different SNR levels. The simulation interval was taken to be 100 million slots

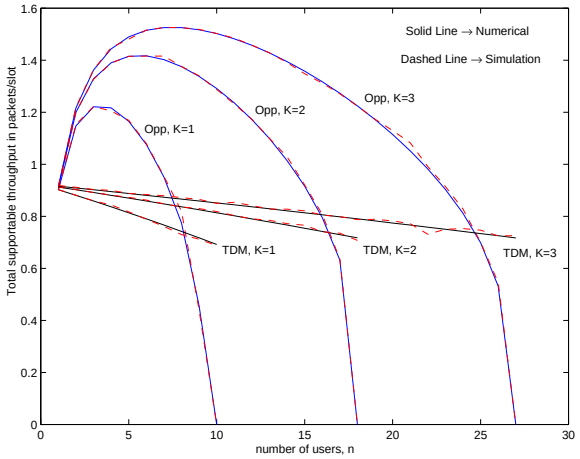

Figure 3.10 Simulations versus numerical computations for all cases. The simulation interval was taken to be 300 million slots

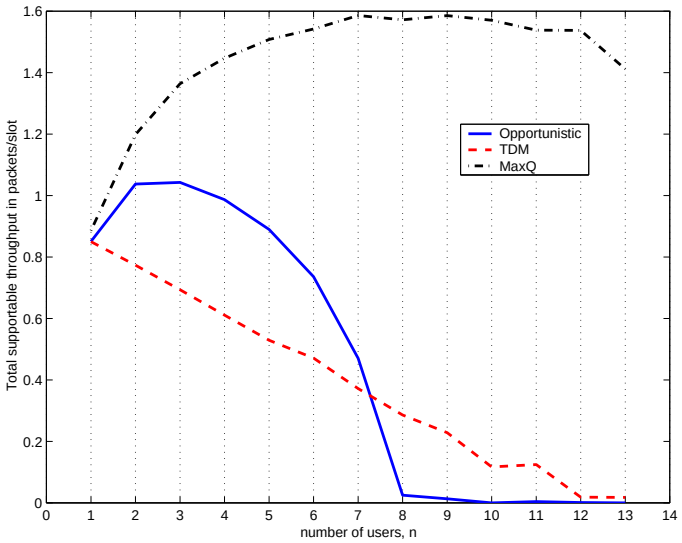

Figure 3.11 The performance of various schedulers with Poisson arrival distribution.

In Figure 3.11, we simulate various schedulers in the random arrival scenario, where the arrivals to each of the queues are Poisson distributed with mean λ at each time slot. We observe that the behavior of the opportunistic and TDM schedulers are not modified, while the supportable rate levels are dropped due to the stochastic nature of the arrivals. For comparison purposes, we also plot the performance of a queue length based scheduler, which we refer to as MAXQ. At time slot k, this scheduler chooses the flow ,i^*, for which $\mu^{(i)}[k]x^{(i)}[k]$ is maximized, where $x^{(i)}[k]$ denotes the length of queue i at the beginning of slot k. Such a scheduler is shown to be throughput optimal in earlier works [8, 35]. The performance of the scheduler in the case when each flow has the same mean arrival rate is denoted in Figure 3.11. As expected, the MaxQ scheduler outperforms all of the schedulers considered since it exploits both the channel state information and the queue length information. However, as we argued earlier, this scheduler may be unfair to users with low rates in an asymmetric scenario. To demonstrate this effect, we simulated the case when the arrivals to queue 1 is Poisson distributed with a fixed mean rate of $0.3\ packets/slot$. The remaining $N-1$ users generate data at mean rate λ. Here, the first flow represents non-real time data, that has no delay constraints. In Figure 3.13, we plot the total mean rate of the delay constrained traffic that is supportable by the MaxQ scheduler with the same delay constraints (i.e. 100 msecs). We observe that the asymmetry

causes a considerable decrease in the total supportable throughput level. In other words, the first flow gains advantage due to its aggressive nature and deteriorates the performance of the remaining flows. Nevertheless, the MaxQ scheduler still provides significant improvement to the opportunistic scheduler, which may be more fair to all the flows. As a compromise between the two, we further simulate a token based scheduler depicted in Figure 3.12.

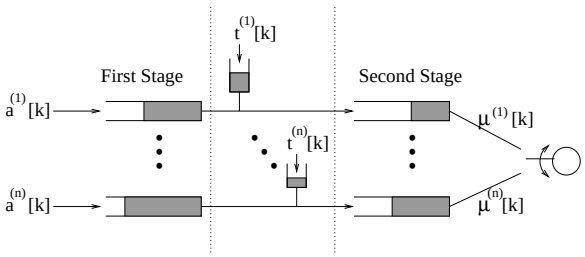

Figure 3.12 Structure of the PF+MaxQ Scheduler.

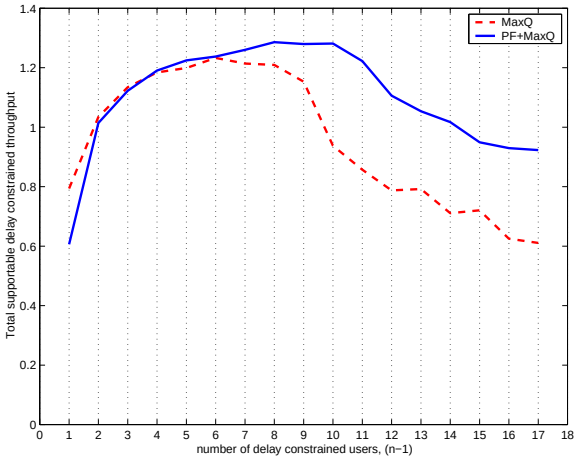

Figure 3.13 Comparison of MaxQ and PF+MaxQ schedulers.

This scheduler, which we refer to as PF+MAXQ, implements a combination of flow isolation and queue-based scheduling. A first stage queue is maintained for each flow, and the packets are moved to the second stage queue depending on the availability of tokens. In time slot k, the amount of token generated for each flow is given by $\frac{1}{n}\max_{1\leq i\leq n}\mu^{(i)}[k]$. Therefore, a proportionally fair allocation of the available service rates is maintained through this screening process among all the flows sharing the system. Then, the actual queues that will be served is determined according to the MaxQ rule by using the *second stage* buffer occupancy levels. The delay experienced by each packet is the amount of time spent between the time it first enters the first stage queue and the time it is served. The performance of this scheduler for the asymmetric scenario described above is plotted in Figure 3.13. We observe that MaxQ+PF scheduler provides higher supportable throughputs compared to MaxQ when N gets large. This is because the token based screening maintains a fairness among the flows, which improves the delay characteristics of low rate flows.

CHAPTER 4

JOINT CONGESTION CONTROL AND SCHEDULING FOR FAIR RESOURCE ALLOCATION IN CELLULAR NETWORKS

4.1 Background and Motivation

The wireless channel is a shared medium over which many users compete for resources. Since there are many users, it is important to allocate this shared resource in a fair manner among the users. Further, since the available spectrum is limited, it is also important to efficiently use the channel. However, the time-varying nature of the wireless environment, coupled with different channel conditions for different users, poses significant challenges to accomplishing these goals. Moreover, the lack of availability of channel and arrival statistics further complicates the solution.

In this section, we restrict our attention to the downlink in cellular networks where there is a base station that allocates resources to many competing users. We assume that the packets destined for the different receivers are stored in separate queues. The scheduler at the base station is responsible for allocating resources to the different queues as a function of the current channel conditions as well as the queue lengths. Prior work on this problem can be largely classified into two main categories:

- *Throughput-optimal scheduling*: Here it is assumed that the mean arrival rates of the packets into each queue lie within the capacity region (the set of sustainable arrival rates) of the channel. However, neither the actual arrival rates nor the channel capacity region is assumed to be known. The scheduler is allowed to know the current queue lengths and the current channel conditions. It was then shown in [6] that allocating resources to maximize a queue-length-weighted sum of the rates (which are feasible in the current time slot) is a stabilizing policy. This result was then generalized in many different directions in Chapter 2 and in other works [8–11, 16, 36, 37].

- *Fair Scheduling:* An obvious drawback of throughput-optimal policies is that no traffic policing is enforced. For instance, if one or more sources misbehave and increase their arrival rates so that the set of arrival rates lies outside the capacity region, then the system becomes unstable. In other words, all flows will be penalized due to the behavior of a few misbehaving flows. Thus, an alternative is to provide some degree of flow isolation at least in the long term, by allocating resources in a fair manner to the various queues. A commonly-used framework for such allocation is the concept of proportional fairness [38]. It was shown in [27] that proportional fairness can be achieved in TDMA cellular networks by scheduling the user which has the largest ratio of the achievable data rate at the current instant to the average rate that it has been allocated so far. The properties of such a policy have been studied empirically in [39] and analytically in [40, 41], and a multiple antenna implementation of such an algorithm over slowly time-varying channels has been proposed in [20]. Related work on channel-state-aware scheduling in wireless networks can also be found in [19, 28, 42–44].

From an applications point of view, throughput-optimal scheduling as described above is more suitable for inelastic traffic where the sources do not adapt their transmission rate based on congestion in the network. In this case, admission control is required to ensure that the arrival rates lie within the capacity region of the network and further, in the case of wireless networks, due to the time-varying nature of the network, an appropriate scheduling algorithm is required to ensure that the network can stably serve the admitted traffic. On the other hand,

fair scheduling is more suited for elastic traffic sources which can adjust their traffic rates in response to feedback from the network regarding the network conditions. Without such a rate-control mechanism, fair scheduling would either lead to under utilization (when a traffic source is not generating enough data to make use of the bandwidth allocated to it) or packet losses or large delays (when a traffic source is generating data at a much larger rate than the rate allocated to it by the base station).

In this chapter, we are interested in allocating resources to elastic sources whose utilities are described by concave functions. Specifically, user i derives a utility $U_i(x_i)$ when it transmits at rate x_i. For ease of exposition, we consider utility functions of the form

$$U_i(x_i) = \beta_i \frac{x_i^{(1-m)}}{(1-m)}, \qquad i = 1, \cdots, N,$$

where m is a positive constant and β_i is some fixed weight, which can be different for different users. Thus, we consider $m-$weighted proportionally fair resource allocation. Notice that as $m \to 1$, this allocation converges to the weighted proportionally fair allocation and as $m \to \infty$, it gives the weighted max-min fair allocation. We assume that congestion information is conveyed to the sources by putting the corresponding congestion price in the ACK packets. Each source react to its congestion price by choosing its transmission rates such that its marginal utility ($U_i'(x_i)$) is equal to the congestion price. We take the queue length at the base station to be the congestion price. In the Internet context, this is a special case of the dual algorithm proposed in [2, 45, 46]. In wireline networks, this interpretation of queue length (or delay) as the congestion price naturally arises from an convex optimization perspective where the resource constraints are linear [3]. However, in wireless networks, this interpretation is not immediately obvious since the resource constraints are not necessarily linear. Despite this, we show that the dual algorithm at the sources, along with queue-length-based scheduling at the base station, can be used to approximate weighted proportional fairness arbitrarily closely, where the approximation depends on the choice of a certain parameter used in the congestion control algorithm. Instead of the dual algorithm other algorithms such as the primal algorithm [1, 4] and the primal-dual algorithm [47, 48] can also be used. For a comprehensive description of the many algorithms that can be used to solve the resource allocation problem, see [3]. In this

chapter, we restrict ourselves to the dual algorithm. The problem studied in this chapter has also been considered in [49]. The results in [49] are independent and contemporaneous to our work. However, the solution proposed in [49] is quite different. The solution in [49] uses a greedy source rate update rule while we use a static update rule as we will see later. We also note that [50] is a recent work that provides an alternate analysis of a similar problem to ours. There, the authors use a new Lyapunov drift argument to measure the proximity of the achieved performance of their algorithm to the optimal performance.

The chapter is organized as follows. Section 4.2 introduces the scheduler and congestion controller that will analyzed in the rest of the chapter. In Section 4.3, we first analyze a heuristic continuous-time, deterministic fluid model of the system and then use the intuition thus obtained to study the original stochastic system model. Generalizations and implementation considerations are discussed in Section 4.4. Various simulation results are presented in Section 4.5.

4.2 Description of the Cross-layer Mechanism

We consider a cellular network shared by N flows in the downlink as in Chapter 2. The system model for the base station and the channel state process is the same as before. Figure 4.1 depicts the combination of the congestion controller and the base station from the perspective of a single flow. In this chapter, we change our notation of the number of arriving packets from $a_i[t]$ to $x_i[t]$ to indicate the fact that we no longer assume the traffic to be inelastic. We assume that $\mu_i[t]$ and $x_i[t]$ can only take non-negative integer values. Then, the evolution of the size of the i^{th} queue is given by

$$q_i[t+1] = (q_i[t] + x_i[t] - \mu_i[t])^+, \qquad i = 1, \cdots, N.$$

The channel state process is assumed to be independent and identically distributed in each time slot (although it is straightforward to generalize our results to allow Markovian channel state processes), but we do not require that the statistics be known at the base station. We recall the definition of the *mean achievable rate region* as $\bar{\mathcal{C}} = \{\eta : \eta = \sum_{j=1}^{J} \pi_j^{ch} \eta^{(j)}, \eta^{(j)} \in \mathcal{C}_j\}$,

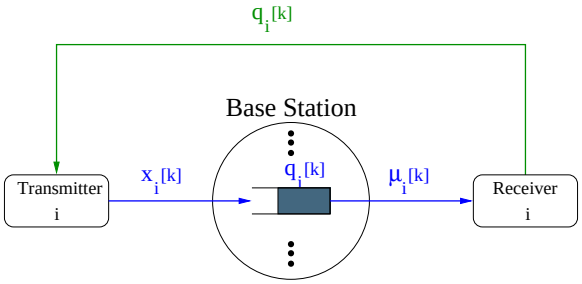

Figure 4.1 A pictorial depiction of the system.

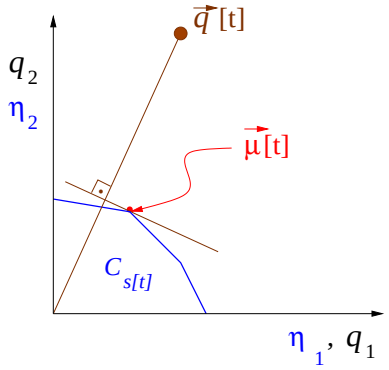

Figure 4.2 Given $\mathbf{q}[t]$ and $s[t]$, the vector $\mu[t]$ is chosen on the boundary of the current achievable rate region as in this figure.

where π_j^{ch} stands for the stationary probability of the channel state process being in state j. The scheduler implemented at the base station is described as follows.

QUEUE-LENGTH-BASED SCHEDULER: In time slot t, given the current queue length vector, $\mathbf{q}[t] := (q_1[t], \cdots, q_N[t])'$, and the current channel state, $s[t]$, the scheduler chooses a service rate vector $\mu[t] := (\mu_1[t], \cdots, \mu_N[t])' \in \mathcal{C}_{s[t]}$ that satisfies

$$\mu[t] \in \arg\max_{\eta \in \mathcal{C}_{s[t]}} \sum_{i=1}^{n} q_i[t]\eta_i. \tag{4.1}$$

A geometric interpretation of the above policy for two users is given in Figure 4.2, where the queue-length state space and the achievable service rate region are superimposed on each other. We observe that the allocated service rates always lies on the boundary of the current achievable rate region, and that if the rate vector $\mu[t]$ satisfies (4.1) for some $\mathbf{q}[t]$, then it satisfies the same condition for all $\xi\mathbf{q}[t]$, for all $\xi > 0$. As mentioned earlier, this policy is known to be throughput-optimal for inelastic flows.

The packet arrival rate into the queue is assumed to be congestion controlled according to the dual controller [2, 45]. We note that the dual controller is derived for the Internet applications where all users sharing a common resource can receive the same treatment from the router. However, here the situation is fundamentally different due the fact that the channel conditions for the different users can be different. One of the contributions of this chapter is show that, somewhat surprisingly, the dual controller still leads to fair resource allocation provided

that the base station uses the scheduler described above. Such a scheduling mechanism is not necessary in the Internet, but is crucial in the wireless network context studied here. We now describe the congestion controller.

CONGESTION CONTROLLER: For the i^{th} flow, given its current buffer occupancy $q_i[t]$, the data generation rate in slot t, equal to $x_i[t]$ in our notation, is a random variable satisfying the following:

$$E[x_i[t] \mid q_i[t]] = \min\left\{\frac{\alpha_i K}{(q_i[t])^m}, M\right\} \qquad (4.2)$$
$$E[x_i^2[t] \mid q_i[t]] \leq A < \infty, \qquad \forall q_i[t]$$

where $m, \{\alpha_i\}, A$ and $M > 2\hat{\eta}$ are positive constants. We also assume $x_i[t]$ is independent across time slots for each i. (Again, it is straightforward to generalize this assumption to allow dependence in the arrivals across time slots.) $\diamond$

We have allowed $x_i[t]$ to be a random variable to allow for various sources of randomness in the actual implementation (e.g., window-based implementations of congestion control) that are not precisely modeled here. Further, we have used $M > 2\hat{\eta}$ to ensure that the arrival rate is bounded when $q_i[t]$ is close to zero. We note the well-known basic characteristics of a congestion controller from the above mechanism: the higher the congestion level, which is indicated by an increased level of buffer occupancy, the lower the data generation rate.

Notice that we have introduced a constant K in the congestion control algorithm. This corresponds to assuming that the utility function of user i is $K\alpha_i \frac{x_i^{(1-m)}}{1-m}$. Since K is the same for all users, this will not affect the relative resource allocation among the users. However, this constant plays a crucial role in determining how well we approximate weighted m-fair resource allocation in a wireless network. Indeed, we will show that weighted m-fair allocation is closely approximated for large K.

4.3 Characterizing the System Performance

In this section, we will analyze the system described in the previous section. To accomplish this, we will start with a heuristic continuous-time fluid model and understand its behavior.

Later, we will use these observations in the analysis of the original model and show that the original model behaves like the fluid model for large K.

4.3.1 Continuous-time Fluid Model

In the fluid-model, we assume that the channel state process is not random, but constant at its mean level. In other words, the achievable rate region is fixed at $\bar{\mathcal{C}}$. Also, the arrival rate is no longer a random variable, but is taken to be equal to its mean, i.e., $x_i(t) = \min\left\{\frac{\alpha_i K}{(q_i(t))^m}, M\right\}$. Here, (t), instead of $[t]$, is used to signify that time is a continuous variable. Then, the evolution of the i^{th} queue-length is described by

$$\dot{q}_i(t) = \left(\min\left\{\frac{\alpha_i K}{(q_i(t))^m}, M\right\} - \bar{\mu}_i(t)\right)^+_{q_i(t)}, \tag{4.3}$$

where $\bar{\mu}(t) \in \arg\max_{\eta\in\bar{\mathcal{C}}} \sum_{i=1}^{N} q_i(t)\eta_i$ and $(y)^+_z$ is equal to y when $z > 0$ and is equal to $\max(y, 0)$ when $z \leq 0$. In this formulation, the queue-length state space is assumed to be continuous. We now identify the set of service rates and queue lengths such that if the these queue lengths are chosen as the initial state and at each time instant, resources are allocated to achieve these service rates, then the queue lengths will remain at the initial conditions forever.

Definition 4.1 (Invariant pair). *The pair* $(\mathbf{q}^\star, \mathbf{x}^\star)$ *forms an* invariant pair *(more precisely,* $\mathbf{x}^\star$ *is an* invariant service rate vector *and* $\mathbf{q}^\star$ *is an* invariant queue-length vector*) if they satisfy both of the following conditions:*

$$(D_1)\ \mathbf{x}^\star \in \arg\max_{\eta\in\bar{\mathcal{C}}} \sum_{i=1}^{N} q_i^\star \eta_i, \qquad (D_2)\ q_i^\star = \left(\frac{\alpha_i K}{x_i^\star}\right)^{1/m} \qquad \forall i \in \{1, \cdots, n\}. \diamond$$

Notice that, if at any time t' we have $\mathbf{q}(t') = \mathbf{q}^\star$ and $\mu(t') = \mathbf{x}^\star$, then, due to (D_1) and (D_2), $\dot{q}(t)$ given by (4.3) will be zero for all $t \geq t'$. We now show that the invariant pair exists and is unique.

Proposition 4.1. *[Existence and Uniqueness of* $(\mathbf{q}^\star, \mathbf{x}^\star)$*] An invariant pair of rates and queue lengths exists and is unique.*

Proof. Note that the conditions on $x^\star$ given by (D_1) and (D_2) can be concisely written as

$$\sum_{i=1}^{N}(x_i^\star - \eta_i)\left(\frac{\alpha_i K}{x_i^\star}\right)^{1/m} \geq 0 \qquad \forall \eta \in \bar{\mathcal{C}}.$$

This is simply the condition for $x^\star$ to be an optimal solution to the following problem of maximizing a concave function over a convex set [22]:

$$\max_{\mu \in \bar{\mathcal{C}}} \sum_{i=1}^{N} \frac{(K\alpha_i)^{\frac{1}{m}}}{\left(1-\frac{1}{m}\right)} \mu_i^{1-\frac{1}{m}}.$$

Since $\bar{\mathcal{C}}$ is a bounded set, clearly a solution exists to the above optimization problem. Further, since the objective is strictly concave the solution is unique. □

The above proof shows that the invariant point is simply the set of rates and queue lengths achieved under fair resource allocation, which is our goal. Next, we are interested in showing that the queue lengths described by the invariant point is attractive, i.e., all trajectories eventually converge to it.

Proposition 4.2. *Starting from any initial queue-length vector,* $\mathbf{q}(0)$*, the queue-length vector* $\mathbf{q}(t)$ *eventually reaches* $\mathbf{q}^\star$ *as* $t \to \infty$.

Proof. Consider the Lyapunov function $W(\mathbf{q}) = \frac{1}{2}\sum_{i=1}^{N}(q_i - q_i^\star)^2$. Next, we study the time derivative of this Lyapunov function at time t.

$$\begin{aligned}
\dot{W}(\mathbf{q}(t)) &= \sum_{i=1}^{N}(q_i(t) - q_i^\star)\dot{q}_i(t) \\
&= \sum_{i=1}^{N}(q_i(t) - q_i^\star)\left(\min\left\{\frac{\alpha_i K}{(q_i(t))^m}, M\right\} - \bar{\mu}_i(t) + u_i(t)\right),
\end{aligned}$$

where $u_i(t)$ is a non-negative quantity which denotes the wasted service given to queue i at time t. Note that $u_i(t) = 0$ whenever $q_i(t) > 0$. Thus, it is easy to see that

$$\begin{aligned}
\dot{W}(\mathbf{q}(t)) &\leq \sum_{i=1}^{N}(q_i(t) - q_i^\star)\left(\min\left\{\frac{\alpha_i K}{(q_i(t))^m}, M\right\} - \bar{\mu}_i(t)\right) \\
&= \sum_{i=1}^{N}(q_i(t) - q_i^\star)\left(\min\left\{\frac{\alpha_i K}{(q_i(t))^m}, M\right\} - x_i^\star\right) \qquad (4.4) \\
&\quad + \sum_{i=1}^{N}(q_i(t) - q_i^\star)(x_i^\star - \bar{\mu}_i(t)), \qquad (4.5)
\end{aligned}$$

where the last step follows from adding and subtracting $x_i^\star$ to each term in the summation. Consider (4.4): if $q_i(t) > q_i^\star$, then $\min\left\{\frac{\alpha_i K}{(q_i(t))^m}, M\right\} - x_i^\star < 0$; and if $q_i(t) < q_i^\star$, then $\min\left\{\frac{\alpha_i K}{(q_i(t))^m}, M\right\} - x_i^\star > 0$. Therefore, unless $\mathbf{q}_i^\star = \mathbf{q}_i(t)$, the expression (4.4) is negative and when $\mathbf{q}_i^\star = \mathbf{q}_i(t)$, the expression (4.4) is zero.

Next we consider (4.5). We show that this expression is negative unless $\mathbf{q}^\star = \mathbf{q}(t)$. First we note the following two inequalities which follow from the definition of the invariant point and our scheduling policy, which is the solution to the optimization problem (4.1).

$$\sum_{i=1}^{N} q_i^\star x_i^\star \;\geq\; \sum_{i=1}^{N} q_i^\star \bar{\mu}_i(t) \tag{4.6}$$

$$\sum_{i=1}^{N} q_i(t) \bar{\mu}_i(t) \;\geq\; \sum_{i=1}^{N} q_i(t) x_i^\star \tag{4.7}$$

Adding both sides of the inequalities (4.6) and (4.7), and re-arranging the terms yields

$$\sum_{i=1}^{N} (q_i(t) - q_i^\star)(x_i^\star - \bar{\mu}_i(t)) \;\leq\; 0.$$

Combining this result with our earlier observation regarding (4.4) leads to

$$\dot{W}(\mathbf{q}(t)) < 0, \quad \text{if } \mathbf{q}(t) \neq \mathbf{q}^\star, \text{ and}$$
$$\dot{W}(\mathbf{q}(t)) = 0, \quad \text{if } \mathbf{q}(t) = \mathbf{q}^\star.$$

The result follows from Lyapunov's global stability theorem [51]. □

4.3.2 Original System Model

In this section, we return to our original system model, where the arrivals and departures are integer-valued and random. We observe that the queue-length state vector $\mathbf{q}[t]$ evolves according to a discrete-time, discrete-space Markov chain. We first show that this Markov chain is stable, i.e., positive recurrent. The fact that the Markov chain is stable is not surprising since by our choice of congestion control, we have ensured that the mean arrival rate into a queue reduces when the queue length is large. However, the Lyapunov function used to establish stability can be used to obtain a useful upper bound on the Euclidean distance between the invariant queue-length vector $\mathbf{q}^\star$ and $\mathbf{q}[t]$ for large K and large t. This upper bound is then used to establish the properties of our joint congestion control-scheduling algorithm.

Lemma 4.1. *For the Lyapunov function* $W(\mathbf{q}) = \sum_{i=1}^{N} \frac{(q_i - q_i^\star)^2}{2}$, *there exist positive constants* δ, ζ *and* c *such that*

$$\begin{aligned} E[\Delta W_t(\mathbf{q})] &:= E[W(\mathbf{q}[t+1]) - W(\mathbf{q}[t]) \mid \mathbf{q}[t] = \mathbf{q}] \\ &\leq -\frac{\delta}{(K)^{\frac{1}{2m}}} \|\mathbf{q} - \mathbf{q}^\star\| \mathcal{I}_{\mathbf{q} \in \mathcal{D}^c} + \zeta \mathcal{I}_{\mathbf{q} \in \mathcal{D}}, \end{aligned} \tag{4.8}$$

where $\mathcal{D} := \{\mathbf{y} \,:\, \|\mathbf{y} - \mathbf{q}^\star\| < c(K)^{\frac{1}{2m}}\}$ *and* $\mathcal{D}^c$ *is the complement of* $\mathcal{D}$ *in* $(\Re^+)^N$.

Proof. The proof is provided in the appendix. □

Theorem 4.1 (Positive Recurrence). *The Markov chain* $\mathbf{q}[t]$ *is positive recurrent.*

Proof. It is easy to see that the Markov chain has a countable state space and is irreducible and aperiodic.

We showed in Lemma 4.1 that there is a Lyapunov function that has negative conditional mean drift for all queue-length vectors that have sufficiently large magnitude. Now the result follows from Foster-Lyapunov criterion [52, Proposition 5.3]. □

Inequality (4.8) is stronger than what is necessary to prove the stability of the Markov chain. However, it is useful in establishing the following theorem which characterizes the mean distance between $\mathbf{q}[t]$ for large t and the invariant queue-length vector $\mathbf{q}^\star$.

Theorem 4.2 (Mean Distance Bound). *There exists a positive constant* $\bar{c}$, *that depends on the mean achievable rate region, the algorithm parameters* $\{\alpha_i, \gamma_i\}$, *and the moments of the channel and arrival processes, such that*

$$E\left[\|\mathbf{q}^\infty - \mathbf{q}^\star\|\right] \leq \bar{c}(K)^{\frac{1}{2m}}, \qquad \text{for large } K \tag{4.9}$$

where $\mathbf{q}^\infty$ *is a notation used to denote the state of the Markov chain in steady-state and* $\|\cdot\|$ *denotes the Euclidean distance in the* $\Re^N$.

Proof. We use (4.8) and the idea behind the proof of Pakes' lemma [53, 54] to prove the theorem. We consider the following $T-$step mean drift. For any $\mathbf{y} \geq \mathbf{0}$,

E[W(**q**[T])—**q**[0]=**y**]-W(**y**)

$$
\begin{aligned}
&= \sum_{t=0}^{T-1} E[W(\mathbf{q}[t+1]) - W(\mathbf{q}[t])|\mathbf{q}[0] = \mathbf{y}] \\
&= \sum_{t=0}^{T-1} \sum_{\mathbf{q}\in\mathcal{Z}_+^N} P\left(\mathbf{q}[t] = \mathbf{q}|\mathbf{q}[0] = \mathbf{y}\right) E[W(\mathbf{q}[t+1]) - W(\mathbf{q}[t])|\mathbf{q}[t] = \mathbf{q}] \qquad (4.10) \\
&\leq \zeta \sum_{\mathbf{q}\in\mathcal{D}} \sum_{t=0}^{T-1} P\left(\mathbf{q}[t] = \mathbf{q}|\mathbf{q}[0] = \mathbf{y}\right) - \sum_{\mathbf{q}\in\mathcal{D}^c} \frac{\delta\|\mathbf{q} - \mathbf{q}^\star\|}{(K)^{\frac{1}{2m}}} \sum_{t=0}^{T-1} P\left(\mathbf{q}[t] = \mathbf{q}|\mathbf{q}[0] = \mathbf{y}\right), \qquad (4.11)
\end{aligned}
$$

where $\mathcal{Z}_+^N$ denotes the set of all non-negative n dimensional integer valued vectors. In the above derivation, (4.10) follows from the fact that $\mathbf{q}[t]$ is a Markov chain, and we have used (4.8) to get the inequality in (4.11). We note that for any $\mathbf{q} \in \mathcal{Z}_+^N$,

$$\lim_{T\to\infty} \frac{1}{T} \sum_{t=0}^{T-1} P\left(\mathbf{q}[t-1] = \mathbf{q}|\mathbf{q}[0] = \mathbf{y}\right) = \pi_{\mathbf{q}}^{\infty},$$

for all $\mathbf{y}$, where $\vec{\pi}^{\infty}$ denotes the stationary distribution of the Markov chain $\mathbf{q}[t]$. Next, we move $W(\mathbf{y})$ to the other side of the inequality in (4.11), divide both sides by T, and let T go to infinity. This operation yields

$$0 \leq \zeta \sum_{\mathbf{q}\in\mathcal{D}} \pi_{\mathbf{q}}^{\infty} - \frac{\delta}{(K)^{\frac{1}{2m}}} \sum_{\mathbf{q}\in\mathcal{D}^c} \|\mathbf{q} - \mathbf{q}^\star\| \pi_{\mathbf{q}}^{\infty}.$$

Re-arranging the terms and with minor manipulations, this inequality can be written as

$$\frac{\delta}{(K)^{\frac{1}{2m}}} \sum_{\mathbf{q}\in\mathcal{Z}_+^N} \|\mathbf{q} - \mathbf{q}^\star\| \pi_{\mathbf{q}}^{\infty} \leq \sum_{\mathbf{q}\in\mathcal{D}} \left(\zeta + \frac{\delta}{(K)^{\frac{1}{2m}}} \|\mathbf{q} - \mathbf{q}^\star\|\right) \pi_{\mathbf{q}}^{\infty} \leq (\zeta + \delta c) \sum_{\mathbf{q}\in\mathcal{D}} \pi_{\mathbf{q}}^{\infty} \leq (\zeta + \delta c),$$

where the second inequality follows from the definition of $\mathcal{D}$. Here, the left-hand-side is nothing but $\frac{\delta E[\|\mathbf{q}^\infty - \mathbf{q}^\star\|]}{(K)^{\frac{1}{2m}}}$. So we multiply both sides with $\frac{(K)^{\frac{1}{2m}}}{\delta}$ to get

$$E[\|\mathbf{q}^\infty - \mathbf{q}^\star\|] \leq \left(c + \frac{\zeta}{\delta}\right) (K)^{\frac{1}{2m}},$$

which completes the proof for $\bar{c} := \left(c + \frac{\zeta}{\delta}\right)$. □

Notice that Theorem 4.2 implies, due the Markov's inequality, that $\forall \epsilon > 0$

$$P\left(\frac{1}{(K)^{\frac{1}{m}}} |q_i^\infty - q_i^\star| > \epsilon\right) \leq \frac{\bar{c}}{\epsilon (K)^{\frac{1}{m} - \frac{1}{2m}}}.$$

Therefore, the right-hand-side can be made arbitrarily small by choosing K sufficiently large. On the other hand, observe that $\frac{q_i^\star}{(K)^{\frac{1}{m}}} = \left(\frac{\alpha_i}{x_i^\star}\right)^{\frac{1}{m}}$. Hence, in the above probabilistic sense, $\frac{q_i^\infty}{(K)^{\frac{1}{m}}}$ is approximately equal to $\left(\frac{\alpha_i}{x_i^\star}\right)^{\frac{1}{m}}$. We also know from Theorem 4.1, that $\mathbf{q}[t] \to \mathbf{q}^\infty$ as $t \to \infty$. Combining these arguments, we can expect a typical sample path of $q[t]$ to converge to a region around the vector $(\left(\frac{\alpha_1}{x_1^\star}\right)^{\frac{1}{m}}, \cdots, \left(\frac{\alpha_N}{x_N^\star}\right)^{\frac{1}{m}})$ when K is large. In Section 4.5, we will present simulation results which will reinforce this observation.

Next, we address the implications of the above analysis on the delay and fairness characteristics of the system. It was observed in the above analysis that, for sufficiently large values of K, the queue-length vector will evolve towards the invariant point $\mathbf{q}^\star$ and stay relatively close to it in a probabilistic sense. Therefore, we can make the following approximation: $\mathbf{q}[t] \approx \mathbf{q}^\star$, when t becomes large. Consequently, the local scheduler described by (4.1) will make its decision at time t, roughly as

$$\mu[t] \in \arg\max_{\eta \in \mathcal{C}_{s[t]}} \sum_{i=1}^{N} q_i^\star \eta_i.$$

Thus, from the proof of Proposition 4.1, our proposed combination of the local scheduler with the end-to-end congestion controller guarantees stability and *weighted m-fair resource allocation* among the flows. In Section 4.5, we will present simulation results to support the above arguments.

Recalling Theorem 4.2 and the discussion following it, we can expect the mean of $\mathbf{q}^\infty$ to be very close to $\mathbf{q}^\star$. In fact, using a Lyapunov function of the form $L(\mathbf{q}) = \frac{1}{2}\sum_{i=1}^{N} q_i^2$, and using arguments very similar to the ones used in the proof of Theorem 4.2, we can prove that for large enough K, $E[\mathbf{q}^\infty] = \Theta(\mathbf{q}^\star)$.[1] Therefore, Little's Law suggests that the delays experienced by flow i is

$$E[\text{Delay}_i] \;=\; \frac{1}{x_i^\star}\Theta(q_i^\star) \approx \frac{\alpha_i}{(x_i^\star)^2}\Theta((K)^{1/m}),$$

where the last step is true for large K. Since we need large K to ensure a close approximation to weighted proportional fairness, this also implies large delays in the queues. This can

[1] $f(u) = \Theta(g(u))$ implies that for large enough u, there exist positive constants, $c_1 \leq c_2$, such that $c_1 g(u) \leq f(u) \leq c_2 g(u)$.

be alleviated by a virtual queue implementation of the scheduling mechanism which will be discussed in the next section.

4.4 Generalizations and Implementation Considerations

4.4.1 Reducing Delays Using Virtual Queues

As we have discussed earlier, one penalty for achieving user-defined fairness (as opposed to network-dictated fairness) is the possibility of large delays at the base station buffers. We can alleviate this problem by implementing the base station scheduler using virtual queues [55–57]. For each flow, the base station maintains a counter called the virtual queue. As an example, consider flow i. The virtual queue of flow i keeps track of a virtual queue length, where the virtual queue length of flow i is simply the length of a queue whose arrivals are the same as that of flow i, but whose service rate is always a fixed fraction $\rho < 1$ of the actual service rate. Therefore, the size of the virtual queue (denoted by $\tilde{q}_i$ for flow i) will always be larger than the actual queue-length q_i. The congestion feedback given to user i is $\tilde{q}_i[t]$ and therefore, user i will reduce its arrival rate well before its real queue builds up significantly. See Figure 4.3 for the model from flow i's perspective.

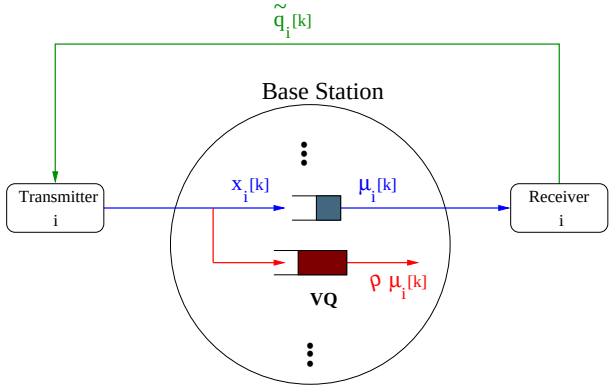

Figure 4.3 The virtual queue implementation at the base station.

By choosing the ρ parameter appropriately the delay levels and the packet loss probabilities can be adjusted: the lower the ρ, the lower the actual queue lengths. However, there is a possible loss in throughput by choosing $\rho < 1$. In Section 4.5, we will provide simulation

results which show that, by choosing ρ close to $1,$ but not equal to $1,$ we can reduce the queue lengths dramatically while maintaining close to 100% throughput.

4.4.2 End-to-End versus Last-Hop Congestion Control

The advantage of end-user-implemented congestion control is that it allows each user to choose a congestion control algorithm based on its utility function. Thus, instead of the base station imposing a particular notion of fairness, the resource allocation truly reflects the needs (as defined by the user utility functions) of the users. Further, resource allocation based on a base station-defined notion of fairness could result in under-utilization of the resources or large backlogs if the allocated data rate is not matched to the users' transmission rates.

An argument against congestion control at the end-user is that it does not provide for isolation among the flows. In other words, if a user misbehaves by transmitting at a much larger rate than is dictated by its congestion control algorithm, then there is no policing at the base station to prevent other users from experiencing poor quality-of-service. A base-station-defined fair resource allocation solves this problem by allocating resources to the users independent of the user's behavior. Here, we discuss a last-hop congestion control strategy, in place of the end-user congestion control algorithm, which can provide the same type of flow isolation albeit with the same drawbacks as described in the previous paragraph.

LOCAL IMPLEMENTATION STRATEGY: The base station imitates the effect of the end-to-end congestion controller by maintaining a two-stage queueing system. The queue at the first stage for each user is used to store packets arriving from the user. The contents of this first-stage are drained into another queue at a rate specified by the congestion control algorithm. The second-stage queues are the one used to implement the queue-length-based controller. Figure 4.4 depicts this model from flow i's perspective. $\diamond$

In the original implementation of proportional fairness given in [20, 27], the base station must decide on a time window over which the average rate allocated to each user is computed. This parameter is now replaced by the choice of the parameter K in our algorithm. It is inter-

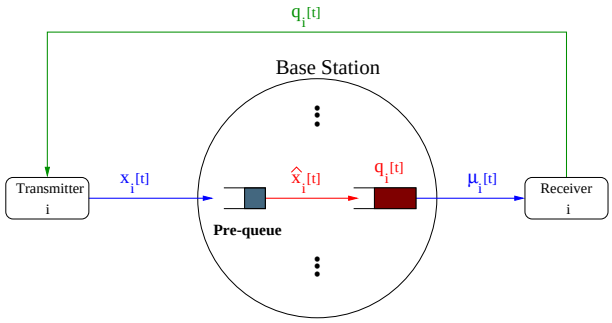

Figure 4.4 With the use of a pre-queue, the number of packets arriving at the second stage queue, denoted in the figure by $\hat{x}_i[t]$, can be chosen as a function of $q_i[t]$, thus mimicking the behavior of the congestion controller.

esting to note that both parameters directly impact the ability of the respective algorithms to precisely mimic weighted proportional fairness.

4.5 Simulation Results

In this section, we provide simulation results to complement the analysis in the previous sections. We present results for a ten-user scenario, and make the reasonable assumption that the channels between the base station and each of the users fade independently. The base station is only allowed to serve a single queue in a given slot. For this scenario, the scheduling algorithm (4.1) is equivalent to serving the user that solves $i^*[t] = \underset{i\in\{1,\cdots,10\}}{\arg\max}\, \eta_i q_i[t]$, at the rate $\eta_{i^*}[t]$. Ties are broken randomly. We let the rate vectors, $(\eta_1[t], \cdots, \eta_{10}[t])$, be Poisson distributed with mean $0.4 + (0.1)k$ for the k^{th} user. Also, the number of arrivals in each slot to each queue is Poisson distributed with the mean determined by the congestion controller. In the simulations, we set $\alpha_i = 1$ for all i and investigated the behavior of the queue lengths as a function of K for different m values.

We start with the case of $m = 2$. Figure 4.5 plots the average queue length levels experienced by each flow, as a function of K. We observe that the queue lengths are proportional to $\sqrt{K}$ in accordance with our analysis. In Figure 4.6, the variances of the queue lengths are depicted and it can be seen that they are also of the form $\sqrt{K}$. Therefore, the queue lengths are

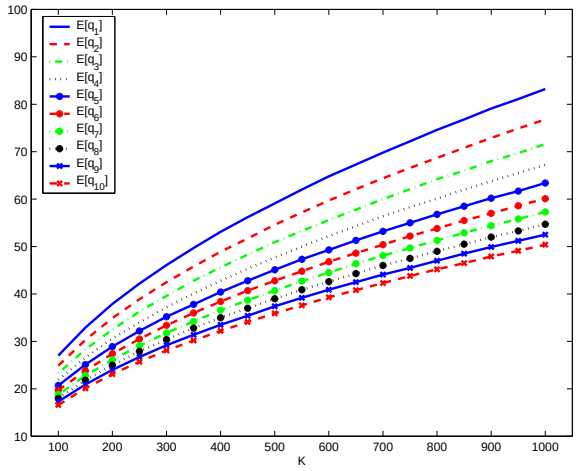

Figure 4.5 Empirical change in the mean of users' queue-lengths with K, when $m = 2$.

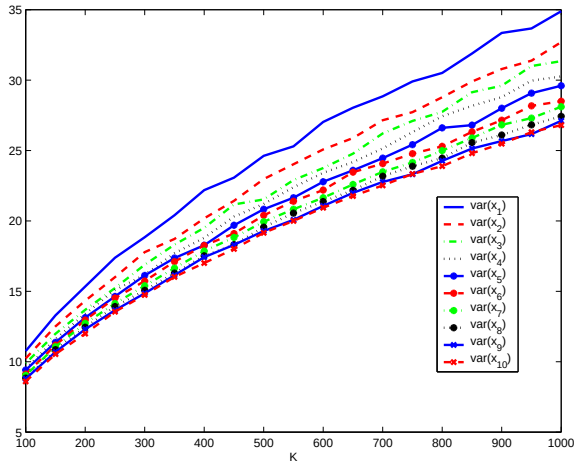

Figure 4.6 Empirical variance of the queue lengths with increasing K, when $m = 2$.

more and more clustered around the mean level as K increases. This observation agrees with our theoretical arguments in Section 4.3.

The average service rates provided to the flows is plotted in Figure 4.7 with differing K, when $m = 2$. Clearly, K does not have a significant impact on these levels. It is of interest to determine whether these rates are allocated in a fair manner. We will study this aspect later on in this section.

Next, we take $m = 1$. In this case, our analysis predicts that the mean queue length levels change linearly with K. Figure 4.8 verifies this expectation and Figure 4.9 plots the mean service rate levels as a function of K. Again, we observe that the average service rates appear to be the same for different K.

Finally, we consider the case when $m = 0.5$. Figure 4.10 plots the mean queue length levels of the queues as a function of K. Figure 4.11 depicts the change in the mean service rates with K. We observe once again that the mean service rates are not significantly affected by the K parameter. On the other hand, the average queue length levels increase as K^2, in agreement with our theoretical analysis.

Next, we compare the above implementation of a queue-length-based base station scheduler and an end-to-end congestion controller with the $m-$weighted proportionally-fair scheduler, similarly designed with the scheduler suggested by [27]. This scheduler is described next.

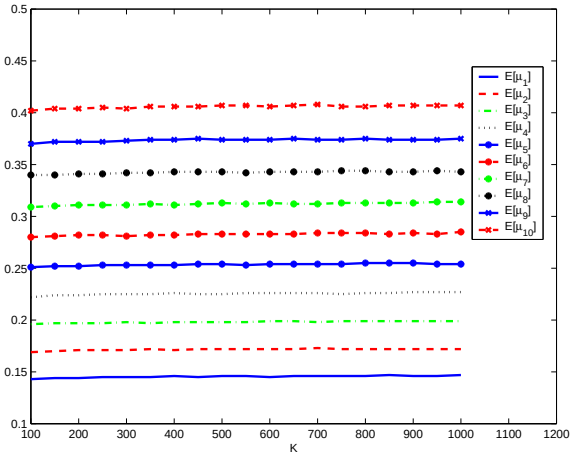

Figure 4.7 Empirical average of the service rates provided to the flows for various K with $m = 2$.

$m-$WEIGHTED PROPORTIONALLY FAIR SCHEDULER [27]: The scheduler keeps track of the average service rates provided to each of the flows in the last t_c slots. We denote this parameter by $T_i[t]$ for the i^{th} flow in slot t. Then, given the achievable service rates $\{\eta_i[t]\}$, the scheduler serves the queue, $i^*[t]$, that satisfies

$$i^*[t] = \arg\max_{i=1,2} \frac{\eta_i[t]}{(T_i[t])^{\frac{1}{m}}},$$

where $T_i[t]$ is updated using an exponential weighted low-pass filter as follows:

$$T_i[t+1] = \begin{cases} \left(1 - \frac{1}{t_c}\right) T_i[t] + \frac{\eta_i[t]}{t_c} & i = i^*[t] \\ \left(1 - \frac{1}{t_c}\right) T_i[t] & i \neq i^*[t] \end{cases}$$

$\diamond$

In our simulations, we let t_c to be 100. Notice that $T_i[t]$ serves as an empirical average service rate provided to flow i until time t. Hence, this scheduler gives priority to those flows that haven't received enough service in the history.

Table 1 shows the empirical average obtained by this proportionally fair scheduler along with our results for differing m parameters. We observe that the empirical mean service rate allocated to the users under the m-weighted proportionally fair algorithm in [27] and our scheduler are in fact nearly identical as is to be expected.

Finally, we simulate the virtual queue implementation described in Section 4.4 for the case when $m = 1$ and $K = 100$. We demonstrate the effect of ρ on the mean queue-length levels

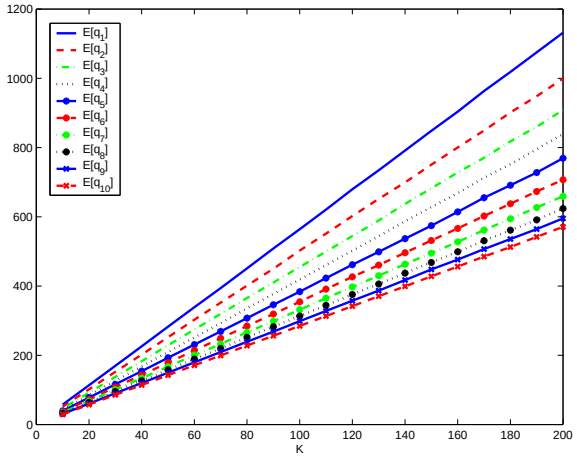

Figure 4.8 Empirical change in the mean of users' queue-lengths with K, when $m = 1$.

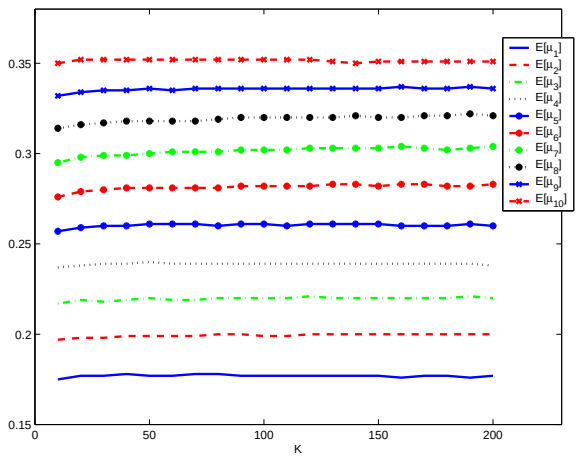

Figure 4.9 Mean service rates with increasing K, when $m = 1$.

	Ours ($m = 2$)	PF ($m = 2$)	Ours ($m = 1$)	PF ($m = 1$)	Ours ($m = 1/2$)	PF ($m = 1/2$)
User 1	0.147	0.147	0.177	0.177	0.206	0.202
User 2	0.172	0.173	0.200	0.198	0.217	0.217
User 3	0.199	0.199	0.220	0.218	0.238	0.231
User 4	0.227	0.228	0.238	0.239	0.249	0.244
User 5	0.254	0.258	0.260	0.259	0.259	0.256
User 6	0.285	0.288	0.283	0.279	0.273	0.267
User 7	0.314	0.316	0.304	0.297	0.291	0.277
User 8	0.343	0.345	0.321	0.316	0.295	0.287
User 9	0.375	0.373	0.336	0.333	0.303	0.296
User 10	0.407	0.403	0.351	0.351	0.308	0.306

Table 4.1 Comparison of our results to those of the m-weighted proportionally fair scheduler.

of queues 1 and 10 in Figure 4.12. Here, we plot the users that experience the largest and smallest mean queue lengths in order to avoid confusion. The rest of the queues exhibit similar behaviors.

It can be seen from this simulation that modifying ρ has a dramatic impact on the mean queue-length levels as we had argued. Of course, the choice of virtual queue parameter ρ will also have an effect on the mean service rates as shown in Figure 4.13. For example, if ρ is chosen to be 0.99 (which leads to a dramatic decrease in the queue lengths as seen from Figure 4.12), the mean service rate for users do not decrease significantly. Thus, we see that

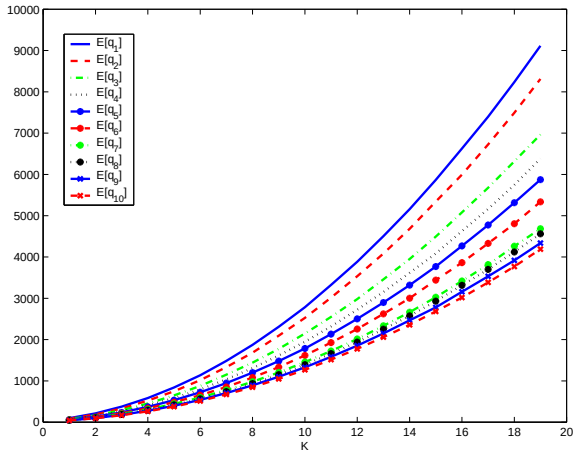

Figure 4.10 Empirical change in the mean of users' queue-lengths with K, when $m = 0.5$.

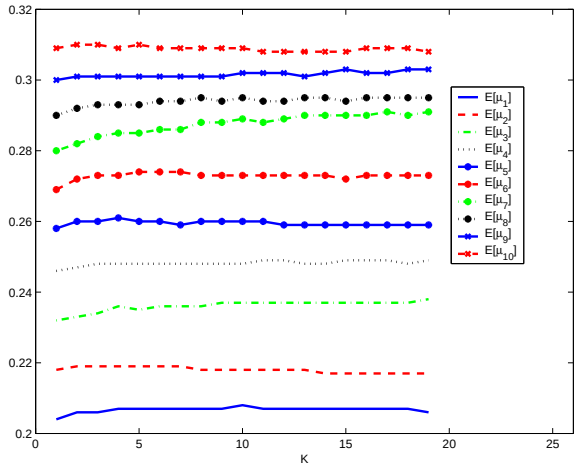

Figure 4.11 Mean service rates with increasing K, when $m = 0.5$.

by sacrificing throughput minimally one can dramatically reduce the queue lengths which is consistent with the observation for the Internet [55–57].

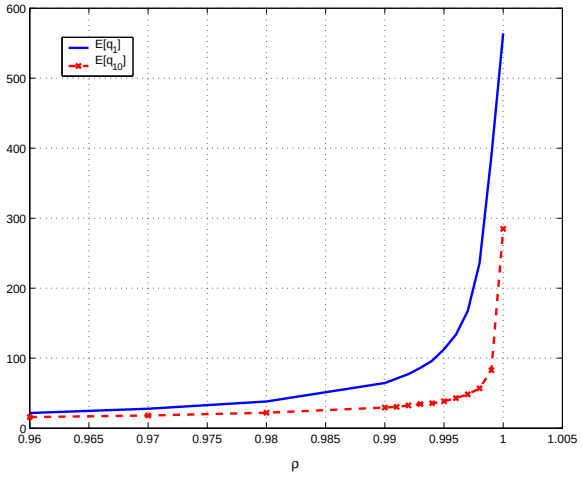

Figure 4.12 Empirical change in the mean of users' queue-lengths with ρ, when $m = 1, K = 100$.

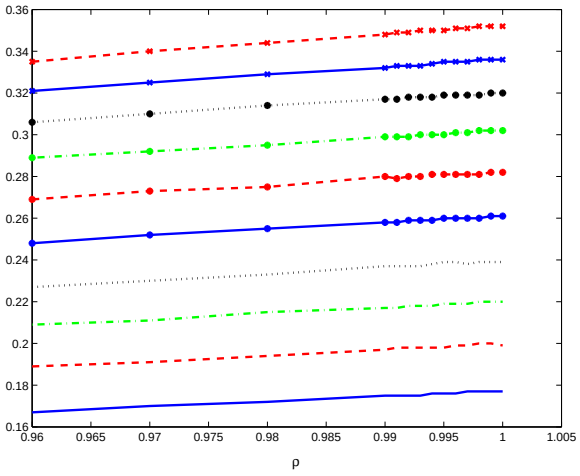

Figure 4.13 Mean service rates with increasing ρ, when $m = 1, K = 100$.

CHAPTER 5

RESOURCE ALLOCATION IN MULTI-HOP WIRELESS NETWORKS

In the previous chapters, we have concentrated on the case of single-hop wireless networks. In this chapter, we will generalize the analysis of the previous chapter to cover the case of multi-hop wireless networks, where each flow traverses multiple intermediate nodes to reach its destination. Even though the core analysis technique will be the same as in the single-hop case, there are nevertheless important differences in the approach and the results. In particular, the queue-length-based scheduler is different than the set of schedulers we studied. Also, we develop an interesting relationship between the queue length of the nodes and the *Lagrange multipliers* of the optimization problem being considered. In [58], the authors provide a similar relationship, but using a different technique. Also, in our analysis, we include the effect of unused service and the stochastic nature of the traffic generation that is not modeled in [58].

The chapter is organized as follows. In Section 5.1, we introduce the network and traffic models. Section 5.2 contains the optimization problem that we aim to solve along with the characterization of the optimal point. The scheduling policy and the dual congestion controller for the network is introduced in Section 5.3 and analyzed in Section 5.4.

5.1 Network model

We assume that the network is represented by a graph, $\mathcal{G} = (\mathcal{N}, \mathcal{L})$, where $\mathcal{N}$ is the set of nodes and $\mathcal{L}$ is the set of directed links. If a link (n, m) is in $\mathcal{L}$, then it is possible to send packets from node n to node m subject to the interference constraints to be described shortly. We let $\mu = \{\mu_l\}_{l \in \mathcal{L}}$ denote the rate vector at which data can be transfered over each link $l \in \mathcal{L}$. We assume that there is an upper bound, $\hat{\eta} < \infty$, on each μ_l. In this chapter, for ease of presentation we assume that there is no fading in the environment. Time variations can be added to the analysis as in previous chapters. However, it complicates the expressions without providing additional insight.

We let Γ denote a bounded region in the $|\mathcal{L}|$ dimensional real space, representing the set of μ that can be achieved in a given time slot, i.e. it represents the interference constraint. Without loss of generality, we can assume that Γ is a convex region, because a non-convex region can be made convex by time-sharing.

We use $\mathcal{F}$ to denote the set of flows that share the network resources. We assume that each flow, f, has a unique, loop-free route and a utility function associated with it. We use H_l^f to denote the indicator function that is equal to 1 when link l is in the route of flow f, and zero otherwise. In the analysis, we also use the following notation:

$\rightarrow$ $b(f)$: beginning node of flow f.

$\rightarrow$ $e(f)$: end node of flow f.

$\rightarrow$ $p(n, f)$: parent node of node n for flow f.

$\rightarrow$ $c(n, f)$: child node of node n for flow f. [1]

Figure 5.1 illustrates an example network with three flows passing through it.

Associated with each flow f is a utility function $U_f(x_f)$, which is a function of the flow rate x_f. The utility function, denoted by $U_f(\cdot)$ for flow f, is assumed to satisfy the following conditions:

[1] With this notation, the route of flow f is $(b(f), c(b(f), f)), \cdots, (p(e(f), f), e(f))$.

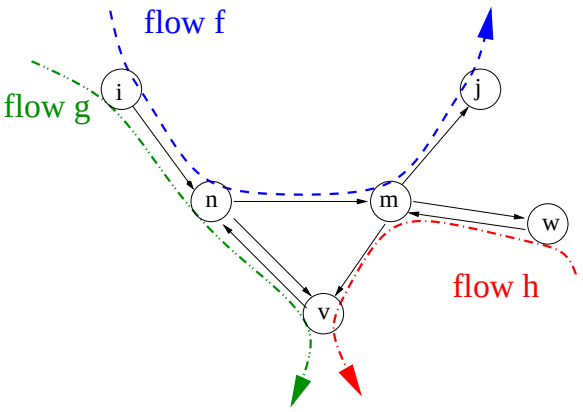

Figure 5.1 An example network model with $b(f) = i$, $e(f) = j$, $p(n, f) = i$ and $c(n, f) = m$.

- $U_f(\cdot)$ is a twice differentiable, strictly concave, nondecreasing function of the mean flow rate, x_f.

- For every $\bar{M} \in (0, \infty)$, there exists a constant $m < \infty$ such that

$$0 \leq -\frac{1}{U_f''(x)} \leq m \qquad \forall x \in [0, \bar{M}] \tag{5.1}$$

- $U_f'^{-1}(\cdot)$ is a convex function, and satisfies[2]

$$1 - \frac{U_f'^{-1}(\kappa + \frac{\beta}{K^{1-\sigma}})}{U_f'^{-1}(\kappa)} = O(K^{-\gamma}) \tag{5.2}$$

  for any fixed $\kappa, \beta > 0$ and for some $\gamma \in (0, 1)$ that is determined as a function of $\sigma \in (0, 1)$.

We note that these conditions are not restrictive and hold for the following class of utility functions.

$$U_f(x) = \beta_f \frac{x^{1-\alpha_f}}{(1-\alpha_f)} \qquad \forall\, \alpha_f > 0. \tag{5.3}$$

This class of utility functions is known to characterize a large class of fairness concepts [59].

Given the routes of each of the flows, the flow rate vector, $\mathbf{x} = \{x_f\}_{f \in \mathcal{F}}$, can be translated into the link rate vector, $\mathbf{y}(\mathbf{x}) = \{y_l(\mathbf{x})\}_{l \in \mathcal{L}}$ as follows:

$$y_l(\mathbf{x}) \;\; = \;\; \sum_{f \in \mathcal{F}} x_f H_l^f, \qquad \text{for all } l \in \mathcal{L}.$$

[2] $f(x) = O(g(x))$ implies that $\limsup_{x \to \infty} \left| \frac{f(x)}{g(x)} \right| < \infty$.

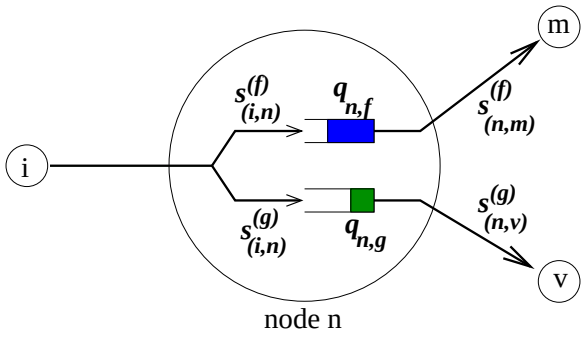

Figure 5.2 Each node contains a queue for each flow traversing it. This figure zooms into node n of Figure 5.1.

Next, we describe the capacity region of the network.

Definition 5.1 (Capacity region). *The* capacity region, Λ, *of the network contains the set of flow rates* $\mathbf{x}$ *that satisfies the link constraints,* Γ, *i.e.* $\Lambda = \{\mathbf{x} : \mathbf{y}(\mathbf{x}) \in \Gamma\}$. *Observe that* Λ *represents a region in the* $|\mathcal{F}|$ *dimensional space.*

It is assumed that each node maintains a separate queue for each of the flows that traverses it. We use $q_{n,f}[t]$ to denote the queue length of flow f at node n at the beginning of time-slot t. See Figure 5.2 for an example node model. Then, for each $n \in \mathcal{N}$, and $f \in \mathcal{F}$, the evolution of $q_{n,f}$ is given by

$$q_{n,f}[t+1] = q_{n,f}[t] + x_f[t]\,\mathcal{I}_{n=b(f)} + s^{(f)}_{(p(n,f),n)}[t]\,\mathcal{I}_{n\neq b(f)} - s^{(f)}_{(n,c(n,f))}[t],$$

where we use $s^{(f)}_{(n,m)}[t]$ to denote the rate provided to flow f over link (n,m) at slot t. Notice that, this is the actual amount of packets served over the link, not the potential amount denoted by $\mu^{(f)}_{(n,m)}[t]$. Clearly, we have $s_{(n,m)}[t] = \sum_f s^{(f)}_{(n,m)}[t]$. Also, the following relationship exists between $s^{(f)}_{(n,m)}[t]$ and $\mu^{(f)}_{(n,m)}[t]$:

$$s^{(f)}_{(n,m)}[t] = \min(\mu^{(f)}_{(n,m)}[t], q_{n,f}[t]) \qquad \forall\,(n,m) \in \mathcal{L}.$$

In order to keep the state space of queue lengths discrete, we assume that $\mu^{(f)}_l[t]$, and $x_f[t]$ take on a discrete set of values.

5.2 Problem Statement and Characterization of the Optimal Point

Our goal is to design a congestion control/scheduling mechanism such that the flow rate vector, $\mathbf{x}$, solves the following optimization problem,

$$\begin{aligned} \max_{\mathbf{x}} \quad & \sum_{f \in \mathcal{F}} U_f(x_f) \\ s.t. \quad & \mathbf{x} \in \Lambda \end{aligned} \tag{5.4}$$

which we will also refer to as the *primal problem.* We use $v^\star$ to denote the optimum value of (5.4). Due to strict concavity assumption of $U_i(\cdot)$ and the convexity of the capacity region Λ, there exists a unique optimizer of the primal problem, which we refer to as $\mathbf{x}^\star$.

Before we study the *dual* of the primal problem, we cast the primal problem in a slightly different manner.

$$\max_{\mathbf{x},\, \mu} \quad \sum_{f \in \mathcal{F}} U_f(x_f) \tag{5.5}$$

$$s.t. \quad y_l(\mathbf{x}) \leq \mu_l \qquad \forall\, l \in \mathcal{L}, \tag{5.6}$$

$$\mu \in \Gamma,$$

$$\mathbf{x} \geq 0. \tag{5.7}$$

We let $\lambda_l \geq 0$ be the Lagrange multiplier associated with the condition (5.6) for link l. Then, the *Lagrangian* of (5.5) is given by

$$\begin{aligned} L(\mathbf{x}, \mu, \lambda) &= \sum_{f \in \mathcal{F}} U_f(x_f) - \sum_{l \in \mathcal{L}} \lambda_l (y_l(\mathbf{x}) - \mu_l) \\ &= \sum_{f \in \mathcal{F}} \{U_f(x_f) - x_f \lambda_f\} + \sum_{l \in \mathcal{L}} \lambda_l \mu_l, \end{aligned}$$

where we have made an abuse of notation by defining $\lambda_f = \sum_{l \in \mathcal{L}} H_l^f \lambda_l$. Here, λ_l can be interpreted as the price of transferring a unit amount of data over link l. Thus, λ_f is nothing but the price of transferring a unit amount of data from the source of flow f to its destination.

We define the *dual function* as:

$$D(\lambda) = \max_{\mathbf{x}\geq 0,\, \mu\in\Gamma} \quad L(\mathbf{x},\mu,\lambda) \tag{5.8}$$

$$= \sum_{f\in\mathcal{F}} \max_{x_f\geq 0}\{U_f(x_f) - x_f\lambda_f\} + \max_{\mu\in\Gamma} \sum_{l\in\mathcal{L}} \mu_l\lambda_l, \tag{5.9}$$

Observe that, due to the decomposition in (5.9), we can easily specify the optimizing flow rate and link rate vector as a function of λ as follows.

$$\begin{aligned} x_f^\star(\lambda) &= U_f'^{-1}(\lambda_f) \\ \mu^\star(\lambda) &\in \arg\max_{\mu\in\Gamma} \sum_{l\in\mathcal{L}} \mu_l\lambda_l \end{aligned}$$

The *dual* of the primal problem is given by

$$\min_{\lambda\geq 0}\ D(\lambda) \tag{5.10}$$

We let $d^\star$ denote the minimum attained by the dual problem. The following is a well-known result in duality theory.

Fact 5.1 (Weak Duality). *The following always holds:* $d^\star \geq v^\star$.

Now, we present some properties of the optimal solution. First, we define the following.

Definition 5.2. $\lambda^\star$ *is said to be an* optimal Lagrange multiplier *of the primal problem in (5.5) if it satisfies:* $\lambda^\star \geq 0$ *and*

$$v^\star = \max_{\mathbf{x}\geq 0,\, \mu\in\Gamma} L(\mathbf{x},\mu,\lambda^\star)$$

The next two propositions are straight forward extensions of their similar versions presented in [22].

Proposition 5.1. *Let* $\lambda^\star$ *be an optimal Lagrange multiplier. Then* $(\mathbf{x}^\star,\mu^\star)$ *is a global maximum of the primal problem if and only if*

$$\begin{aligned} (\mathbf{x}^\star,\mu^\star) &\quad \textit{is feasible, i.e.,}\ y_l(\mathbf{x}) \leq \mu_l^\star \textit{ and } \mu^\star\in\Gamma, \\ (\mathbf{x}^\star,\mu^\star) &\in \arg\max_{\mathbf{x}\geq 0,\mu\in\Gamma} L(\mathbf{x},\mu,\lambda^\star), \\ \lambda_l^\star(y_l(\mathbf{x}^\star) - \mu_l^\star) &= 0, \qquad \forall\, l\in\mathcal{L}. \end{aligned}$$

Proof. If $(\mathbf{x}^\star, \mu^\star)$ is a global maximum, then it must be feasible and

$$\begin{aligned} v^\star &= \sum_{f\in\mathcal{F}} U_f(x_f^\star) \\ &\overset{(a)}{\leq} \sum_{f\in\mathcal{F}} U_f(x_f^\star) - \sum_{l\in\mathcal{L}} \lambda_l^\star(y_l(\mathbf{x}^\star) - \mu_l^\star) \\ &= L(\mathbf{x}^\star, \mu^\star, \lambda^\star) \\ &\leq \max_{\mathbf{x}\geq 0, \mu\in\Gamma} L(\mathbf{x}, \mu, \lambda^\star), \end{aligned}$$

where inequality (a) is true because $\lambda_l^\star \geq 0$ for all $l \in \mathcal{L}$ and $y_l(\mathbf{x}^\star) \leq \mu_l^\star$ for all feasible $(\mathbf{x}^\star, \mu^\star)$ pair. But, due to Definition 5.2, the last inequality must be an equality. Therefore, we must have

$$\begin{aligned} L(\mathbf{x}^\star, \mu^\star, \lambda^\star) &= \max_{\mathbf{x}\geq 0, \mu\in\Gamma} L(\mathbf{x}, \mu, \lambda^\star), \qquad \text{and,} \\ \lambda_l^\star(y_l(\mathbf{x}^\star) - \mu_l^\star) &= 0, \qquad \forall\, l \in \mathcal{L}. \end{aligned}$$

Conversely, if the given conditions hold, then

$$\begin{aligned} \sum_{f\in\mathcal{F}} U_f(x_f^\star) &= \sum_{f\in\mathcal{F}} U_f(x_f^\star) - \sum_{l\in\mathcal{L}} \lambda_l^\star(y_l(\mathbf{x}^\star) - \mu_l^\star) \\ &= L(\mathbf{x}^\star, \mu^\star, \lambda^\star) \\ &= \max_{\mathbf{x}\geq 0, \mu\in\Gamma} L(\mathbf{x}, \mu, \lambda^\star) \\ &= v^\star. \end{aligned}$$

Therefore, $(\mathbf{x}^\star, \mu^\star)$ must be a global maximum. □

Proposition 5.2. *The triple $(\mathbf{x}^\star, \mu^\star, \lambda^\star)$ is an optimal solution, i.e., satisfies $D(\lambda^\star) = \sum_{f\in\mathcal{F}} U_f(x_f^\star)$, if and only if*

(a) $\mathbf{x}^\star \geq 0$, $\mu^\star \in \Gamma$ *and* $x_l^\star \leq \mu_l^\star$.

(b) $\lambda^\star \geq 0$.

(c) $(\mathbf{x}^\star, \mu^\star) \in \arg\max_{\mathbf{x}\geq 0, \mu\in\Gamma} L(\mathbf{x}, \mu, \lambda^\star)$ *or equivalently,*
$x_f^\star = U_f'^{-1}(\lambda_f^\star)$ *for all* $f \in \mathcal{F}$, *and* $\mu^\star \in \arg\max_{\mu\in\Gamma} \sum_{l\in\mathcal{L}} \lambda_l^\star \mu_l$.

(d) $\lambda_l^\star(y_l(\mathbf{x}^\star) - \mu_l^\star) = 0$, *for all* $l \in \mathcal{L}$.

Proof. If $(\mathbf{x}^\star, \mu^\star, \lambda^\star)$ is an optimal solution, then $(\mathbf{x}^\star, \mu^\star)$ must be primal feasible and $\lambda^\star$ must be dual feasible, which proves (a) and (b). Then, parts (c) and (d) follow from Proposition 5.1.

Conversely, using conditions (a)-(d), we can write

$$\begin{aligned} v^\star &\geq \sum_{f\in\mathcal{F}} U_f(x_f^\star) \\ &= L(\mathbf{x}^\star, \mu^\star, \lambda^\star) \\ &= \max_{\mathbf{x}\geq 0, \mu\in\Gamma} L(\mathbf{x}, \mu, \lambda^\star) \\ &= D(\lambda^\star) \\ &\geq d^\star. \end{aligned}$$

Using the weak duality result of Fact 5.1, the equality must hold in the previous set of equations. Therefore, if conditions (a)-(d) hold, then $(\mathbf{x}^\star, \mu^\star, \lambda^\star)$ must be an optimal solution, and there is no duality gap. □

Proposition 5.3 (Strong Duality). *For the primal-dual problem pair defined in (5.4) and (5.10), there is no duality gap, i.e.,* $d^\star = v^\star$.

Proof. The proof uses a result from [60], and is moved to the appendix. □

Since we already know that $x^\star$ is unique, Proposition 5.3 states that there exists a nonempty set, $\Psi^\star$, of optimal Lagrange multipliers that satisfy

$$\sum_{f\in\mathcal{F}} U_f(x_f^\star) = D(\lambda^\star) \qquad \text{for all } \lambda^\star \in \Psi^\star,$$

and there is an associated rate vector $\mu^\star \in \Gamma$ for each $\lambda^\star$ which satisfies:

- $y_l(\mathbf{x}^\star) \leq \mu_l^\star \;\forall\, l \in \mathcal{L}$,
- if $y_l(\mathbf{x}^\star) < \mu_l^\star$, then $\lambda_l^\star = 0$,
- $\mu^\star \in \arg\max_{\mu\in\Gamma} \sum_{l\in\mathcal{L}} \lambda_l^\star \mu_l$.

The last property implies that $\sum_{l\in\mathcal{L}} \lambda_l^\star \mu_l^\star \geq \sum_{l\in\mathcal{L}} \lambda_l^\star \mu_l$ for any $\mu \in \Gamma$. But, from (d) of Proposition 5.2, we know that $\lambda_l^\star \mu_l^\star = \lambda_l^\star y_l(x^\star)$ for all $l \in \mathcal{L}$. Therefore, we have

$$\sum_{l\in\mathcal{L}} \lambda_l^\star y_l(x^\star) \geq \sum_{l\in\mathcal{L}} \lambda_l^\star \mu_l \qquad \forall\, \mu \in \Gamma. \tag{5.11}$$

We will make use of this inequality in a later section.

The optimization problem (5.4) is obviously equivalent to the following optimization problem.

$$\begin{aligned} \max \quad & \sum_{f\in\mathcal{F}} KU_f(x_f) \\ s.t. \quad & \mathbf{x} \in \Lambda \end{aligned} \tag{5.12}$$

where $K < \infty$ is a positive parameter that we are free to choose. Clearly, for any fixed K, the optimizer of (5.12) is the same as that of (5.4), namely, $\mathbf{x}^\star$. However, the set of optimal Lagrange multipliers of (5.12), which we denote with $\Psi_K^\star$, is given by $\Psi_K^\star = K\Psi^\star$, i.e. there is a one-to-one correspondence between any $\lambda^\star \in \Psi^\star$ and $K\lambda^\star \in \Psi_K^\star$. All the propositions and arguments made for $\Psi^\star$ applies to $\Psi_K^\star$. In particular, (5.11) holds for all Lagrange multipliers $\lambda^\star \in \Psi_K^\star$ because both sides of the inequality are multiplied by the same constant K. We will see later that the constant K plays an important role in the convergence analysis as in the previous chapter.

5.3 Scheduling and Congestion Control Algorithm

In this section, we introduce the two mechanisms that work in parallel to guarantee stability of the queues and fair allocation of the resources. The queue-length-based scheduler that is also referred to as the *back-pressure scheduler* is due to a work by Tassiulas [12], and uses differential backlog at the two end nodes of a link to determine the rate of that link. This is actually an extension of the queue-length-based scheduler that we studied in the single-hop scenario to the multi-hop networks.

At the transport layer, we introduce the *dual congestion controller* mechanism that aims to change the end-to-end flow rates in a direction so as to minimize the dual objective of (5.12). It turns out that the optimal Lagrange multipliers of (5.12) is related to the queue lengths at the nodes. In particular, the differential backlog over each link tracks the optimal Lagrange multiplier vector. We will clarify these claims in the analysis.

Definition 5.3 (Back-pressure Scheduler). *At slot t, for each $(n,m) \in \mathcal{L}$, we define the differential backlog for flow f over link (n,m) as*

$$W_{(n,m),f}[t] \;=\; (q_{n,f}[t] - q_{m,f}[t]).$$

Then, choose the rate vector $\mu[t] \in \Gamma$ that satisfies

$$\mu[t] \in \underset{\left\{\eta\in\Gamma,\ \sum_{\{f:H^f_{(n,m)}=1\}} \eta^{(f)}_{(n,m)} = \eta_{(n,m)}\right\}}{\arg\max} \sum_f \sum_{\{(n,m):H^f_{(n,m)}=1\}} \eta^{(f)}_{(n,m)} W_{(n,m),f}[t]. \tag{5.13}$$

We note that among those flows that share link l, the one, say $\hat{f}$, with maximum $W_{l,f}[t]$ over all $f \in \{f : H^f_l = 1\}$ will be the only one to be served over link l at slot t, i.e., $\mu^{(\hat{f})}_l[t] = \mu_l[t]$. The following fact is a natural consequence of the optimization (5.13) employed by the back-pressure policy.

Fact 5.2. *Under the back-pressure scheduling policy, those flows that have $W_{l,f}[t] < 0$ will get $\mu^{(f)}_l[t] = 0$, because the objective of the optimization in (5.13) can only decrease by choosing $\mu^{(f)}_l[t] > 0$, if $W_{l,f}[t] < 0$.*

Definition 5.4 (Dual Congestion Controller). *At the beginning of time slot t, each flow, say f, has access to the queue length of its first node, i.e. $q_{b(f),f}[t]$. Then the data rate $x_f[t]$ of flow f is an independently distributed random variable that satisfies*

$$\begin{aligned} E[x_f[t] \mid q_{b(f),f}[t]] &= \min\left\{U'^{-1}_f\left(\frac{q_{b(f),f}[t]}{K}\right), M\right\} \\ E[x^2_f[t] \mid q_{b(f),f}[t]] &\le A < \infty, \qquad \forall q_{b(f),f}[t], \end{aligned}$$

where $M \geq 2\hat{\eta}$ is a constant that guarantees that the amount of data pumped into the network is bounded in its mean.

5.4 Analysis of the System

In this section, we will start by describing and analyzing a heuristic continuous-time fluid model of the system, which will lay a foundation for the subsequent discrete-time analysis.

5.4.1 Continuous-time Fluid model Analysis

Under this model, as we did in Chapter 4, we assume that the time is continuous and the evolution of each queues is given by a differential equation as follows: for each $n \in \mathcal{N}$, and $f \in \mathcal{F}$,

$$\dot{q}_{n,f}(t) \;=\; (x_f(t)\,\mathcal{I}_{n=b(f)} + \mu^{(f)}_{(p(n,f),n)}(t)\,\mathcal{I}_{n\neq b(f)} - \mu^{(f)}_{(n,c(n,f))}(t))^{+}_{q_{n,f}(t)}.$$

Here, (t) is used instead of $[t]$ to signify that we are working in continuous-time. The back-pressure algorithm computes the rates at every instant of time implementing the same algorithm as described in Section 5.3. Finally, the congestion controller is assumed to determine the instant flow rates such that

$$x_f(t) \;=\; U_f'^{-1}\left(\frac{q_{b(f),f}(t)}{K}\right) \qquad \forall\, f \in \mathcal{F}. \tag{5.14}$$

Next, we describe $\mathbf{W}^\star = \{W^\star_{l,f}\}^{f\in\mathcal{F}}_{l\in\mathcal{L}}$ and $\mathbf{q}^\star = \{q^\star_{n,f}\}^{f\in\mathcal{F}}_{n\in\mathcal{N}}$ as a function of the Lagrange multipliers of the optimization problem (5.12).

Definition 5.5 (Optimal $(\mathbf{W}^\star, \mathbf{q}^\star)$). *For any $\lambda^\star \in \Psi^\star_K$, we define*

$$W^\star_l \;=\; \lambda^\star_l, \qquad \forall\, l \in \mathcal{L}, \qquad \textit{and} \qquad W^\star_{l,f} = W^\star_l, \quad \forall\, f \in \{f : H^f_l = 1\} \tag{5.15}$$

$$q^\star_{n,f} \;=\; W^\star_{(n,c(n,f))} + W^\star_{(c(n,f),c(c(n,f),f))} + \cdots + W^\star_{(p(e(f),f),e(f))}, \qquad \forall\, f,\, n, \tag{5.16}$$

where (5.15) sets the optimal differential backlog values to be equal to the corresponding optimal Lagrange multipliers (or link prices) of (5.12), and (5.16) sets the optimal queue length value at node n for flow f to be equal to the sum of all the downstream link prices.

Notice that for each $\lambda^\star \in \Psi^\star_K$, Definition 5.5 yields a possibly different pair $(\mathbf{W}^\star, \mathbf{q}^\star)$. We let $\mathbb{Q}^\star_K$ denote the set of possible $\mathbf{q}^\star$. We know that this set is not empty because $\Psi^\star_K$ is not empty due to the strong duality property. Also, it must be true that $q^\star_{b(f),f}$ must be equal for all $\mathbf{q}^\star \in \mathbb{Q}^\star_K$ because the following relationship between $\mathbf{x}^\star$ and $\mathbf{q}^\star$ must hold: $x^\star_f = U_f'^{-1}(q^\star_{b(f),f}/K)$ for each $f \in \mathcal{F}$.

Then, the following global asymptotic stability result holds.

Theorem 5.1. *Starting from any* $\mathbf{x}(0)$ *and* $\mathbf{q}(0)$*, the continuous-time algorithm described above converges to* $\mathbf{x}^\star$ *and* $\mathbb{Q}_K^\star$ *as* $t \to \infty$*.*

Proof. Consider the following Lyapunov function

$$V(\mathbf{q};\mathbf{q}^\star) = \frac{1}{2}\sum_{n\in\mathcal{N}}\sum_{f\in\mathcal{F}}(q_{n,f}-q_{n,f}^\star)^2,$$

where $\mathbf{q}^\star \in \mathbb{Q}_K^\star$. Next, we write the time-derivative of this function.

$$\begin{aligned}
&\dot{V}(\mathbf{q}(t);\mathbf{q}^\star)\\
&= \sum_{n,f}(q_{n,f}(t)-q_{n,f}^\star)\left(x_f(t)\mathcal{I}_{n=b(f)} + \mu^{(f)}_{(p(n,f),n)}(t)\mathcal{I}_{n\neq b(f)} - \mu^{(f)}_{(n,c(n,f))}(t) + u_{n,f}(t)\right)\\
&\leq \sum_{n,f}(q_{n,f}(t)-q_{n,f}^\star)\left(x_f(t)\mathcal{I}_{n=b(f)} + \mu^{(f)}_{(p(n,f),n)}(t)\mathcal{I}_{n\neq b(f)} - \mu^{(f)}_{(n,c(n,f))}(t)\right) \qquad (5.17)\\
&\overset{(a)}{=} \sum_{f}(q_{b(f),f}(t)-q_{b(f),f}^\star)(x_f(t)-x_f^\star)\\
&\quad + \sum_{n,f}(q_{n,f}(t)-q_{n,f}^\star)\left(x_f^\star(t)\mathcal{I}_{n=b(f)} + \mu^{(f)}_{(p(n,f),n)}(t)\mathcal{I}_{n\neq b(f)} - \mu^{(f)}_{(n,c(n,f))}(t)\right)\\
&= \sum_{f}(q_{b(f),f}(t)-q_{b(f),f}^\star)\left(U_f'^{-1}\left(\frac{q_{b(f),f}(t)}{K}\right) - U_f'^{-1}\left(\frac{q^\star_{b(f),f}}{K}\right)\right) \qquad (5.18)\\
&\quad + \sum_{n,f} q_{n,f}\left(x_f^\star(t)\mathcal{I}_{n=b(f)} + \mu^{(f)}_{(p(n,f),n)}(t)\mathcal{I}_{n\neq b(f)} - \mu^{(f)}_{(n,c(n,f))}(t)\right) \qquad (5.19)\\
&\quad + \sum_{n,f} q_{n,f}^\star(t)\left(\mu^{(f)}_{(n,c(n,f))}(t) - \mu^{(f)}_{(p(n,f),n)}(t)\mathcal{I}_{n\neq b(f)} - x_f^\star(t)\mathcal{I}_{n=b(f)}\right) \qquad (5.20)
\end{aligned}$$

where (5.17) follows from noting that the unused service $u_{n,f}(t) = 0$ whenever $q_{n,f}(t) > 0$. Equality (a) is obtained by adding and subtracting $x_f^\star\mathcal{I}_{n=b(f)}$ for all n, f to (5.17). Equation (5.18) is obtained by substituting the expression in (5.14) and noting that we can write $x_f^\star = U_f'^{-1}(q^\star_{b(f),f}/K)$.

The strict concavity of $U_f(\cdot)$ implies that $(5.18) \leq 0$ for all $\mathbf{q}$ with strict inequality whenever $\mathbf{q} \notin \mathbb{Q}_K^\star$. Next, we study the (5.20) and (5.19) separately to argue that they are both non-positive quantities.

We start with (5.20). Notice that we can write

$$\sum_{f\in\mathcal{F}} q^\star_{b(f),f}x_f^\star = \sum_{f\in\mathcal{F}}\sum_{\{(n,m):H^f_{(n,m)}=1\}} x_f^\star(q_{n,f}^\star - q_{m,f}^\star) = \sum_{f\in\mathcal{F}}\sum_{\{(n,m):H^f_{(n,m)}=1\}} x_f^\star W^\star_{(n,m),f}, \quad (5.21)$$

by adding and subtracting $q^\star_{n,f}$ for all the nodes on the route of each flow f. Also notice that we can write

$$\sum_{n,f} q^\star_{n,f}\left(\mu^{(f)}_{(n,c(n,f))}(t) - \mu^{(f)}_{(p(n,f),n)}(t)\mathcal{I}_{n\neq b(f)}\right)$$

$$\begin{aligned} &= \sum_{f\in\mathcal{F}}\sum_{\{(n,m):H^f_{(n,m)}=1\}} \mu^{(f)}_{(n,m)}(t)(q^\star_{n,f} - q^\star_{m,f}) \\ &= \sum_{f\in\mathcal{F}}\sum_{\{(n,m):H^f_{(n,m)}=1\}} \mu^{(f)}_{(n,m)}(t)W^\star_{(n,m),f}, \end{aligned} \tag{5.22}$$

by making a change in the order of summation. Now, by definition, we have $W^\star_{(n,m),f} = W^\star_{(n,m)}$ for all f that share link (n,m). Thus, we can rearrange the terms of (5.22) to get

$$\begin{aligned} (5.22) &= \sum_{(n,m)\in\mathcal{L}} W^\star_{(n,m)} \sum_{\{f:H^f_{(n,m)}=1\}} \mu^{(f)}_{(n,m)}(t) \\ &= \sum_{l\in\mathcal{L}} W^\star_l \mu_l(t) \end{aligned}$$

Similarly, we can write (5.21) as

$$\begin{aligned} (5.21) &= \sum_{(n,m)\in\mathcal{L}} W^\star_{(n,m)} \sum_{\{f:H^f_{(n,m)}=1\}} x^\star_f \\ &= \sum_{l\in\mathcal{L}} W^\star_l y_l(\mathbf{x}^\star) \\ &\overset{(a)}{\geq} \sum_{l\in\mathcal{L}} W^\star_l \mu_l \\ &= (5.22) \end{aligned}$$

where the the inequality (a) follows from (5.11). Noting that $(5.20) = (5.22) - (5.21)$ concludes that we must have $(5.20) \leq 0$.

Next, we consider the expression (5.19). Following similar arguments as above, we can write

$$\sum_{f\in\mathcal{F}} x^\star_f q_{b(f),f}(t) = \sum_{f\in\mathcal{F}}\sum_{\{(n,m):H^f_{(n,m)}=1\}} x^\star_f W_{(n,m),f}(t). \tag{5.23}$$

On the other hand, we have

$$\sum_{n,f} q_{n,f}\left(\mu^{(f)}_{(n,c(n,f))}(t) - \mu^{(f)}_{(p(n,f),n)}(t)\mathcal{I}_{n\neq b(f)}\right) = \sum_{f\in\mathcal{F}}\sum_{\{(n,m):H^f_{(n,m)}=1\}} \mu^{(f)}_{(n,m)}(t)W_{(n,m),f}(t) \tag{5.24}$$

Now, since $\mathbf{y}(\mathbf{x}^\star) \in \Gamma$ and $\mu(t)$ maximizes $\sum_{f\in\mathcal{F}} \sum_{\{(n,m):H^f_{(n,m)}=1\}} \eta^{(f)}_{(n,m)} W_{(n,m),f}(t)$ over all $\eta \in \Gamma$ due to the back-pressure scheduler, we must have $(5.19) = (5.23) - (5.24) \leq 0$. This completes our claim.

Finally, it is not difficult to see that $\dot{V}(\mathbf{q}(t); \mathbf{q}^\star) = 0$ if $\mathbf{q}(t) = \mathbf{q}^\star$. Thus, for any other $\tilde{\mathbf{q}}^\star \in \mathbb{Q}^\star_K$, we must also have $\dot{V}(\mathbf{q}(t); \tilde{\mathbf{q}}^\star) = 0$ for $\mathbf{q}(t) = \mathbf{q}^\star$. This argument implies that we have $\dot{V}(\mathbf{q}(t); \mathbf{q}^\star) = 0$ for any $\mathbf{q}(t) \in \mathbb{Q}^\star_K$.

Combining all of these arguments, we are able to claim that

$$\dot{V}(\mathbf{q}(t); \mathbf{q}^\star) \begin{cases} < 0 & \text{if } \mathbf{q}(t) \notin \mathbb{Q}^\star_K, \\ = 0 & \text{if } \mathbf{q}(t) \in \mathbb{Q}^\star_K \end{cases}$$

Hence, $\mathbf{q}(t) \to \mathbb{Q}^\star_K$ and $\mathbf{x}(t) \to \mathbf{x}^\star$ as $t \to \infty$.

□

5.4.2 Discrete-time Stochastic model Analysis

Our analysis of the continuous-time, fluid model in Section 5.4.1 showed that the system evolves toward the optimal rate allocation and the queue lengths change in such a way that the differential backlogs converge to the optimal Lagrange multiplier set. In this section, we return to our original discrete-time, stochastic system model described in Section 5.3 and study its performance. In the analysis, we will utilize the intuition we obtained from the fluid model.

The following lemma provides a relationship between potential service rate and the actual service rate, that will be used in the proof of the subsequent theorem.

Lemma 5.1. *For our system, the following relationship holds for any* $\mathbf{q}[t]$ *and some* $B < \infty$:

$$\sum_{f\in\mathcal{F}} \sum_{\{(n,m):H^f_{(n,m)}=1\}} s^{(f)}_{(n,m)}[t](q_{n,f}[t] - q_{m,f}[t]) \geq \sum_{f\in\mathcal{F}} \sum_{\{(n,m):H^f_{(n,m)}=1\}} \mu^{(f)}_{(n,m)}[t](q_{n,f}[t] - q_{m,f}[t]) - B$$

Proof. We prove this lemma by covering all the possible cases. Before we start, we note that $s^{(f)}_{(n,m)}[t] = \min(\mu^{(f)}_{(n,m)}[t], q_{n,f}[t])$.

CASE 1: $q_{n,f}[t] < q_{m,f}[t]$: then, due to Fact 5.2, we have $\mu^{(f)}_{(n,m)}[t] = 0$ and subsequently, we

must have $s^{(f)}_{(n,m)}[t] = 0$. Thus, the claim holds with equality.

CASE 2: $q_{n,f}[t] \geq q_{m,f}[t]$ and $q_{n,f}[t] \geq \hat{\eta}$: then there can be no unused service since $\mu^{(f)}_{(n,m)}[t] < \hat{\eta}$ by assumption. Thus, we have $s^{(f)}_{(n,m)}[t] = \mu^{(f)}_{(n,m)}[t]$ and the claim holds with equality.

CASE 3: $\hat{\eta} > q_{n,f}[t] \geq q_{m,f}[t]$: then, we have $s^{(f)}_{(n,m)}[t] < \hat{\eta}$ and

$$\mu^{(f)}_{(n,m)}[t](q_{n,f}[t] - q_{m,f}[t]) \leq \hat{\eta}^2.$$

Thus, we have

$$\sum_{f\in\mathcal{F}} \sum_{\{(n,m):H^f_{(n,m)}=1\}} \mu^{(f)}_{(n,m)}[t](q_{n,f}[t] - q_{m,f}[t]) \leq |\mathcal{L}||\mathcal{F}|\hat{\eta}^2 =: B.$$

Noting that $\sum_{f\in\mathcal{F}} \sum_{\{(n,m):H^f_{(n,m)}=1\}} s^{(f)}_{(n,m)}[t](q_{n,f}[t] - q_{m,f}[t]) \geq 0$, since $s^{(f)}_{(n,m)}[t] = 0$ whenever $q_{n,f}[t] \leq q_{m,f}[t]$, we finish the proof of this lemma. □

The following lemma finds an upper bound on an expression that will arise in the proof of the following theorem.

Lemma 5.2. *Given any $\bar{B} < \infty$, we can find some $\gamma \in (0,1)$ such that for K large enough, we have*

$$\bar{B} + \sum_f \left\{ \left(q_{b(f),f} - q^\star_{b(f),f}\right) \left(\min\left\{ U_f'^{-1}\left(\frac{q_{b(f),f}}{K}\right), M\right\} - U_f'^{-1}\left(\frac{q^\star_{b(f),f}}{K}\right)\right)\right\}$$
$$\leq -\frac{\delta}{K^\gamma}\|\mathbf{q}-\mathbf{q}^\star\|\mathcal{I}_{\|\mathbf{q}-\mathbf{q}^\star\|\geq cK^\gamma} + \zeta\mathcal{I}_{\|\mathbf{q}-\mathbf{q}^\star\|<cK^\gamma}$$

where δ, ζ and c are positive constants which are independent of L.

Proof. We define

$$\Phi = \sum_f \left(q_{b(f),f} - q^\star_{b(f),f}\right) \left(\min\left\{ U_f'^{-1}\left(\frac{q_{b(f),f}}{K}\right), M\right\} - U_f'^{-1}\left(\frac{q^\star_{b(f),f}}{K}\right)\right),$$

$$\hat{f} = \arg\max_f |q_{b(f),f} - q^\star_{b(f),f}|.$$

Noting that for all f we have

$$\left(q_{b(f),f} - q^\star_{b(f),f}\right) \left(\min\left\{ U_f'^{-1}\left(\frac{q_{b(f),f}}{K}\right), M\right\} - U_f'^{-1}\left(\frac{q^\star_{b(f),f}}{K}\right)\right) \leq 0$$

due to the fact that $U_f'^{-1}(\cdot)$ is decreasing in its parameter. Then, we can write

$$\Phi \leq -|q_{b(\hat{f}),\hat{f}} - q^\star_{b(\hat{f}),\hat{f}}| \left| \min\left\{ U_f'^{-1}\left(\frac{q_{b(\hat{f}),\hat{f}}}{K}\right), M \right\} - U_f'^{-1}\left(\frac{q^\star_{b(\hat{f}),\hat{f}}}{K}\right) \right|$$

There are two cases to consider: If $\min\left\{ U_f'^{-1}\left(\frac{q_{b(\hat{f}),\hat{f}}}{K}\right), M \right\} = M$, then

$$\min\left\{ U_f'^{-1}\left(\frac{q_{b(\hat{f}),\hat{f}}}{K}\right), M \right\} - x^\star_{\hat{f}} > M - \hat{\eta} > \hat{\eta},$$

since M is chosen to be larger than $2\hat{\eta}$.

If, on the other hand, $\min\left\{ U_f'^{-1}\left(\frac{q_{b(\hat{f}),\hat{f}}}{K}\right), M \right\} < M$, then we have

$$\left| \min\left\{ U_f'^{-1}\left(\frac{q_{b(\hat{f}),\hat{f}}}{K}\right), M \right\} - x^\star_{\hat{f}} \right| = x^\star_{\hat{f}} \left| \frac{U_{\hat{f}}'^{-1}\left(\frac{q_{b(\hat{f}),\hat{f}}}{K}\right)}{U_{\hat{f}}'^{-1}\left(\frac{q^\star_{b(\hat{f}),\hat{f}}}{K}\right)} - 1 \right|. \tag{5.25}$$

Notice that

$$q_{b(\hat{f}),\hat{f}} = \begin{cases} q^\star_{b(\hat{f}),\hat{f}} - |q_{b(\hat{f}),\hat{f}} - q^\star_{b(\hat{f}),\hat{f}}| \geq 0 & \text{if } q_{b(\hat{f}),\hat{f}} - q^\star_{b(\hat{f}),\hat{f}} \leq 0, \\ q^\star_{b(\hat{f}),\hat{f}} + |q_{b(\hat{f}),\hat{f}} - q^\star_{b(\hat{f}),\hat{f}}| \geq 0 & \text{if } q_{b(\hat{f}),\hat{f}} - q^\star_{b(\hat{f}),\hat{f}} \geq 0. \end{cases}$$

Since $U_{\hat{f}}'^{-1}(\cdot)$ is assumed to be a decreasing, convex function, we can write

$$\left| \frac{U_{\hat{f}}'^{-1}\left(\frac{q^\star_{b(\hat{f}),\hat{f}}}{K} - \frac{|q_{b(\hat{f}),\hat{f}} - q^\star_{b(\hat{f}),\hat{f}}|}{K}\right)}{U_{\hat{f}}'^{-1}\left(\frac{q^\star_{b(\hat{f}),\hat{f}}}{K}\right)} - 1 \right| \geq \left| \frac{U_{\hat{f}}'^{-1}\left(\frac{q^\star_{b(\hat{f}),\hat{f}}}{K} + \frac{|q_{b(\hat{f}),\hat{f}} - q^\star_{b(\hat{f}),\hat{f}}|}{K}\right)}{U_{\hat{f}}'^{-1}\left(\frac{q^\star_{b(\hat{f}),\hat{f}}}{K}\right)} - 1 \right|.$$

Therefore, we have

$$\left| \frac{U_{\hat{f}}'^{-1}\left(\frac{q_{b(\hat{f}),\hat{f}}}{K}\right)}{U_{\hat{f}}'^{-1}\left(\frac{q^\star_{b(\hat{f}),\hat{f}}}{K}\right)} - 1 \right| \geq \left| \frac{U_{\hat{f}}'^{-1}\left(\frac{q^\star_{b(\hat{f}),\hat{f}}}{K} + \frac{|q_{b(\hat{f}),\hat{f}} - q^\star_{b(\hat{f}),\hat{f}}|}{K}\right)}{U_{\hat{f}}'^{-1}\left(\frac{q^\star_{b(\hat{f}),\hat{f}}}{K}\right)} - 1 \right|$$

We consider the set of $\mathbf{q}$ which satisfies $\|\mathbf{q} - \mathbf{q}^\star\| \geq cK^\sigma$, where c and K are positive constants and $\sigma \in (0,1)$. We are interested in the behavior of the system as K tends to infinity. The exact values of c and σ depend on the utility functions and other system parameters, and will be provided later in the proof.

Notice that if $\|\mathbf{q}-\mathbf{q}^\star\| \geq cK^\sigma$, then $|q_{b(\hat{f}),\hat{f}} - q^\star_{b(\hat{f}),\hat{f}}| \geq \frac{c}{\sqrt{|\mathcal{N}|}}K^\sigma$. Then, we can write

$$(5.25) \geq \left| \frac{U'^{-1}_{\hat{f}}\left(\frac{q^\star_{b(\hat{f}),\hat{f}}}{K} + \frac{c}{\sqrt{\mathcal{N}}K^{1-\sigma}}\right)}{U'^{-1}_{\hat{f}}\left(\frac{q^\star_{b(\hat{f}),\hat{f}}}{K}\right)} - 1 \right|$$

We claim that $q^\star_{b(\hat{f}),\hat{f}} = \varrho K$ for some $\varrho > 0$. This follows from the fact that by definition, each $q^\star_{b(f),f}$ is a sum of a finite number of link prices, i.e., $q^\star_{b(f),f} = \sum_{\{l:H^f_l=1\}} W^\star_l$. Also, by definition, $\mathbf{W}^\star = K\lambda^\star$ for some fixed $\lambda^\star \in \Psi^\star$. Hence, $q^\star_{b(f),f}$ must be linearly increasing with K, which proves our claim. By invoking the condition (5.2) on the utility functions, we can write: for $\|\mathbf{q}-\mathbf{q}^\star\| \geq cK^\sigma$,

$$\Phi(t) + \bar{B} \;\leq\; -|q_{b(\hat{f}),\hat{f}} - q^\star_{b(\hat{f}),\hat{f}}| \left(x^\star_f c_1 K^{-\gamma} + \frac{\bar{B}\sqrt{|\mathcal{N}|}}{c} K^{-\sigma} \right).$$

If we choose $\sigma \in (0,1)$ such that $\gamma = \sigma$, then for large enough c, we get the following expression for some $\delta > 0$ and $\zeta < \infty$.

$$\Phi(t) + \bar{B} \;\leq\; -\frac{\|\mathbf{q}-\mathbf{q}^\star\|}{K^\sigma}\delta\mathcal{I}_{\{\|\mathbf{q}-\mathbf{q}^\star\|\geq cK^\sigma\}} + \zeta\mathcal{I}_{\{\|\mathbf{q}-\mathbf{q}^\star\|<cK^\sigma\}}$$

□

Next, we consider the single-step mean drift of the Lyapunov function $V(\mathbf{q};\mathbf{q}^\star)$ that we studied in Section 5.4.1 and provide an upper bound on it.

Theorem 5.2. *For any $\mathbf{q}^\star \in \mathbb{Q}^\star_K$, the one-step mean drift of the Lyapunov function*

$$V(\mathbf{q};\mathbf{q}^\star) = \frac{1}{2}\sum_{n\in\mathcal{N}}\sum_{f\in\mathcal{F}}(q_{n,f} - q^\star_{n,f})^2$$

can be upper-bounded as follows:

$$\begin{aligned} E[\Delta V_t(\mathbf{q};\mathbf{q}^\star)] \;&:=\; E[V(\mathbf{q}[t+1];\mathbf{q}^\star) - V(\mathbf{q}[t];\mathbf{q}^\star) \mid \mathbf{q}[t] = \mathbf{q}] \\ &\leq\; -\frac{\|\mathbf{q}-\mathbf{q}^\star\|}{K^\sigma}\delta\mathcal{I}_{\{\|\mathbf{q}-\mathbf{q}^\star\|\geq cK^\sigma\}} + \zeta\mathcal{I}_{\{\|\mathbf{q}-\mathbf{q}^\star\|<cK^\sigma\}} \end{aligned}$$

for some $\sigma \in (0,1)$, and positive constants δ, c and ζ.

Proof. We start by expanding the drift expression and dropping the $[t]$ term for notational convenience

$E[\Delta V_t(\mathbf{q};\mathbf{q}^\star)]$

$$
\begin{aligned}
:= \quad & \frac{1}{2}\sum_{n,f} E\left[\left(q_{n,f}[t+1]-q^\star_{n,f}\right)^2-\left(q_{n,f}[t]-q^\star_{n,f}\right)^2 \mid \mathbf{q}[t]=\mathbf{q}\right] \\
= \quad & \frac{1}{2}\sum_{n,f} E\left[\left(q_{n,f}[t]-q^\star_{n,f}+x_f[t]\mathcal{I}_{n=b(f)}+s^{(f)}_{(p(n,f),n)}[t]\mathcal{I}_{n\neq b(f)}-s^{(f)}_{(n,c(n,f))}[t]\right)^2\right. \\
& \qquad \left.-\left(q_{n,f}[t]-q^\star_{n,f}\right)^2 \mid \mathbf{q}[t]=\mathbf{q}\right] \\
= \quad & \sum_{n,f}(q_{n,f}-q^\star_{n,f})\left(\min\left\{U_f'^{-1}\left(\frac{q_{b(f),f}}{K}\right),M\right\}\mathcal{I}_{n=b(f)}+s^{(f)}_{(p(n,f),n)}\mathcal{I}_{n\neq b(f)}-s^{(f)}_{(n,c(n,f))}\right) \\
& +\frac{1}{2}\sum_{n,f} E\left[\left(x_f\mathcal{I}_{n=b(f)}+s^{(f)}_{(p(n,f),n)}\mathcal{I}_{n\neq b(f)}-s^{(f)}_{(n,c(n,f))}\right)^2 \mid \mathbf{q}[t]=\mathbf{q}\right]. \qquad (5.26)
\end{aligned}
$$

It is not difficult to see that we can find some $B_1<\infty$ such that $(5.26)<B_1$ since we have $E[x_f[t]\mid\mathbf{q}]\leq M$, and $E[x_f^2[t]\mid\mathbf{q}]\leq A$, and $s_l[t]<\hat{\eta}$ for all $l\in\mathcal{L}$.

By adding and subtracting $\sum_{n,f} x^\star_f\mathcal{I}_{n=b(f)}$ to the previous expression, we can write

$E[\Delta V_t(\mathbf{q};\mathbf{q}^\star)]$

$$
\begin{aligned}
\leq \quad & \sum_{f\in\mathcal{F}}(q_{b(f),f}-q^\star_{b(f),f})\left(\min\left\{U_f'^{-1}\left(\frac{q_{b(f),f}}{K}\right),M\right\}-U_f'^{-1}\left(\frac{q^\star_{b(f),f}}{K}\right)\right) \qquad (5.27) \\
& +\sum_{n,f} q_{n,f}(x_f\mathcal{I}_{n=b(f)}+s^{(f)}_{(p(n,f),n)}\mathcal{I}_{n\neq b(f)}-s^{(f)}_{(n,c(n,f))}) \qquad (5.28) \\
& +\sum_{n,f} q^\star_{n,f}(s^{(f)}_{(n,c(n,f))}-s^{(f)}_{(p(n,f),n)}\mathcal{I}_{n\neq b(f)}-x_f\mathcal{I}_{n=b(f)}) \qquad (5.29) \\
& +B_1. \qquad (5.30)
\end{aligned}
$$

Notice the similarity of (5.27), (5.28) and (5.29) to (5.18), (5.19) and (5.20), respectively. We will use our arguments in the proof of Theorem 5.1 to complete this proof.

Let us first concentrate on (5.28). Notice that we have

$$\begin{aligned}\sum_{n,f} q_{n,f}(s^{(f)}_{(n,c(n,f))} - s^{(f)}_{(p(n,f),n)}\mathcal{I}_{n\neq b(f)}) &= \sum_{f\in\mathcal{F}} \sum_{\{(n,m):H^f_{(n,m)}=1\}} s^{(f)}_{(n,m)}(q_{n,f} - q_{m,f}) \\ &\geq \sum_{f\in\mathcal{F}} \sum_{\{(n,m):H^f_{(n,m)}=1\}} \mu^{(f)}_{(n,m)}(q_{n,f} - q_{m,f}) - B \\ &= \sum_{n,f} q_{n,f}(\mu^{(f)}_{(n,c(n,f))} - \mu^{(f)}_{(p(n,f),n)}\mathcal{I}_{n\neq b(f)}) - B\end{aligned}$$

where the inequality is due to Lemma 5.1. Therefore, we can write

$$\begin{aligned}(5.28) &\leq B + (5.19) \\ &\leq B\end{aligned}$$

where the last inequality is due to our analysis of (5.19) in the proof of Theorem 5.1.

Next, we focus on (5.29). But, we already know from our analysis of (5.20) that

$$\begin{aligned}\sum_{f\in\mathcal{F}} x^\star_f q^\star_{b(f),f} &\geq \sum_{l\in\mathcal{L}} W^\star_l \mu_l \\ &\overset{(a)}{\geq} \sum_{l\in\mathcal{L}} W^\star_l s_l \\ &= \sum_{n,f} q^\star_{n,f}(s^{(f)}_{(n,c(n,f))} - s^{(f)}_{(p(n,f),n)}\mathcal{I}_{n\neq b(f)})\end{aligned}$$

where inequality (a) follows from the fact that $s_l \leq \mu_l$ for all $l \in \mathcal{L}$. Thus, we must have $(5.29) \leq 0$.

After combining these results, and letting $\bar{B} = B + B_1$, we get the following upper bound on the mean drift expression.

$$E[\Delta V_t(\mathbf{q};\mathbf{q}^\star)] \leq \bar{B} + \sum_{f\in\mathcal{F}}(q_{b(f),f} - q^\star_{b(f),f})\left(\min\left\{U'^{-1}_f\left(\frac{q_{b(f),f}}{K}\right), M\right\} - U'^{-1}_f\left(\frac{q^\star_{b(f),f}}{K}\right)\right),$$

which is in the exact same form with the expression studied in Lemma 5.2. Thus, we have

$$E[\Delta V_t(\mathbf{q};\mathbf{q}^\star)] \leq -\frac{\delta}{K^\sigma}\|\mathbf{q}-\mathbf{q}^\star\|\mathcal{I}_{\|\mathbf{q}-\mathbf{q}^\star\|\geq cK^\sigma} + \zeta\mathcal{I}_{\|\mathbf{q}-\mathbf{q}^\star\|<cK^\sigma},$$

as claimed. □

Theorem 5.3. *The Markov chain* $\mathbf{q}[t]$ *is positive recurrent.*

Proof. The result follows from the application of Foster-Lyapunov criterion [52, Proposition 5.3] using the result of Theorem 5.2. □

Theorem 5.4. *There exists a positive constant* $\bar{c}$*, that depends on* Λ*, the utility function set* $\{U_f(\cdot)\}$*, and the moments of the arrival processes, such that for each* $\mathbf{q}^\star \in \mathbb{Q}_K^\star$*,*

$$E\left[\|\mathbf{q}^\infty - \mathbf{q}^\star\|\right] \;\leq\; \bar{c}(K)^\sigma, \qquad \textit{for large } K \tag{5.31}$$

where $\mathbf{q}^\infty$ *is a notation used to denote the state of the Markov chain in steady-state and* $\|\cdot\|$ *denotes the Euclidean distance.*

Proof. We follow the same line of reasoning as we did in the proof of Theorem 4.2. Hence, we move it to the appendix. □

Theorem 5.4 puts an upper bound on the difference of the queue lengths of the network to the set $\mathbb{Q}_K^\star$ that is obtained from the Lagrange multipliers of the optimization problem. The next theorem, uses this result to state that the mean rate vector can be made to get arbitrarily close the the optimal rate vector $\mathbf{x}^\star$ by choosing K large enough.

Theorem 5.5. *The mean of the stationary rate vector converges to* $\mathbf{x}^\star$ *as* K *increases, i.e.*

$$E[\mathbf{x}^\infty] \to \mathbf{x}^\star \qquad \textit{as } K \to \infty,$$

where $\mathbf{x}^\infty$ *is defined by* $x_f^\infty = \min\left\{U_f'^{-1}\left(\frac{q^\infty_{b(f),f}}{K}\right), M\right\}$ *for all* $f \in \mathcal{F}$*.*

Proof. If we divide both sides of the expression (5.31) by K, then we can write: for each $f \in \mathcal{F}$,

$$E[|\frac{q^\infty_{b(f),f}}{K} - \frac{q^\star_{b(f),f}}{K}|] \leq \bar{c}(K)^{\sigma-1} \to 0, \qquad \text{as } K \to \infty. \tag{5.32}$$

Recall the relationship between the queue-lengths and the rates:

$$E[x_f \mid \mathbf{q}] = \min\left\{U_f'^{-1}\left(\frac{q_{b(f),f}}{K}\right), M\right\}.$$

If we take the expectation of both sides using the stationary distribution of the Markov chain, $\mathbf{q}[t]$, we get

$$E[x_f^\infty] = E\left[\min\left\{U_f'^{-1}\left(\frac{q^\infty_{b(f),f}}{K}\right), M\right\}\right].$$

Then, we can write

$$\begin{aligned}
|E[x_f^\infty] - x_f^\star| &\leq E[|x_f^\infty - x_f^\star|] \\
&= E\left[\left|\min\left\{U_f'^{-1}\left(\frac{q_{b(f),f}}{K}\right), M\right\} - U_f'^{-1}\left(\frac{q^\star_{b(f),f}}{K}\right)\right|\right] \\
&= |\frac{1}{U_f''(\tilde{x})}|E\left[\left|\frac{q^\infty_{b(f),f}}{K} - \frac{q^\star_{b(f),f}}{K}\right|\right]
\end{aligned}$$

for some $\tilde{x} \in [0, M]$ due to Taylor's expansion. Thus, we can invoke the condition (5.1) on the utility functions to claim that

$$\begin{aligned}
|E[x_f^\infty] - x_f^\star| &\leq mE\left[\left|\frac{q^\infty_{b(f),f}}{K} - \frac{q^\star_{b(f),f}}{K}\right|\right] \\
&\leq \bar{c}m(K)^{\sigma-1} \\
&\to 0 \qquad \text{as } K \to \infty,
\end{aligned}$$

where the second inequality follows from (5.32). □

CHAPTER 6

ASYNCHRONOUS CONGESTION CONTROL IN MULTI-HOP WIRELESS NETWORKS

The congestion controllers that we studied in Chapters 4 and 5 used the actual buffer length information as an indicator of the price of the routes in order to determine the flow rate levels. Alternatively, the prices of the resources could be computed separately and communicated between the nodes to indicate their congestion levels. However, in an actual implementation, the price and rate information at a node may take a random and unbounded amount of time to reach far away from it. In this chapter, we will consider a multi-hop wireless network over which such an asynchronous congestion controller operates. The details of the underlying scheduler is not known to the congestion controller, but it is assumed that the it satisfies a few reasonable conditions that will be described later.

The chapter is organized as follows. In Section 6.1, we present the interference model and the asynchronous congestion controller mechanism along with the problem statement. In Section 6.2, we analyze the system and prove its convergence properties.

6.1 System model and Problem Statement

We consider a multi-hop wireless network model as in 5.1 except that we assume the following simple interference model: in every slot, each node can only transmit to (or receive from) at most one of its neighbors. There are no other interference constraints. Thus, the set of

links that can be simultaneously active form a matching if the wireless network is represented as a graph.

In addition, we assume the following additional condition on the utility functions:

- For every $\bar{M} \in (0, \infty)$, there exists a constant C such that

$$\left| U_f'' \left(U_f'^{-1}(y) \right) \right| \geq Cy \qquad \forall y \geq \bar{M} \tag{6.1}$$

This condition is also satisfied by all the functions in the form (5.3). We assume that the link rates are the same and equal to c packets/slot, when they are scheduled. For ease of presentation, we will take $c = 1$. Thus, the maximum rate at which any node $n \in \mathcal{N}$ can be receive and transmit data is 1.

For such an interference model, it is not difficult to see that the capacity region, Λ, satisfies

Fact 6.1.

$$\Lambda \subset \{\mathbf{x} : 2 \sum_{f \in R_n} x_f + \sum_{f \in S_n \cup D_n} x_f \leq 1, \, \forall n \in \mathcal{N}\},$$

where we define

$$\begin{aligned} S_n &= \{\text{Set of flows that are generated at node } n\} \\ D_n &= \{\text{Set of flows that are destined to node } n\} \\ R_n &= \{\text{Set of flows that for which } n \text{ is a relay node}\} \end{aligned}$$

Also, we can state the following fact that puts a lower bound on the capacity region.

Fact 6.2.

$$\Lambda \supset \{\mathbf{x} : 2 \sum_{f \in R_n} x_f + \sum_{f \in S_n \cup D_n} x_f \leq \frac{2}{3}, \, \forall n \in \mathcal{N}\},$$

This fact is discussed in [61, 62], and is based on a work by Shannon [63].

In our formulation, we will simply assume that the scheduling algorithm can stabilize the system for those flow rates that lies within a region $\Omega \subset \Lambda$ that is defined by

$$\Omega = \{\mathbf{x} : 2 \sum_{f \in R_n} x_f + \sum_{f \in S_n \cup D_n} x_f \leq \beta, \, \forall n \in \mathcal{N}\}$$

for some $\beta \in (0,1)$. It is known that a greedy distributed scheduler will yield an Ω with $\beta = 1/3$ [64, 65]. Also, it is not difficult to see that Ω is a convex region.

Our goal is to have the flow rates converge to the point that satisfies:

$$\begin{aligned} \mathbf{x}^\star \in \quad & \arg\max \quad \sum_{f\in\mathcal{F}} U_f(x_f) \\ & s.t. \qquad \mathbf{x} \in \Omega, \end{aligned} \tag{6.2}$$

Since Ω is convex, and $\{U_f(\cdot)\}$ is strictly concave, there exists a unique $\mathbf{x}^\star$. Next, we describe the Asynchronous Congestion Controller that we are going to study.

Definition 6.1 (Asynchronous Congestion Controller). *At the beginning of each time slot,* t,

Source f computes:

$$x_f[t] = min\left\{M, U_f'^{-1}\left(\frac{q_f(\tau^{(f)}[t])}{K}\right)\right\}$$

Node n computes:

$$p_n[t+1] \quad = \quad \left(p_n[t] + \sum_{f\in S_n\cup D_n} x_f(\tau_f^{(n)}[t]) + 2\sum_{f\in R_n} x_f(\tau_f^{(n)}[t]) - \beta\right)^+,$$

where $q_f(\tau^{(f)}[t])$ *is defined to be equal to*

$$\sum_{n\in Route(f)} \left(2p_n(\tau_n^{(f)}[t])\mathcal{I}_{f\in R_n} + p_n(\tau_n^{(f)}[t])\mathcal{I}_{f\in S_n\cup D_n}\right),$$

and $M > 2c$*, and we define* $\tau_n^{(f)}[t] \in [0,t]$ *to be the time slot at which the price information of node* n *(i.e.* $p_n[\cdot]$*) was sent, given that it is received at source* f *at slot* t*. And similarly,* $\tau_f^{(n)}(t) \in [0,t]$ *is the time slot at which the rate information of source* f *(i.e.* $x_f[\cdot]$*) was sent, given that it is received by node* n *at slot* t*.*

In this algorithm, $p_n[t]$, represents the price of using a unit amount of time of node n. Then, $q_f(\cdot)$ is the price of transferring unit amount of flow f traffic over its route. Also, note that $t - \tau_n^{(f)}(t)$ is the random variable representing the number of slots it took for $p_n(\cdot)$ to be transfered from node n to source f by the underlying scheduling mechanism, given that it is received at time slot t. Further, let $\tau^{(f)}(t)$ is the vector of $\tau_n^{(f)}(t)$ for source f at time t, and

also, $\tau^{(n)}(t)$ be the vector of $\tau_f^{(n)}(t)$ for node n at time t. Finally, K is a positive constant, and we are interested in the behavior of the system when K is large.

This model contains the essential components of the asynchronous operation of the network. It is referred to as "Totally Asynchronous" in [5]. Specifically, the amount of time it takes for the flow rate and node price information to reach any node or a source is captured by a random variable. In the next section, we will prove that it asymptotically solves the resource allocation problem described in (6.2). We note that the system is still assumed to operate in a time slotted fashion, where slots are synchronized at all the nodes.

Since the flow rate and price information can only be conveyed by the underlying scheduler, the statistics of the feedback delays are dependent on the specific scheduler design. In our analysis, we will impose a single constraint on the tail of the delay distribution, without specifying the exact characteristics of the scheduler.

Assumption 6.1 (Delay condition). *There exists a large D such that*

$$\mathbf{P}\left(\left|t-\tau_n^{(f)}[t]\right|>TD\right)\leq e^{-\nu(D)T} \qquad \forall n,f$$

$$\mathbf{P}\left(\left|t-\tau_f^{(n)}[t]\right|>TD\right)\leq e^{-\eta(D)T} \qquad \forall n,f$$

where ν and η are some positive numbers depending on D.

This assumption can be made to hold by allowing links to be active with small probability even when there is no data to transmit, but congestion information is conveyed.

In the following sections, we will provide an analysis of the convergence properties of the asynchronous congestion controller.

6.2 Analysis of the Asynchronous Congestion Controller

We will start this section by characterizing the optimal rate allocation following the same line of reasoning as we did in Chapter 5. Then, we will prove the global asymptotic stability of the mechanism for the fluid model. And finally, we will provide the proof for the original discrete-time model.

6.2.1 Characterization of the Optimal Rate Allocation

We start by noting that the optimization problem in (6.2) can be solved by using Lagrange multipliers. The Lagrangian and the Dual function of the problem (6.2) are:

$$\begin{aligned} L(\mathbf{x},\lambda) &= \sum_{f\in\mathcal{F}} U_f(x_f) - \sum_{n\in\mathcal{N}} \left\{ \lambda_n \left(\sum_{f\in S_n\cup D_n} x_f + 2\sum_{f\in R_n} x_f - \beta \right) \right\} \\ D(\lambda) &= \max_{\mathbf{x}\geq 0} L(\mathbf{x},\lambda) \\ &= \sum_{f\in\mathcal{F}} \max_{x_f\geq 0} \left(U_f(x_f) - x_f \sum_{n\in Route(f)} (2\lambda_n \mathcal{I}_{f\in R_n} + \lambda_n \mathcal{I}_{f\in S_n\cup D_n}) \right) \\ &\quad +\beta\sum_n \lambda_n \end{aligned}$$

where λ_n is the Lagrange multiplier associated with the n^{th} constraint of (6.2). Then, the dual optimization problem to (6.2) is given by: $\min_{\lambda\geq 0} D(\lambda)$. It can be shown that for the problem we consider, there is no duality gap [60]. Thus, there exists a nonempty set of Lagrange multipliers, $\Psi^\star$, any element (say $\lambda^\star$) of which satisfies: $D(\lambda^\star) = \sum_f U_f(x_f^\star)$. But for any feasible $\mathbf{x}$ of the primal problem (6.2), we must have:

$$\sum_{n\in\mathcal{N}} \lambda_n^\star \left(\sum_{f\in S_n\cup D_n} x_f + 2\sum_{f\in R_n} x_f - \beta \right) \leq 0$$

because the expression in the parenthesis can never be positive for a feasible rate vector, and $\lambda^\star$ is a nonnegative vector. Thus, we must have $\mathbf{x}^\star$ as the optimizer of the Lagrangian $L(\mathbf{x},\lambda^\star)$, and also have the pair $(\mathbf{x}^\star,\lambda^\star)$ satisfy:

$$\sum_{n\in\mathcal{N}} \lambda_n^\star \left(\sum_{f\in S_n\cup D_n} x_f^\star + 2\sum_{f\in R_n} x_f^\star - \beta \right) \leq 0, \tag{6.3}$$

which is also called the *complementary slackness condition* in the optimization literature. From the Lagrangian, it is easy to see that $(\mathbf{x}^\star,\lambda^\star)$ should also satisfy:

$$x_f^\star = U_f'^{-1} \left(\sum_{n\in Route(f)} (2\lambda_n^\star \mathcal{I}_{f\in R_n} + \lambda_n^\star \mathcal{I}_{f\in S_n\cup D_n}) \right) \tag{6.4}$$

Let us define $\mathbf{p}^\star$ and $\mathbf{q}^\star$ as follows: $p_n^\star \stackrel{\triangle}{=} K\lambda^\star$,

$$q_f^\star \stackrel{\triangle}{=} \sum_{n\in Route(f)} (2p_n^\star \mathcal{I}_{f\in R_n} + p_n^\star \mathcal{I}_{f\in S_n\cup D_n}) \tag{6.5}$$

where K is some multiplicative factor. We define $\Psi^\star_K = K\Psi^\star$, i.e., if $\lambda^\star \in \Psi^\star$ then the corresponding $\mathbf{p}^\star \in \Psi^\star_K$. Notice that we can re-write (6.4) and the complementary slackness condition (6.3) in terms of $\mathbf{p}^\star$ and $\mathbf{q}^\star$:

$$\begin{aligned} x^\star_f &= U'^{-1}_f\left(\frac{q^\star_f}{K}\right) \\ 0 &= \left(\sum_{f\in S_n\cup D_n} x^\star_f + 2\sum_{f\in R_n} x^\star_f - \beta\right)^+_{p^\star_n} \end{aligned} \tag{6.6}$$

where we recall the definition of $(y)^+_z$ as being equal to y if $z \geq 0$ and zero if $y \leq 0$ and $z = 0$.

Given the characterization of the optimal point, we start our analysis of the system starting with the continuous-time fluid model.

6.2.2 Continuous-time Fluid model of the Congestion Controller

The congestion control algorithm for the fluid model is described as follows:

Definition 6.2 (Continuous-time Congestion Controller). *At time t,*

Source f computes:

$$x_f(t) = U'^{-1}_f\left(\frac{q_f(t)}{K}\right)$$

Node n computes:

$$\dot{p}_n(t) = \left(\sum_{f\in S_n\cup D_n} x_f(t) + 2\sum_{f\in R_n} x_f(t) - \beta\right)^+_{p_n(t)}$$

where

$$q_f(t) \stackrel{\triangle}{=} \sum_{n\in Route(f)} [2p_n(t)\mathcal{I}_{f\in R_n} + p_n(t)\mathcal{I}_{f\in S_n\cup D_n}] \tag{6.7}$$

Notice that here we have assumed synchronous computation: information updates at the sources and the nodes occur instantaneously and simultaneously at every time instant. In later sections, when considering the discrete-time model, we will remove this key assumption and develop a fully asynchronous algorithm for congestion control. Nevertheless, the analysis of the continuous-time system will be useful in understanding the more realistic model. Next, we state the theorem that proves the convergence properties of the congestion controller.

Theorem 6.1. *Starting from any initial* $\mathbf{p}(0)$, $\mathbf{x}(t)$ *eventually reaches* $\mathbf{x}^\star$ *as* $t \to \infty$.

Proof. Consider the Lyapunov function:

$$V(\mathbf{p};\mathbf{p}^\star) = \frac{1}{2}\sum_n (p_n - p_n^\star)^2,$$

which is defined for some $\mathbf{p}^\star \in \Psi_K^\star$. Then, the time derivative of this function at t satisfies

$$\dot{V}(\mathbf{p}(t),\mathbf{p}^\star) \;=\; \sum_n \left\{ (p_n(t) - p_n^\star) \left(\sum_{f\in S_n \cup D_n} x_f(t) + 2\sum_{f\in R_n} x_f(t) - \beta \right)^+_{p_n(t)} \right\}$$

We first consider the case when $\mathbf{p}(t) \in \Psi_K^\star$: note that the rate vector associated with $\mathbf{p}(t)$ has to be the unique optimizer of (6.2), i.e. $\mathbf{x}^\star$. But, by utilizing the complementary slackness condition provided in (6.6) we can easily conclude that

$$\dot{V}(\mathbf{p}(t),\mathbf{p}^\star) = 0 \qquad \text{for all } \mathbf{p}(t) \in \Psi_K^\star. \tag{6.8}$$

Next, we consider $\dot{V}(\mathbf{p}(t),\mathbf{p}^\star)$ for any $\mathbf{p}(t) \geq 0$: define

$$y_n(t) \;\stackrel{\triangle}{=}\; \sum_{f\in S_n\cup D_n} x_f(t) + 2\sum_{f\in R_n} x_f(t) \tag{6.9}$$

Then we have:

$$\begin{aligned}
\dot{V}(\mathbf{p}(t),\mathbf{p}^\star) &= \sum_n (p_n(t) - p_n^\star)\,(y_n - \beta)^+_{p_n(t)} \\
&\leq \sum_n (p_n(t) - p_n^\star)\,(y_n(t) - \beta) \\
&= \sum_n (p_n(t) - p_n^\star)\,(y_n(t) - y_n^\star) + \sum_n (p_n(t) - p_n^\star)\,(y_n^\star - \beta)
\end{aligned}$$

where the inequality follows from the fact that if $p_n(t) = 0$ and $y_n(t) - \beta \leq 0$, then $(y_n(t) - \beta)^+_{p_n(t)} = 0$. Otherwise, $(y_n(t) - \beta)^+_{p_n(t)} = (y_n(t) - \beta)$.

Also, from the complementary slackness condition, we have that if $p_n^\star > 0$, then $y_n^\star = \beta$. Otherwise, if $p_n^\star = 0$, then $y_n^\star \leq \beta$. This fact implies

$$\sum_n (p_n(t) - p_n^\star)\,(y_n^\star - \beta) \leq 0 \tag{6.10}$$

Therefore,

$$\begin{aligned}
\dot{V}(\mathbf{p}(t),\mathbf{p}^\star) &\leq \sum_n (p_n(t)-p_n^\star)\,(y_n(t)-y_n^\star) \\
&= \sum_n (p_n(t)-p_n^\star)\left(\sum_{f\in S_n\cup D_n}(x_f(t)-x_f^\star)+2\sum_{f\in R_n}(x_f(t)-x_f^\star)\right) \\
&= \sum_f \left(x_f(t)-x_f^\star\right)\left(\sum_{n\in Route(f)}[(p_n(t)-p_n^\star)\mathcal{I}_{f\in S_n\cup D_n}+2(p_n(t)-p_n^\star)\mathcal{I}_{f\in R_n}]\right) \\
&= \sum_f \left(x_f(t)-x_f^\star\right)\left(q_f(t)-q_f^\star\right) \\
&= K\sum_f \left(x_f(t)-x_f^\star\right)\left(U_f'(x_f(t))-U_f'(x_f^\star)\right) \\
&\leq 0,
\end{aligned}$$

with strict inequality when $\mathbf{p}(t)\notin\Psi_K^\star$, due to the strict concavity assumption of $U_f(\cdot)$. Then, by combining this result with (6.8) and by invoking LaSalle's theorem [66, Theorem 4.4], we conclude that $\mathbf{p}(t)\stackrel{t\to\infty}{\longrightarrow}\Psi_K^\star$ and hence $\mathbf{x}(t)\stackrel{t\to\infty}{\longrightarrow}\mathbf{x}^\star$. □

6.2.3 Discrete-time Congestion Controller

In this section, we will prove the stability of the congestion controller that was described in Definition 6.1. We start our analysis by introducing the notation:

$$y_n(\tau^{(n)}[t])\stackrel{\triangle}{=}\sum_{f\in S_n\cup D_n}x_f(\tau_f^{(n)}[t])+2\sum_{f\in R_n}x_f(\tau_f^{(n)}[t])$$

Notice that $q_f(\tau^{(f)}[t])$ is the estimated price of flow f's path at time t which is computed using delayed versions of the actual prices. On the other hand, $q_f[t]$ [defined in (6.7)] assumes the instantaneous knowledge of all the prices on flow f's path. Similar interpretation holds for $y_n(\tau^{(n)}[t])$ and $y_n[t]$ [defined in (6.9)].

Consider the Lyapunov function, $V(\cdot)$, used in the continuous-time analysis. The following theorem characterizes the drift of this Lyapunov function:

Theorem 6.2. *Let $\mathcal{P}(t)$ be the sequence of vectors $(\mathbf{p}(t), \mathbf{p}(t-1), \cdots, \mathbf{p}(0))$. Then the mean drift satisfies:*

$$\begin{aligned} E[\Delta V_t] &\stackrel{\triangle}{=} E[V(\mathbf{p}[t+1]; \mathbf{p}^\star) - V(\mathbf{p}[t]; \mathbf{p}^\star) \mid \mathcal{P}[t]] \\ &\leq -\frac{\delta}{K^\sigma}\|\mathbf{q}[t] - \mathbf{q}^\star\| + \hat{B} \end{aligned} \tag{6.11}$$

for some constant $\hat{B} < \infty$ and $\delta > 0$, $\sigma \in (0,1)$. Recall that, $\|\cdot\|$ denotes Euclidean distance.

Furthermore, there exists some $\tilde{B} < \infty$, and $c > 0$ such that

$$E[\Delta V_t] \leq -cK\|\hat{\mathbf{x}}[t] - \mathbf{x}^\star\|^2 + \tilde{B}, \tag{6.12}$$

where we define $\hat{x}_f[t] = \min\left\{M, U_f'^{-1}\left(\frac{q_f[t]}{L}\right)\right\}$, i.e., it is the rate of flow f at time t if all the price information were instantaneously available at the sources.

Before we provide the proof of Theorem 6.2 we give the following lemma that will be used in the proof.

Lemma 6.1. *We have*

$$\sum_f \left\{\left(q_f[t] - q_f^\star\right)\left(\hat{x}_f[t] - x_f^\star\right)\right\} \leq -cK\|\hat{\mathbf{x}}[t] - \mathbf{x}^\star\|^2,$$

where c is a positive constant which is independent of K.

Proof. We start by adding and subtracting $KU_f'(\hat{x}_f[t])$ into the first factor within the summation, which yields

$$\begin{aligned} \sum_f \left\{\left(q_f[t] - q_f^\star\right)\left(\hat{x}_f[t] - x_f^\star\right)\right\} &= \sum_f \left(q_f[t] - KU_f'(\hat{x}_f[t])\right)\left(\hat{x}_f[t] - x_f^\star\right) \qquad (6.13) \\ &\quad + \sum_f \left(KU_f'(\hat{x}_f[t] - KU_f'(x_f^\star)\right)\left(\hat{x}_f[t] - x_f^\star\right) \qquad (6.14) \end{aligned}$$

We will analyze the terms (6.13) and (6.14) separately. We claim that (6.13)≤ 0. To see this, we first note that, if $\hat{x}_f[t] < M$, then $q_f[t] = KU_f'(\hat{x}_f[t])$ and hence we have

$$\left(q_f[t] - KU_f'(\hat{x}_f[t])\right)\left(\hat{x}_f[t] - x_f^\star\right) = 0.$$

If, on the other hand, we have $\hat{x}_f[t] = M > x_f^\star$, then $q_f[t] < U_f'(\hat{x}_f[t])$ which implies that

$$\left(q_f[t] - KU_f'(\hat{x}_f[t])\right)\left(\hat{x}_f[t] - x_f^\star\right) \leq 0.$$

Combining these two observations proves our claim.

Next, we turn our attention to (6.14). We start by noting that

$$\left(KU_f'(\hat{x}_f[t] - KU_f'(x_f^\star)\right)\left(\hat{x}_f[t] - x_f^\star\right) \;\; = \;\; -K\left|U_f'(\hat{x}_f[t] - U_f'(x_f^\star)\right|\,|\hat{x}_f[t] - x_f^\star|, \quad (6.15)$$

which follows from the strict concavity assumption on $U_f(\cdot)$. Also, due to Taylor expansion, we can find some $z_f[t]$ between $\hat{x}_f[t]$ and $x_f^\star$ for which,

$$U_f'(\hat{x}_f[t]) - U_f'(x_f^\star) = (\hat{x}_f[t] - x_f^\star)U_f''(z_f[t]).$$

Using the assumption in (5.1), we can thus claim that there exists some $c > 0$ which yields

$$\left|U_f'(\hat{x}_f[t]) - U_f'(x_f^\star)\right| \geq c|\hat{x}_f[t] - x_f^\star|.$$

Substituting this into (6.15) and then (6.15) into (6.14) yields the result. □

Now, we provide the proof of Theorem 6.2.

Proof of Theorem 6.2. Notice that we can write

$$p_n[t+1] \;\; = \;\; p_n[t] + y_n(\tau^{(n)}[t]) - \beta + u_n[t],$$

where $u_n[t]$ is a nonnegative parameter that assures the non-negativity of $p_n[t+1]$. We first start by showing that we can ignore the $u_n[t]$ term in the iteration. Towards this end, we can write

$$\begin{aligned}(p_n[t+1] - p_n^\star)^2 \;\; &= \;\; \left(p_n[t] + y_n(\tau^{(n)}[t]) - \beta - p_n^\star\right)^2 && (6.16)\\ &\quad\;\; \left(p_n[t] + y_n(\tau^{(n)}[t]) - \beta\right) + u_n^2[t] && (6.17)\\ &\quad\;\; -2u_n[t]p_n^\star, && (6.18)\end{aligned}$$

for any n. Since $p_n^\star, u_n[t] \geq 0$, we have (6.18)≤ 0. We also claim that (6.17)≤ 0. To see this, we observe that: $u_n[t] = 0$ if $p_n[t] + y_n(\tau^{(n)}[t]) - \beta > 0$, and that $u_n[t] = -(p_n[t] + y_n(\tau^{(n)}[t]) - \beta)$

if $u_n[t] > 0$. These two observations imply that (6.17)$= -u_n^2[t] \leq 0$. This completes the proof of the claim that $(p_n[t+1] - p_n^\star)^2 \leq (6.16)$.

By using this result in the definition of ΔV_t we get

$$\begin{aligned}
E[\Delta V_t] &\leq B + \sum_n (p_n[t] - p_n^\star)\, E\left[y_n(\tau^{(n)}[t]) - \beta \mid \mathcal{P}[t]\right] \\
&= B + \sum_n (p_n[t] - p_n^\star)\, E\left[y_n(\tau^{(n)}[t]) - y_n^\star \mid \mathcal{P}[t]\right] + \sum_n (p_n[t] - p_n^\star)\,(y_n^\star - \beta) \\
&\overset{(a)}{\leq} B + \sum_n (p_n[t] - p_n^\star)\, E\left[y_n(\tau^{(n)}[t]) - y_n^\star \mid \mathcal{P}[t]\right] \\
&= B + \sum_n (p_n[t] - p_n^\star)\, E\left[y_n[t] - y_n^\star \mid \mathcal{P}[t]\right] \\
&\quad + \sum_n (p_n[t] - p_n^\star)\, E\left[y_n(\tau^{(n)}[t]) - y_n[t] \mid \mathcal{P}[t]\right],
\end{aligned}$$

where inequality (a) follows from (6.10). Now, looking at the last term:

$$\begin{aligned}
&E\left[\textstyle\sum_n (p_n[t] - p_n^\star)\,(y_n[t] - y_n^\star) \mid \mathcal{P}[t]\right] \\
&= E\left[\sum_n (p_n[t] - p_n^\star)\left(\sum_{f \in S_n \cup D_n} x_f[t] + 2\sum_{f \in R_n} x_f[t] - \sum_{f \in S_n \cup D_n} x_f^\star - 2\sum_{f \in R_n} x_f^\star\right) \mid \mathcal{P}[t]\right] \\
&= E\left[\sum_f \left(x_f[t] - x_f^\star\right)\left(\sum_{n \in f} [(p_n[t] - p_n^\star).\mathcal{I}_{f \in S_n \cup D_n} + 2(p_n[t] - p_n^\star).\mathcal{I}_{f \in R_n}]\right) \mid \mathcal{P}[t]\right] \\
&= \sum_f E\left[\left(x_f[t] - x_f^\star\right) \mid \mathcal{P}[t]\right]\left(q_f[t] - q_f^\star\right) \\
&= \sum_f \left(q_f[t] - q_f^\star\right) E\left[x_f[t] - \hat{x}_f[t] \mid \mathcal{P}[t]\right] + \sum_f \left(q_f[t] - q_f^\star\right)\left(\hat{x}_f[t] - x_f^\star\right)
\end{aligned}$$

Therefore, we can rewrite the upper bound of $E[\Delta V_t]$ as:

$$\begin{aligned}
E[\Delta V_t] \leq\ & B + \sum_f \left(q_f[t] - q_f^\star\right)\left(\hat{x}_f[t] - x_f^\star\right) && (6.19)\\
& + \sum_f \left(q_f[t] - q_f^\star\right) E\left[x_f[t] - \hat{x}_f[t] \mid \mathcal{P}[t]\right] && (6.20)\\
& + \sum_n (p_n[t] - p_n^\star)\, E\left[y_n(\tau^{(n)}[t]) - y_n[t]] \mid \mathcal{P}[t]\right], && (6.21)
\end{aligned}$$

where we recall that $x_f[t] = \min\left\{M, U_f'^{-1}\left(\frac{q_f(\tau^{(f)}[t])}{K}\right)\right\}$ and $\hat{x}_f[t] = \min\left\{M, U_f'^{-1}\left(\frac{q_f[t]}{K}\right)\right\}$.

By the Lemma 5.2, we know that for some $\sigma \in (0,1)$,

$$(6.19) \leq -\frac{\delta}{K^\sigma}\|\mathbf{q}[t] - \mathbf{q}^\star\|\mathcal{I}_{\|\mathbf{q}[t]-\mathbf{q}^\star\| \geq cK^\sigma} + \zeta\mathcal{I}_{\|\mathbf{q}[t]-\mathbf{q}^\star\| \leq cK^\sigma} \tag{6.22}$$

Alternatively, by Lemma 6.1, we can write

$$(6.19) \quad \leq \quad -cK\|\hat{\mathbf{x}}[t] - \mathbf{x}^\star\|^2. \tag{6.23}$$

We will utilize these two alternative bounds to get the two results stated in Theorem 6.2.

Next, let us consider (6.20). From the Taylor's expansion, we have:

$$|x_f[t] - \hat{x}_f[t]| \leq \left| \frac{q_f[t] - q_f(\tau^{(f)}[t])}{K.U_f''(\tilde{x})} \right|$$

for some $\tilde{x} \in [0, M]$.

It is not difficult to see that we can find some $\bar{B} < \infty$ which satisfies $|q_f[t+1] - q_f[t]| \leq \bar{B}, \forall f$. Then invoking the Assumption 6.1 yields

$$E\left[\left| \frac{q_f[t] - q_f(\tau^{(f)}[t])}{K} \right| \mid \mathcal{P}[t] \right] \quad \leq \quad \left(\sum_T \frac{\bar{B}TD}{K} e^{-\nu(D)T} \right) \leq \frac{c_1}{K}$$

for some constant c_1. This fact implies that across time slots the q_f values does not change much compared with K.

Now, for each flow f, we have the following cases:

Case 1: $q_f[t] \leq KU_f'(M)$

Using the assumption (5.1) on the utility functions, we have:

$$\begin{aligned} \left| q_f[t] - q_f^\star \right| E\left[|x_f[t] - \hat{x}_f[t]| \mid \mathcal{P}[t] \right] &\leq \left| q_f[t] - q_f^\star \right| E\left[\left| \frac{q_f[t] - q_f(\tau^{(f)}[t])}{K.U_f''(\tilde{x})} \right| \mid \mathcal{P}[t] \right] \\ &\leq \left| q_f[t] - q_f^\star \right| \frac{mc_1}{K} \leq C_1 \end{aligned}$$

for some constant $C_1 < \infty$. The last step follows from the fact that $q_f^\star = \varrho K$ for some constant ϱ. This is true, because $p_n^\star = K\lambda_n^\star$ and $q_f^\star$ satisfies (6.5).

Case 2: $q_f[t] \geq KU_f'(M)$ or $\frac{q_f[t]}{K} \geq U_f'(M)$

From the assumption (6.1) on utility functions, we have:

$$\left| U_f'' \left(U_f'^{-1} \left(\frac{q_f[t]}{K} \right) \right) \right| \geq c_2 \frac{q_f[t]}{K}$$

for some constant $c_2 > 0$.

Therefore,

$$\begin{aligned}
\left|q_f[t]-q_f^\star\right| E\left[|x_f[t]-\hat{x}_f[t]| \mid \mathcal{P}[t]\right] &\leq \left|q_f[t]-q_f^\star\right| E\left[\left|\frac{q_f[t]-q_f(\tau^{(f)}[t])}{K.U_f''(\tilde{x})}\right| \mid \mathcal{P}[t]\right] \\
&\overset{(a)}{\leq} \left|q_f[t]-q_f^\star\right| \left|\frac{c_1}{K.U_f''\left(U_f'^{-1}(\frac{q_f[t]}{K})\right)}\right| \\
&\leq \left|q_f[t]-q_f^\star\right| \frac{c_1}{K}.\frac{1}{c_2\frac{q_f[t]}{K}} \\
&\leq \left|1-\frac{q_f^\star}{q_f[t]}\right| \frac{c_1}{c_2} \overset{(b)}{\leq} C_2
\end{aligned}$$

for some constant $C_2 < \infty$. The inequality (a) follows from the fact that, compared to K, the q_f values do not change much across time slots, and inequality (b) is due to the fact that $q_f^\star = \varrho K$ for some constant $\varrho > 0$.

Thus, combining the two cases and defining $C_3 = \max\{C_1, C_2\}$, we have

$$(6.20) \leq \sum_f \left|q_f[t]-q_f^\star\right| E\left[|x_f[t]-\hat{x}_f[t]| \mid \mathcal{P}[t]\right] \leq C_3.$$

Finally, we consider (6.21). Observe that:

$$\begin{aligned}
y_n(\tau^{(n)}[t]) - y_n[t] &= \sum_{f\in S_n\cup D_n}\left(x_f(\tau_f^{(n)}[t]) - x_f[t]\right) + 2\sum_{f\in R_n}\left(x_f(\tau_f^{(n)}[t]) - x_f[t]\right) \\
x_f(\tau_f^{(n)}[t]) &= \min\left\{M, U_f'^{-1}\left(\frac{q_f(\tau^{(f)}(\tau_f^{(n)}[t]))}{K}\right)\right\}
\end{aligned}$$

Then we can write (6.21) as

$$\begin{aligned}
(6.21) &= \sum_n (p_n[t]-p_n^\star)\, E\Bigg[\sum_{f\in S_n\cup D_n}\left(x_f(\tau_f^{(n)}[t]) - x_f[t]\right) \\
&\qquad +2\sum_{f\in R_n}\left(x_f(\tau_f^{(n)}[t]) - x_f[t]\right) \mid \mathcal{P}[t]\Bigg] \\
&\leq \sum_n |p_n[t]-p_n^\star|\, E\Bigg[\Bigg|\sum_{f\in S_n\cup D_n}\left(x_f(\tau_f^{(n)}[t]) - x_f[t]\right) \\
&\qquad +2\sum_{f\in R_n}\left(x_f(\tau_f^{(n)}[t]) - x_f[t]\right)\Bigg| \mid \mathcal{P}[t]\Bigg]
\end{aligned}$$

First, we observe that

$$E\left[\left|\sum_{f\in S_n\cup D_n}\Big(x_f(\tau_f^{(n)}[t])-x_f[t]\Big)+2\sum_{f\in R_n}\Big(x_f(\tau_f^{(n)}[t])-x_f[t]\Big)\right|\mid\mathcal{P}[t]\right]$$
$$\leq E\left[2N_{max}\left|x_{\tilde{f}(n)}(\tau_{\tilde{f}(n)}^{(n)}[t])-x_{\tilde{f}(n)}[t]\right|\mid\mathcal{P}[t]\right],$$

where N_{max} is the maximum number of nodes along any flow's path, and

$$\tilde{f}(n)=\underset{f\in R_n\cup S_n\cup D_n}{\arg\max}\left|x_f(\tau_f^{(n)}[t])-x_f[t]\right|$$

Also, for every flow f that go through node n, we always have $p_n\leq q_f$. Therefore,

$$(6.21)\ \leq\ \sum_n 2N_{max}\left|q_{\tilde{f}(n)}[t]+p_n^\star\right|E\left[\left|x_{\tilde{f}(n)}(\tau_{\tilde{f}(n)}^{(n)}[t])-x_{\tilde{f}(n)}[t]\right|\mid\mathcal{P}[t]\right]$$

Now, we can apply the same technique as in the analysis of (6.20), and conclude that: $(6.21)\leq C_4$, for some $C_4<\infty$.

Thus, if we use the upper bound in (6.22), we have

$$\begin{aligned}\mathbf{E}\left[\Delta V_t\right]&\leq -\frac{\delta}{K^\sigma}\|\mathbf{q}[t]-\mathbf{q}^\star\|.\mathcal{I}_{\|\mathbf{q}[t]-\mathbf{q}^\star\|\geq cK^\sigma}+\zeta.\mathcal{I}_{\|\mathbf{q}[t]-\mathbf{q}^\star\|\leq cK^\sigma}+B+C_3+C_4\\&\leq -\frac{\delta}{K^\sigma}\|\mathbf{q}[t]-\mathbf{q}^\star\|+\hat{B}\end{aligned}$$

for some $\hat{B}$.

Instead, if we use the upper bound in (6.23), we get

$$\mathbf{E}\left[\Delta V_t\right]\ \leq\ -cK\|\mathbf{x}[t]-\mathbf{x}^\star\|^2+\tilde{B},$$

This completes the proof of Theorem 6.2. □

Theorem 6.3.

$$\limsup_{T\to\infty}\frac{1}{T}\sum_{t=0}^{T-1}E\left[\frac{\|\mathbf{q}[t]-\mathbf{q}^\star\|}{K}\right]\leq\frac{B}{\delta K^{1-\gamma}}$$

Proof. We start by taking the expectation of both sides of the expression (6.11) over $\mathcal{P}[t]$. Then we vary t from 0 up to T. Thus, we have

$$\begin{aligned}\mathbf{E}\left[V(1)-V(0)\right]&\leq -\frac{\delta}{K^\gamma}E[\|\mathbf{q}(0)-\mathbf{q}^\star\|]+B\\\mathbf{E}\left[V(2)-V(1)\right]&\leq -\frac{\delta}{K^\gamma}E[\|\mathbf{q}(1)-\mathbf{q}^\star\|]+B\\&\vdots\\\mathbf{E}\left[V[T]-V(T-1)\right]&\leq -\frac{\delta}{K^\gamma}E[\|\mathbf{q}(T-1)-\mathbf{q}^\star\|]+B\end{aligned}$$

Therefore, adding both sides of the inequalities and re-arranging the terms, we get

$$\begin{aligned}\frac{1}{T}\sum_{t=0}^{T} E[\|\mathbf{q}[t]-\mathbf{q}^{\star}\|] &\leq \frac{\mathbf{E}\left[V(0)-V[T]\right]K^{\gamma}}{T\delta}+\frac{BK^{\gamma}}{\delta}\\ &\leq \frac{\mathbf{E}\left[V(0)\right]K^{\gamma}}{T\delta}+\frac{BK^{\gamma}}{\delta}\end{aligned}$$

Taking the $\limsup$ as T goes to infinity yields the result. □

Similarly, we can get an upper bound on the rate vectors.

Theorem 6.4.

$$\limsup_{T\to\infty}\frac{1}{T}\sum_{t=0}^{T-1} E\left[\|\hat{\mathbf{x}}[t]-\mathbf{x}^{\star}\|^{2}\right] \leq \frac{B}{K}$$

Proof. The proof follows the exact same arguments as in the proof of Theorem 6.3, applied to (6.12). □

These results establish that we can make the flow rates get arbitrarily close to the optimal rate allocation in the above expected sense by choosing the parameter K to be large enough.

CHAPTER 7

CONCLUSIONS AND DIRECTIONS FOR FUTURE RESEARCH

Scheduling is a vital component that determines the performance of a wireless network. In this dissertation, we have proposed and analyzed schedulers that use local queue-length information to determine the distribution of the available resources. Such schedulers have been shown to possess a desirable feature known as throughput-optimality. Moreover,in conjunction with a congestion controller mechanism, we have shown the asymptotic fairness properties of these schedulers.

However, there are a number of important directions to be pursued for future research.

- In the Chapter 3, we compare the performances of opportunistic and TDM schedulers for serving delay-constrained traffic over a general fading channel. The queue-length-based schedulers' performance is shown to be significantly better through simulations. In [67], this fact is proved using a large deviations analysis. However, only a lower bound has been obtained for the large deviations exponent of queue-length-based policies for general models. Characterization of the large deviations exponent precisely is an open problem.

- A key difficulty in the implementation of queue-length-based schedulers over multi-hop networks is their need of a centralized controller. For a simple interference model, it is possible to achieve fully distributed implementation by sacrificing a fraction of the

capacity. We studied such an extension in [68] and in Chapter 6. Extensions to more general interference models is a direction for future research.

- We have studied a dual congestion controller in Chapter 5. However, primal-dual controllers are better suited to describe various versions of TCP used in the Internet [3]. Thus, it would be interesting to extend the results of Chapter 5 to this class of schedulers.

APPENDIX A

Proofs of Chapter 2

A.1 Proof of Claim 2.1 in Section 2.2.4

Note that solving the maximization in (2.7) is equivalent to

$$\begin{aligned}\max_{\{\eta\in\mathcal{C}_j\}_{j=1}^{J}} \sum_{i=1}^{N} f_i(q_i) \sum_{j=1}^{J} \pi_j \eta_i &= \max_{\{\eta\in\mathcal{C}_j\}_{j=1}^{J}} \sum_{j=1}^{J} \pi_j \sum_{i=1}^{N} f_i(q_i)\eta_i \\ &\leq \sum_{j=1}^{J} \pi_j \max_{\eta(j)\in\mathcal{C}_j} \sum_{i=1}^{N} f_i(q_i)\eta_i(j) \\ &\leq \frac{1}{1-\zeta} \sum_{j=1}^{J} \pi_j \sum_{i=1}^{N} f_i(q_i)\mu_i(j).\end{aligned}$$

But $\bar{\mu} \in \bar{\mathcal{C}}$ and hence the previous upper bound is in fact achievable by $\bar{\mu}$. $\diamond$

A.2 Proof of Theorem 2.1

The stability of the class of scheduling policies is proved in several steps. We first consider a continuous-time model with constant arrival rates and a deterministic channel, and show that the system evolves towards a closed region around the origin in the state space (i.e., the space of queue length vectors). This establishes the boundedness of the queues assuming the system were operating deterministically in continuous-time. As we will see, the continuous-time analysis suggests a natural Lyapunov function to analyze the stability of the original discrete-time stochastic system.

However, before we consider the stochastic system, we study a deterministic discrete-time system, where the arrival rates are again taken to be constant at their means and the achievable rate region is fixed at its average. We show that the corresponding Lyapunov function decreases, except in a bounded region around the origin of the state space. This establishes the stability of the new model.

Finally, we include the randomness of the arrivals and channel states to the model and consider the evolution of the Lyapunov function at time instants that are not consecutive, but that are M steps apart, for some large M. This allows us to use law-of-large-numbers type assumptions to view this system as being nearly deterministic and apply the results of the discrete-time deterministic model to complete the proof of stability.

A.2.1 Deterministic model of the system

In this section, we assume that the arrival process to the i^{th} queue is deterministic and constant at each time slot, with the constant equal to the mean, λ_i, of the corresponding stochastic arrival processes, $a_i[t]$. Further, the evolution of each of the queues is assumed to be

$$q_i[t+1] \;\; = \;\; q_i[t] + \lambda_i - \bar{\eta}_i[t] + u_i[t], \tag{A.1}$$

where $\bar{\eta}[t] = \bar{\mu}(\mathbf{q}[t])$, $\bar{\mu}(\mathbf{q}[t]) := \sum_{j=1}^{J} \pi_j \mu(j, \mathbf{q}[t])$ and $u_i[t]$ is an upper-bounded, positive quantity, which denotes the wasted service provided to the i^{th} queue. Thus, $\bar{\mu}(\mathbf{q}[t])$ can be interpreted as the average service provided to Queue i when the queue state is $\mathbf{q}[t]$, where the averaging is performed over the channel state process. In the following section, we state two lemmas, which will be used in the proof of Theorem 2.1.

Continuous-time model

In this model, time is no longer discrete, but is continuous, and the evolution of the queue lengths is governed by the following differential equation

$$\dot{q}_i(t) = \begin{cases} (\lambda_i - \bar{\mu}_i(t)), & q_i(t) > 0 \\ (\lambda_i - \bar{\mu}_i(t))^+, & q_i(t) = 0 \end{cases} \qquad i = 1, 2, \ldots, N. \tag{A.2}$$

Using the above facts, we will now show that we can find a Lyapunov function for the system (A.2), such that its derivative is negative.

Lemma A.1. *Suppose at any time instant t, the service rate vector $\mu(t)$ is chosen such that it satisfies*

$$\sum_{i=1}^{N} f_i(q_i(t))\mu_i(t) \quad \geq \quad (1-\zeta)\max_{\eta\in\bar{\mathcal{C}}} \quad \sum_{i=1}^{N} f_i(q_i(t))\eta_i,$$

where an upper bound on the parameter ζ is provided in the proof of this lemma. Consider the following Lyapunov function:

$$V(\mathbf{q}) = \sum_{i=1}^{N} g_i(q_i), \tag{A.3}$$

where $g_i'(q) = f_i(q)$. Then for some $\delta > 0$, we have

$$\dot{V}(\mathbf{q}) \leq -||\mathbf{f}(\mathbf{q})||_2\delta, \tag{A.4}$$

holding for all $\mathbf{q}$ outside a bounded region around the origin.

Proof:

Let us start by defining $\mathcal{P} = \{i \in \{1, \cdots, N\} : q_i > 0\}$ to be the set of users that have non-empty queues. Then, we have

$$\begin{aligned}\dot{V}(\mathbf{q}) &= \sum_{i\in\mathcal{P}} f_i(q_i)(\lambda_i - \bar{\mu}_i) + \sum_{i\in\mathcal{P}^c} f_i(0)(\lambda_i - \bar{\mu}_i)^+ \\ &= \sum_{i\in\mathcal{P}} f_i(q_i)(\lambda_i - \bar{\mu}_i) + \sum_{i\in\mathcal{P}^c} f_i(0)(\lambda_i - \bar{\mu}_i + u_i),\end{aligned}$$

where u_i is a non-negative quantity that is bounded above by $\hat{\eta}$. Equivalently, we can write

$$\dot{V}(\mathbf{q}) = \sum_{i=1}^{N} f_i(q_i)(\lambda_i - \bar{\mu}_i) + \underbrace{\sum_{i\in\mathcal{P}^c} f_i(0)u_i}_{=:c}, \tag{A.5}$$

where $c \geq 0$ is a positive constant. Let us denote $||\mathbf{f}(\mathbf{q})||_2 := (\sum_{i=1}^{N} f_i^2(q_i))^{1/2}$ and define $\cos(\theta_i) = \frac{f_i(q_i)}{||\mathbf{f}(\mathbf{q})||_2}$. Then using (2.4), (A.5) can be rewritten as

$$\begin{aligned}\dot{V}(\mathbf{q}) &= ||\mathbf{f}(\mathbf{q})||_2 \left(\sum_{i=1}^{N}\cos(\theta_i)\lambda_i - \sum_{i=1}^{N}\cos(\theta_i)\bar{\mu}_i\right) + c \\ &\leq ||\mathbf{f}(\mathbf{q})||_2 \left(\underbrace{\sum_{i=1}^{N}\cos(\theta_i)\lambda_i}_{=:K_\lambda} - \underbrace{\sum_{i=1}^{N}\cos(\theta_i)\tilde{\mu}_i}_{=:K_{\tilde{\mu}}} + \zeta\sum_{i=1}^{N}\cos(\theta_i)\tilde{\mu}_i\right) + C \qquad \text{(A.6)}\end{aligned}$$

where we define $C = \sum_{i=1}^{N} f_i(0)\hat{\eta}$, and

$$\tilde{\mu} = \arg\max_{\eta \in \bar{\mathcal{C}}} \sum_{i=1}^{N} f_i(q_i)\eta_i = \arg\max_{\eta \in \bar{\mathcal{C}}} \sum_{i=1}^{N} \cos(\theta_i)\eta_i \tag{A.7}$$

since $||\mathbf{f}(\mathbf{q})||_2 \geq 0$ is constant for a fixed $\mathbf{q}$. Let us consider the expression in (A.6). The maximization amounts to finding the point on the boundary of $\bar{\mathcal{C}}$ at which a line with a certain slope (determined by θ) is tangential to the boundary. Note that since λ is not on the boundary, any two lines with the same slope such that one passes through $(\lambda_1, \cdots, \lambda_N)$ and the other is tangent to the boundary of $\bar{\mathcal{C}}$, will have a difference of at least $\delta_j > 0$ in its intercept with the j^{th} axis. Choose $\Delta := \min(\delta_1, \cdots, \delta_N) > 0$.

If $\theta_i = \frac{\pi}{2}$, then $K_\lambda = K_{\tilde{\mu}} = 0$. So consider any other index j such that $\theta_j < \frac{\pi}{2}$, which implies $\cos(\theta_j) \geq \gamma_j$ for some $\gamma_j > 0$. Define $\Gamma = \max(\gamma_1, \cdots, \gamma_N) > 0$. Then the j^{th} intercepts are $\frac{K_\lambda}{\cos(\theta_j)}$ and $\frac{K_{\tilde{\mu}}}{\cos(\theta_j)}$ and we can write

$$K_\lambda - K_{\tilde{\mu}} \leq -\Delta \max_j \cos(\theta_j) \leq -\Delta\Gamma := -2\delta.$$

Hence we can conclude that

$$\dot{V}(\mathbf{q}) \leq ||\mathbf{f}(\mathbf{q})||_2(-2\delta + \zeta N\hat{\eta} + \frac{C}{||\mathbf{f}(\mathbf{q})||_2}) \leq -\delta||\mathbf{f}(\mathbf{q})||_2, \tag{A.8}$$

if $||\mathbf{f}(\mathbf{q})||_2 > \frac{2C}{\delta}$ and $\zeta < \frac{\delta}{2N\hat{\eta}}$. $\diamond$

Notice that in the previous proof the fact that $f_i(0) \neq 0$ is easily compensated for by considering larger queue lengths. Hence, from this point on, we will assume $f_i(0) = 0$ for all i in order to avoid this additional complication. For this case, Lemma A.1 will be true for all q.

In what follows, we will use the above Lyapunov function to first show the stability of the deterministic, discrete-time model and to later show that the original stochastic system is stable.

Discrete-time model

Using the result of Lemma A.1, we will now show that the Lyapunov function (A.3) applied to the system described by (A.1) has a negative drift outside a bounded region.

Lemma A.2. *Consider any policy that satisfies Property 2.1. When such a policy is applied to the discrete-time system (A.1) with constant arrivals and time-invariant channel, for sufficiently large M, the M-step drift of the Lyapunov function V satisfies the following inequality:*

$$E\left[\Delta V^{(M)}(\mathbf{q}[t])\right] \leq -M\epsilon_M||\mathbf{f}(\mathbf{q}[t])||_2\mathcal{I}_{\mathbf{q}[t]\in\mathcal{B}^c_{(M)}[t]} + K_{(M)}[t]\mathcal{I}_{\mathbf{q}[t]\in\mathcal{B}_{(M)}[t]}, \quad \text{(A.9)}$$

for some $\epsilon_M > 0$, where $\Delta V^{(M)}(\mathbf{q}[t]) := V(\mathbf{q}[t+M]) - V(\mathbf{q}[t])$, $\mathcal{B}_{(M)}$ is a bounded region around the origin and $K_{(M)}$ is a finite constant, both dependent on $\mathbf{q}[t]$.

Proof:

$$\begin{aligned}\Delta V^{(1)}(\mathbf{q}[t]) &:= V(\mathbf{q}[t+1]) - V(\mathbf{q}[t]) \\ &= \sum_{i=1}^{N} f_i(y_i[t])(\lambda_i - \bar{\mu}_i[t] + u_i[t]),\end{aligned}$$

where $y_i[t]$ lies between $q_i[t]$ and $q_i[t+1]$ from Taylor's theorem. Then we get,

$$\begin{aligned}\Delta V^{(1)}(\mathbf{q}[t]) &= \sum_{i=1}^{N} f_i(y_i[t])(\lambda_i - \bar{\mu}_i[t]) \quad \text{(A.10)} \\ &\quad + \sum_{i=1}^{N} f_i(y_i[t])u_i[t]. \quad \text{(A.11)}\end{aligned}$$

For (A.11) observe that if $q_i[t] > \hat{\eta}$, then $u_i[t] = 0$ and if $q_i[t] \leq \hat{\eta}$, then $u_i[t] \leq \hat{\eta}$. Hence, using the fact that f_i is nondecreasing, and $y_i[t] \leq q_i[t] + \lambda_i$, we get

$$\sum_{i=1}^{N} f_i(y_i[t])u_i[t] \leq \sum_{i=1}^{N} f_i(\lambda_i + \hat{\eta})\hat{\eta} =: C_1 < \infty.$$

Note that (A.10) can be bounded as

$$\begin{aligned}\sum_{i=1}^{N} f_i(y_i[t])(\lambda_i - \bar{\mu}_i[t]) &\leq \sum_{i=1}^{N} f_i(q_i[t])(\lambda_i - \bar{\mu}_i[t]) \quad \text{(A.12)} \\ &\quad + \sum_{i=1}^{N} |f_i(y_i[t]) - f_i(q_i[t])||\lambda_i - \bar{\mu}_i[t]|. \quad \text{(A.13)}\end{aligned}$$

To upper-bound (A.12), we will make use of Lemma A.1. Note that (A.12) is exactly in the same form as (A.5), except that in this case with probability ρ, (A.4) may not hold. However, by

Property 2.1, ρ can be chosen small enough by making M large. Hence, we can upper-bound (A.12) by $-\frac{\delta}{2}||\mathbf{f}(\mathbf{q}[t])||_2$.

Due to the properties of $\{f_i(\cdot)\}$, (A.13) can be upper-bounded by $\gamma||\mathbf{f}(\mathbf{q})||_2$ outside a bounded, closed region. Hence, by choosing $\epsilon_1 := \frac{\delta}{2} - \gamma > 0$, we get the following result

$$E\left[\Delta V^{(1)}(\mathbf{q}[t])\right] \leq -\epsilon_1||\mathbf{f}(\mathbf{q}[t])||_2\mathcal{I}_{\mathbf{q}[t]\in\mathcal{B}^c_{(1)}[t]} + K_{(1)}[t]\mathcal{I}_{\mathbf{q}[t]\in\mathcal{B}_{(1)}[t]}, \tag{A.14}$$

where $\mathcal{I}_A$ denotes the indicator function of the event A, $\mathcal{B}_{(1)}[t]$ is the closed and bounded region around the origin and $K_{(1)}[t] < \infty$ is appropriately chosen.

Next we extend the previous analysis to examine the M-step drift
$E\left[\Delta V^{(M)}(\mathbf{q}[t])\right]$

$$\begin{aligned}
&= E\left[V(\mathbf{q}[t+M]) - V(\mathbf{q}[t])\right] \\
&= \sum_{i=0}^{M-1} E\left[\Delta V^{(1)}(\mathbf{q}[t+i])\right] \\
&\leq \sum_{i=0}^{M-1}\left[-\epsilon_1||\mathbf{f}(\mathbf{q}[t+i])||_2\mathcal{I}_{\mathbf{q}[t+i]\in\mathcal{B}^c_{(1)}[t+i]} + K_{(1)}[t]\mathcal{I}_{\mathbf{q}[t+i]\in\mathcal{B}_{(1)}[t+i]}\right],
\end{aligned} \tag{A.15}$$

which follows from (A.14). We can write (A.15) as

$$E\left[\Delta V^{(M)}(\mathbf{q}[t])\right] \leq -\epsilon_1\left(\sum_{i=0}^{M-1}||\mathbf{f}(\mathbf{q}[t+i])||_2\right)\mathcal{I}_{\mathbf{q}[t]\in\mathcal{B}^c_{(M)}[t]} + K_{(M)}[t]\mathcal{I}_{\mathbf{q}[t]\in\mathcal{B}_{(M)}[t]}, \tag{A.16}$$

where $\mathcal{B}_{(M)}[t]$, and $K_{(M)}[t] < \infty$ are $M-$step equivalents of $\mathcal{B}_{(1)}[t]$, and $K_{(1)}[t] < \infty$.

Now, consider any $j \in \{1, \cdots, N\}$ and $n \in \{0, \cdots, M-1\}$. Due to the property of f given by (2.3), for any $\gamma_n \in (0,1)$, we have

$$\begin{aligned}
f_j(q_j[t+n]) &\geq f_j(q_j[t] - n\eta^*) \\
&= (1-\gamma_n)f_j(q_j[t]),
\end{aligned}$$

for $q_j[t]$ large enough. Taking squares, summing over j, and taking square roots yields

$$\begin{aligned}
||\mathbf{f}(\mathbf{q}[t])||_2 &= \sqrt{\sum_{j=1}^{N} f_j^2(q_j[t])} \\
&\leq \frac{1}{1-\gamma_n}||\mathbf{f}(\mathbf{q}[t+n])||_2.
\end{aligned}$$

Let us define $\gamma := \max_{n\in\{0,\cdots,M-1\}} \gamma_n < 1$, then we can easily write

$$\sum_{i=0}^{M-1} ||\mathbf{f}(\mathbf{q}[t+i])||_2 \quad \geq \quad M(1-\gamma)||\mathbf{f}(\mathbf{q}[t])||_2.$$

Hence, if we denote $\epsilon_M := \epsilon_1(1-\gamma)$, we can upper-bound the M-step drift as

$$E\left[\Delta V^{(M)}(\mathbf{q}[t])\right] \quad \leq \quad -M\epsilon_M||\mathbf{f}(\mathbf{q}[t])||_2 \mathcal{I}_{\mathbf{q}[t]\in\mathcal{B}^c_{(M)}[t]} + K_{(M)}[t]\mathcal{I}_{\mathbf{q}[t]\in\mathcal{B}_{(M)}[t]}, \quad \text{(A.17)}$$

with $\epsilon_M > 0$. $\diamond$

A.2.2 Stochastic model

In the following proof, we will make use of the result of Section A.2.1 even though the arrivals are now stochastic processes and the channel state is time-varying. To facilitate this, we denote the vectors of queue length, allocated service rates and the unused services, at any time n, under the deterministic model by $\mathbf{q}^d[n]$, $\bar{\mu}^d[n]$, and $\mathbf{u}[n]$, respectively. Let $\mathbf{q}^d[t] = \mathbf{q}$. Next, we write the M-step mean drift for the stochastic model. Recall that, in Section A.2.1, we obtained an expression for the drift of the function V assuming that the arrivals are constant and the service provided at each time instant is an average (over the channel states) of the service that would have been provided had the channel been in a particular state. Now, for the stochastic arrival and channel model,

$$\Delta W^{(M)}(\mathbf{q}[t]) \quad := \quad E\left[V(\mathbf{q}[t+M]) - V(\mathbf{q}^d[t+M]) \quad | \quad \mathbf{q}[t]=\mathbf{q}\right] \quad \text{(A.18)}$$

$$+E\left[V(\mathbf{q}^d[t+M]) - V(\mathbf{q}[t]) \quad | \quad \mathbf{q}[t]=\mathbf{q}\right]. \quad \text{(A.19)}$$

Observe that (A.19) can be upper-bounded using (A.9). Next, we consider (A.18). Note that we can write

$$q_i[t+M] \quad = \quad q_i[t] + \underbrace{\sum_{n=t}^{t+M-1} a_i[n]}_{=:A_i(t,M)} - \underbrace{\sum_{n=t}^{t+M-1} \mu_i(s[n],\mathbf{q}[n])}_{=:C_i(t,M)} + \underbrace{\sum_{n=t}^{t+M-1} u_i[n]}_{=:U_i(t,M)}$$

$$q_i^d[t+M] \quad = \quad q_i[t] + M\lambda_i - \underbrace{\sum_{n=t}^{t+M-1}\sum_{j=1}^{J} \pi_j\mu_i(j,\mathbf{q}^d[n])}_{=:C_i^d(t,M)} + \underbrace{\sum_{n=t}^{t+M-1} u_i^d[n]}_{=:U_i^d(t,M)}.$$

Hence, we can write

$$\begin{aligned}\Sigma_{\Delta,i} &:= q_i[t+M] - q_i^d[t+M] \\ &= \underbrace{A_i(t,M) - M\lambda_i}_{=:\Delta A_i} + \underbrace{C_i^d(t,M) - C_i(t,M)}_{=:\Delta C_i} + \underbrace{U_i(t,M) - U_i^d(t,M)}_{=:\Delta U_i}.\end{aligned}$$

Therefore, (A.18) can be written as

$$\begin{aligned}(A.18) &= E\left[\sum_{i=1}^{N} g_i(q_i[t+M]) - g_i(q_i^d[t+M]) \quad | \quad \mathbf{q}[t] = \mathbf{q}\right] \\ &= \sum_{i=1}^{N} E\left[f_i(z_i(t,M))\Sigma_{\Delta,i} \quad | \quad \mathbf{q}[t] = \mathbf{q}\right],\end{aligned}$$

which can be further written as

$$\begin{aligned}&= \sum_{i=1}^{N} E\left[f_i(z_i(t,M))(A_i(t,M) - M\lambda_i) \quad | \quad \mathbf{q}[t] = \mathbf{q}\right] && \text{(A.20)} \\ &\quad + \sum_{i=1}^{N} E\left[f_i(z_i(t,M))(C_i^d(t,M) - C_i(t,M)) \quad | \quad \mathbf{q}[t] = \mathbf{q}\right] && \text{(A.21)} \\ &\quad + \sum_{i=1}^{N} E\left[f_i(z_i(t,M))(U_i(t,M) - U_i^d(t,M)) \quad | \quad \mathbf{q}[t] = \mathbf{q}\right] && \text{(A.22)}\end{aligned}$$

where $z_i(t,M) := \alpha q_i^d[t+M] + (1-\alpha)q_i[t+M]$ for some $\alpha \in [0,1]$. To upper-bound the above expression, we will consider two events, one when the arrivals to each of the queues are upper-bounded by a finite value A and the other, the complement of this event. Let us denote the first event by

$$\mathcal{A} = \{a_i[n] \leq A : 1 \leq i \leq N, t \leq n \leq (t+M-1)\}.$$

First, let us concentrate on (A.20). In the case when the event $\mathcal{A}$ occurs, we can upper-bound $z_i(t,M)$ as

$$z_i(t,M) \leq q_i[t] + \alpha\lambda_i M + (1-\alpha)AM.$$

Then we can upper-bound (A.20) as

$$\leq \sum_{i=1}^{N} E\left[\left|f_i(q_i[t] + \alpha\lambda_i M + (1-\alpha)AM)\right| \left|A_i(t,M) - M\lambda_i\right| \quad | \quad \mathbf{q}[t] = \mathbf{q}\right].$$

For any fixed M, and $\zeta_1 > 0$ it is possible to find an X_i such that for all $q_i > X_i$, we have

$$f_i(q_i + \alpha\lambda_i M + (1-\alpha)AM) \leq (1+\zeta_1) f_i(q_i).$$

Next, we define $E := \{i : q_i[t] > X_i\}$, which enables us to further upper-bound (A.20) as

$$\begin{aligned} &\leq \quad (1+\zeta_1) \sum_{i \in E} f_i(q_i[t]) ME \left[\left| \frac{A_i(t,M)}{M} - \lambda_i \right| \quad | \quad \mathbf{q}[t] = \mathbf{q} \right] \\ &\quad + \sum_{i \in E^c} f_i(X_i) ME \left[\left| \frac{A_i(t,M)}{M} - \lambda_i \right| \quad | \quad \mathbf{q}[t] = \mathbf{q} \right]. \end{aligned}$$

Now, using Assumption (3) in Section 2.2.3, for any $\epsilon_2 > 0$, we can find a large enough M such that

$$E \left[\left| \frac{A_i(t,M)}{M} - \lambda_i \right| \quad | \quad \mathbf{q}[t] = \mathbf{q} \right] < \epsilon_2 \quad \forall i.$$

This enables us to write

$$\sum_{i=1}^{N} E\left[f_i(z_i(t,M)) \Delta A_i \, \mathcal{I}_{\mathcal{A}} \mid \mathbf{q}[t] = \mathbf{q} \right] \leq \left((1+\zeta_1) M \sum_{i=1}^{N} f_i(q_i[t]) + H_1 \right) \epsilon_2, \qquad \text{(A.23)}$$

where $H_1 := \sum_{i \in E^c} f_i(X_i) < \infty$.

If instead the event $\mathcal{A}^c$ occurs, then Assumption (4) in Section 2.2.3 implies that for any $\epsilon_3 > 0$, we can find A large enough so that

$$\sum_{i=1}^{N} E\left[f_i(z_i(t,M)) (A_i(t,M) - M\lambda_i) \mathcal{I}_{\mathcal{A}^c} \quad | \quad \mathbf{q}[t] = \mathbf{q} \right] < \epsilon_3. \qquad \text{(A.24)}$$

Secondly, we concentrate on (A.21). First we write

$$\begin{aligned} (A.21) \quad &= \quad \sum_{i=1}^{N} E\left[\mathcal{I}_{\mathcal{A}} f_i(z_i(t,M)) (C_i^d(t,M) - C_i(t,M)) \mid \mathbf{q}[t] = \mathbf{q} \right] \qquad \text{(A.25)} \\ &\quad + \sum_{i=1}^{N} E\left[\mathcal{I}_{\mathcal{A}^c} f_i(z_i(t,M)) (C_i^d(t,M) - C_i(t,M)) \mid \mathbf{q}[t] = \mathbf{q} \right]. \qquad \text{(A.26)} \end{aligned}$$

Expand (A.25) as follows.

$$\begin{aligned} \sum_{i=1}^{N} E[I_{\mathcal{A}} f_i(z_i(t,M)) \; (\sum_{n=t}^{t+M-1} \{ \quad & \sum_{j=1}^{J} \pi_j \mu_i(j, \mathbf{q}[n]) - \sum_{j=1}^{J} \pi_j \mu_i(j, \mathbf{q}[t]) \\ & + \sum_{j=1}^{J} \pi_j \mu_i(j, \mathbf{q}[t]) - \mu_i(s[n], \mathbf{q}[t]) \\ & + \mu_i(s[n], \mathbf{q}[t]) - \mu_i(s[n], \mathbf{q}[n]) \quad \} \;) \mid \mathbf{q}[t] = \mathbf{q}], \end{aligned}$$

which can be further bounded as

$$\leq \sum_{i=1}^{N} E[I_{\mathcal{A}} f_i(z_i(t,M)) \sum_{n=t}^{t+M-1} \sum_{j=1}^{J} \pi_j(\mu_i(j,\mathbf{q}[n]) - \mu_i(j,\mathbf{q}[t])) \mid \mathbf{q}[t]=\mathbf{q}] \quad \text{(A.27)}$$

$$+ \sum_{i=1}^{N} E[I_{\mathcal{A}} f_i(z_i(t,M)) M \left| \sum_{j=1}^{J} \mu_i(j,\mathbf{q}[t]) \left(\pi_j - \sum_{n=t}^{t+M-1} \frac{1}{M} \mathcal{I}_{s[n]=j} \right) \right| \mid \mathbf{q}[t]=\mathbf{q}] \quad \text{(A.28)}$$

$$+ \sum_{i=1}^{N} E[I_{\mathcal{A}} f_i(z_i(t,M)) \sum_{n=t}^{t+M-1} (\mu_i(s[n],\mathbf{q}[t]) - \mu_i(s[n],\mathbf{q}[n])) \mid \mathbf{q}[t]=\mathbf{q}]. \quad \text{(A.29)}$$

Note that, under the event $\mathcal{A}$, $z_i(t,M) \in [q_i[t] - M\hat{\eta}, q_i[t] + \alpha\lambda_i M + (1-\alpha)AM]$, for some $\alpha \in [0,1]$. Then for any given M, A and $\zeta > 0$, we can find an $X_i < \infty$ such that for any $q_i > X_i$, we have $(1-\zeta) f_i(q_i) \leq f_i(y_i) \leq (1+\zeta) f_i(q_i)$.

Define the set of indices $E := \{i : q_i[t] > X_i\}$. Then using Assumption (2) of Section 2.2.1, along with a repetition of the argument we had for (A.20), given any $\epsilon_4 > 0$, we can come up with a closed, bounded region, outside of which we have

$$(A.28) \leq \left((1+\zeta) M \sum_{i=1}^{N} f_i(q_i[t]) + H_2 \right) \epsilon_4,$$

with $H_2 < \infty$. Since (A.27) and (A.29) follow the same reasoning, only the latter will be examined in detail. Using our earlier analysis, given any $\epsilon_5 > 0$, it is easy to upper bound the following term:

$$\sum_{i=1}^{N} E[I_{\mathcal{A}} f_i(z_i(t,M)) \sum_{n=t}^{t+M-1} \mu_i(s[n],\mathbf{q}[t]) \mid \mathbf{q}[t]=\mathbf{q}] \leq H_3 + (1 + \frac{\epsilon_5}{2M\hat{\eta}}) \sum_{i=1}^{N} \sum_{n=t}^{t+M-1} \{f_i(q_i[t]) E[I_{\mathcal{A}} \mu_i(s[n],\mathbf{q}[t]) \mid \mathbf{q}[t]=\mathbf{q}]\},$$

with $H_3 < \infty$. As for the second term, note that for all $i \in E$, we have $f_i(z_i(t,M)) \geq (1 - \frac{\epsilon_5}{2M\hat{\eta}}) f_i(q_i[t])$, and for $i \in E^c$, we have $f_i(z_i(t,M)) \geq (1 - \frac{\epsilon_5}{2M\hat{\eta}}) f_i(q_i[t]) - H_4$, with an appropriate choice of $H_4 < \infty$. Hence we obtain the following lower bound:

$$\sum_{i=1}^{N} E[I_{\mathcal{A}} f_i(z_i(t,M)) \sum_{n=t}^{t+M-1} \mu_i(s[n],\mathbf{q}[n]) \mid \mathbf{q}[t]=\mathbf{q}] \geq H_5 + (1 - \frac{\epsilon_5}{2M\hat{\eta}}) \sum_{i=1}^{N} \sum_{n=t}^{t+M-1} \{f_i(q_i[t]) E[I_{\mathcal{A}} \mu_i(s[n],\mathbf{q}[n]) \mid \mathbf{q}[t]=\mathbf{q}]\},$$

with $H_5 < \infty$. Putting the last two bounds together, we get the following upper bound on (A.29):

$(A.29)$

$$\leq \sum_{n=t}^{t+M-1} E[I_{\mathcal{A}} \sum_{i=1}^{N} (f_i(q_i[t])\mu_i(s[n],\mathbf{q}[t]) - f_i(q_i[t])\mu_i(s[n],\mathbf{q}[n])) \mid \mathbf{q}[t]=\mathbf{q}] \quad (A.30)$$

$$+\frac{\epsilon_5}{2M\hat{\eta}} \sum_{i=1}^{N} f_i(q_i[t]) E[I_{\mathcal{A}} \sum_{n=t}^{t+M-1} (\mu_i(s[n],\mathbf{q}[t]) - \mu_i(s[n],\mathbf{q}[n])) \mid \mathbf{q}[t]=\mathbf{q}] \quad (A.31)$$

$$+H_6$$

$$\leq \epsilon_5 \sum_{i=1}^{N} f_i(q_i[t]) + H_6 \quad (A.32)$$

with H_6 bounded, where the last inequality follows by observing that the expectation in (A.31) is upper-bounded by $M\hat{\eta}$, and, given M and A, we can find the bounded region around the origin outside of which the expectation in (A.30) can be upper-bounded by $\frac{\epsilon_5}{2M} \sum_{i=1}^{N} f_i(q_i[t])$. Similarly, an upper bound on (A.27) can be obtained by choosing the bounded region large enough. Such an argument would yield the following expression

$$(A.27) \leq \epsilon_6 \sum_{i=1}^{N} f_i(q_i[t]) + H_7,$$

with H_7 bounded. Putting all these bounds together, we can upper-bound (A.25) as

$$(A.25) \leq \epsilon_7 M ||\mathbf{f}(\mathbf{q}[t])||_2 + H_8, \quad (A.33)$$

where H_8 is finite. As for (A.26), we can choose the parameter A large enough so that, due to Assumption (4) of Section 2.2.3, it converges to zero.

Thirdly, consider (A.22) under the event $\mathcal{A}$. Observe that for any queue, say i, and any fixed M, the sum of unused service may be nonzero over a duration of M slots only if $q_i[n] < \hat{\eta}$ for some $n \in \{t, \cdots, t+M-1\}$. Therefore, if $U_i(t,M) > 0$, it is easy to see that $f_i(z_i(t,M)) \leq f_i(\hat{\eta} + MA)$. Similarly, $U_i^d(t,M) > 0$ only if $f_i(z_i(t,M)) \leq f_i(\hat{\eta} + M\lambda_i)$. Moreover, the cumulative unused service over M slots is upper-bounded by $M\hat{\eta}$, since within each slot, the maximum amount of possible unused service is $\hat{\eta}$. Hence, we can easily upper-bound (A.22) under the event $\mathcal{A}$ as

$$\sum_{i=1}^{N} E\left[\mathcal{I}_{\mathcal{A}} f_i(z_i(t,M))(U_i(t,M) - U_i^d(t,M)) \quad \mid \quad \mathbf{q}[t]=\mathbf{q}\right] \quad \leq \quad M\hat{\eta} \max_i f_i(\hat{\eta} + MA) \quad (A.34)$$

If the event $\mathcal{A}^c$ occurs then we can write, for any $\epsilon_8 > 0$,

$$\begin{aligned} & \sum_{i=1}^{N} E\left[\mathcal{I}_{\mathcal{A}^c} f_i(z_i(t,M))(U_i(t,M) - U_i^d(t,M)) \quad | \quad \mathbf{q}[t] = \mathbf{q}\right] \\ \leq & \sum_{i=1}^{N} M\hat{\eta} E\left[\mathcal{I}_{\mathcal{A}^c} f_i(z_i(t,M)) \quad | \quad \mathbf{q}[t] = \mathbf{q}\right] \\ < & M\epsilon_8, \end{aligned} \tag{A.35}$$

with $A < \infty$ chosen to be large enough, due to Assumption (4) of Section 2.2.3. Putting (A.34) and (A.35) together, (A.22) can be upper-bounded as

$$(A.22) \leq M\epsilon_8 + H_9 \tag{A.36}$$

for any $\epsilon_8 > 0$ and with $H_9 < \infty$ chosen appropriately.

Now, combining (A.23), (A.24), (A.33) and (A.36), for any $\epsilon > 0$, we can come up with a closed, bounded region around the origin outside of which we have

$$E\left[V(\mathbf{q}[t+M]) - V(\mathbf{q}^d[t+M]) \quad | \quad \mathbf{q}[t] = \mathbf{q}\right] \quad \leq \quad M\epsilon||\mathbf{f}(\mathbf{q}[t])||_2 + H,$$

for some $H < \infty$ chosen appropriately. So if we choose $\epsilon_M - \epsilon =: \xi > 0$, then we can come up with a closed region, denoted by $\mathcal{G}_{(M)}[t]$, outside of which $\mathbf{q}[t]$ is sufficiently large, and

$$\Delta W^{(M)}(\mathbf{q}[t]) \quad \leq \quad -M\xi||\mathbf{f}(\mathbf{q}[t])||_2 \mathcal{I}_{\mathbf{q}[t] \in \mathcal{G}^c_{(M)}[t]} + K_{(M)} \mathcal{I}_{\mathbf{q}[t] \in \mathcal{G}_{(M)}[t]}, \tag{A.37}$$

with an appropriate choice of $K_{(M)} < \infty$. We can also write the previous expression as

$$E\left[W(\mathbf{q}[t+M]) - W(\mathbf{q}[t]) \mid \mathbf{q}[t] = \mathbf{q}\right] \quad \leq \quad -M\xi||\mathbf{f}(\mathbf{q}[t])||_2 \mathcal{I}_{\mathbf{q}[t] \in \mathcal{G}^c_{(M)}[t]} + K_{(M)}.$$

Taking expectations on both sides, we get

$$E[W(\mathbf{q}[t+M])] - E[W(\mathbf{q}[t])] \quad \leq \quad -M\xi E\left[||\mathbf{f}(\mathbf{q}[t])||_2 \mathcal{I}_{\mathbf{q}[t] \in \mathcal{G}^c_{(M)}[t]}\right] + K_{(M)}.$$

Then, for any positive integer p, we have

$$E[W(\mathbf{q}[(p-1)M])] - E[W(\mathbf{q}[0])] \quad \leq \quad -M\xi \sum_{t=0}^{p-1} E\left[||\mathbf{f}(\mathbf{q}[tM])||_2 \mathcal{I}_{\mathbf{q}[tM] \in \mathcal{G}^c_{(M)}[tM]}\right] + pK_{(M)}.$$

Since $E[W(\mathbf{q}[(p-1)M])] > 0$, we have

$$-E[W(\mathbf{q}[0])] \;\leq\; -M\xi \sum_{t=0}^{p-1} E\left[||\mathbf{f}(\mathbf{q}[tM])||_2 \mathcal{I}_{\mathbf{q}[tM]\in\mathcal{G}^c_{(M)}[tM]}\right] + pK_{(M)}.$$

Re-arranging the terms, we get

$$\sum_{t=0}^{p-1} E\left[||\mathbf{f}(\mathbf{q}[tM])||_2 \mathcal{I}_{\mathbf{q}[tM]\in\mathcal{G}^c_{(M)}[tM]}\right] \;\leq\; \frac{E[W(\mathbf{q}[0])]}{M\xi} + \frac{pK_{(M)}}{M\xi}.$$

Now observe that $E\left[||\mathbf{f}(\mathbf{q}[tM])||_2 \mathcal{I}_{\mathbf{q}[0]\in\mathcal{G}_{(M)}[tM]}\right] < \infty$ since $\mathcal{G}_{(M)}$ represents a closed bounded region around the origin and $||\mathbf{f}||_2$ is bounded is inside such a region. This allows us to write

$$\sum_{t=0}^{p-1} E\left[||\mathbf{f}(\mathbf{q}[tM])||_2\right] \;\leq\; \frac{E[W(\mathbf{q}[0])]}{M\xi} + \frac{pT_{(M)}}{M\xi},$$

for some finite $T_{(M)}$. Finally, dividing both sides by p and letting $p \to \infty$, we obtain

$$\limsup_{p\to\infty} \frac{1}{p} \sum_{t=0}^{p-1} E\left[||\mathbf{f}(\mathbf{q}[t])||_2\right] \;\leq\; \frac{T_{(M)}}{M\xi} =: \bar{l} < \infty, \tag{A.38}$$

as claimed in the theorem statement. ◇

APPENDIX B

Proof of Lemma 4.1

Proof. We write the evolution of the i^{th} queue as

$$q_i[t+1] = q_i[t] + x_i[t] - \mu_i[t] + u_i[t], \tag{B.1}$$

where $u_i[t]$ denotes the amount of unused service that is offered to the queue. Clearly, $u_i[t] \leq \mu_i[t] \leq \hat{\eta}$. Therefore, if $q_i[t] > \hat{\eta}$, then we have $u_i[t] = 0$.

Now we study the conditional mean drift of $W(\cdot)$.

$$\begin{aligned} E[\Delta W_t(\mathbf{q})] &= \sum_{i=1}^{N} \frac{E[(q_i[t+1]-q_i^\star)^2 - (q_i[t]-q_i^\star)^2 \mid \mathbf{q}[t]=\mathbf{q}]}{2} \\ &= \frac{1}{2}\sum_{i=1}^{N} E[(q_i[t+1]-q_i[t])(q_i[t+1]+q_i[t]+2q_i^\star) \mid \mathbf{q}[t]=\mathbf{q}]. \end{aligned}$$

By substituting (B.1) and dropping the time variable t for convenience, we get

$$\begin{aligned} E[\Delta W_t(\mathbf{q})] &= \frac{1}{2}\sum_{i=1}^{N} E[(x_i-\mu_i+u_i)(2q_i+x_i-\mu_i+u_i-2q_i^\star) \mid \mathbf{q}] \\ &\leq \sum_{i=1}^{N}\{(q_i-q_i^\star)\left(\min\left\{\frac{\alpha_i K}{(q_i)^m}, M\right\} - \bar{\mu}_i + E[u_i|\mathbf{q}]\right) \\ &\quad + \frac{E[x_i^2+\mu_i^2+u_i^2|\mathbf{q}]}{2} + E[u_i(x_i-\mu_i)|\mathbf{q}] - \min\left\{\frac{\alpha_i K}{(q_i)^m}, M\right\}\bar{\mu}_i\}, \end{aligned}$$

where $\bar{\mu} \in \arg\max_{\eta\in\bar{\mathcal{C}}} \sum_{i=1}^{N} q_i\eta_i$, and $\mu \in \arg\max_{\eta\in\mathcal{C}_s} \sum_{i=1}^{N} q_i\eta_i$. Recall that $E[x_i^2|\mathbf{q}] \leq A$, for some finite A. Also, $\mu_i < \hat{\eta}$ implies that $E[u_i^2+\mu_i^2|\mathbf{q}] < 2\hat{\eta}^2$. Further, observing that u_i takes positive

values only if $x_i < \mu_i$ implies that $E[u_i(x_i - \mu_i)|\mathbf{q}] \leq 0$. Therefore, we can upper-bound all the terms in the last line of the above expression by a finite value, say B, independently of K. Hence, we obtain

$$E[\Delta W_t(\mathbf{q})] \;\leq\; \sum_{i=1}^{N}(q_i - q_i^\star)\left(\min\left\{\frac{\alpha_i K}{(q_i)^m}, M\right\} - \bar{\mu}_i + E[u_i|\mathbf{q}]\right) + B.$$

For all j with $q_j > q_j^\star$, we have $u_j = 0$ when K is large since we have $q_j > q_j^\star > \hat{\eta}$ when K is taken large enough. We already argued that there cannot be any unused service if the queue-length is larger than $\hat{\eta}$. On the other hand, for all m with $q_m \leq q_m^\star$, we have $E[u_m|\mathbf{q}] \geq 0$. Combining these two observations, we obtain the following upper bound: $(q_i - q_i^\star)E[u_i|\mathbf{q}] \leq 0,\ \forall i,\ \text{for large K}$. Thus,

$$\begin{aligned}
E[\Delta W_t(\mathbf{q})] \;&\leq\; \sum_{i=1}^{N}(q_i - q_i^\star)\left(\min\left\{\frac{\alpha_i K}{(q_i)^m}, M\right\} - \bar{\mu}_i\right) + B \\
&=\; \sum_{i=1}^{N}(q_i - q_i^\star)\left(\min\left\{\frac{\alpha_i K}{(q_i)^m}, M\right\} - x_i^\star\right) + \sum_{i=1}^{N}(q_i - q_i^\star)(x_i^\star - \bar{\mu}_i) + B \\
&\leq\; \sum_{i=1}^{N}(q_i - q_i^\star)\left(\min\left\{\frac{\alpha_i K}{(q_i)^m}, M\right\} - x_i^\star\right) + B,
\end{aligned}$$

where the last step follows from the observation in the proof of Proposition 2 that

$$\sum_{i=1}^{N}(q_i - q_i^\star)(x_i^\star - \bar{\mu}_i) \leq 0.$$

We let $i^* = \arg\max_i |q_i - q_i^\star|$ and re-write the upper bound as

$$E[\Delta W_t(\mathbf{q})] \leq -|q_{i^*} - q_{i^*}^\star|\left|\min\left\{\frac{\alpha_{i^*} K}{(q_{i^*})^m}, M\right\} - x_{i^*}^\star\right| + B.$$

Now, if $\min\left\{\frac{\alpha_{i^*}K}{(q_{i^*})^m}, M\right\} = M$, then

$$\left|\min\left\{\frac{\alpha_{i^*} K}{(q_{i^*})^m}, M\right\} - x_{i^*}^\star\right| = M - x_{i^*}^\star > \hat{\eta}.$$

If $\min\left\{\frac{\alpha_{i^*}K}{(q_{i^*})^m}, M\right\} = \frac{\alpha_{i^*}K}{(q_{i^*})^m}$, then

$$\left|\min\left\{\frac{\alpha_{i^*} K}{(q_{i^*})^m}, M\right\} - x_{i^*}^\star\right| = x_{i^*}^\star\left|1 - \left(\frac{q_{i^*}^\star}{q_{i^*}}\right)^m\right| \geq x_{i^*}^\star\left|1 - \left(\frac{q_{i^*}^\star}{q_{i^*}^\star + |q_{i^*} - q_{i^*}^\star|}\right)^m\right|$$

Suppose that $\|\mathbf{q}^\star - \mathbf{q}\| \geq c(K)^{\frac{1}{2m}}$, where the choice of $c > 0$ will be specified later. Noting the inequalities $|q_{i^*} - q^\star_{i^*}| \leq \|\mathbf{q} - \mathbf{q}^\star\| \leq \sqrt{n}|q_{i^*} - q^\star_{i^*}|$, we can write

$$\begin{aligned} x^\star_{i^*}\left|1 - \left(\frac{q^\star_{i^*}}{q^\star_{i^*} + |q_{i^*} - q^\star_{i^*}|}\right)^m\right| &\geq x^\star_{i^*}\left|1 - \frac{1}{\left(1 + \frac{c(x^\star_{i^*})^{1/m}}{\sqrt{n}\alpha_{i^*}^{1/m}}(K)^{-\frac{1}{2m}}\right)^m}\right| \\ &\geq x^\star_{i^*}\left|1 - \frac{1}{1+\psi m}\right| = x^\star_{i^*}\frac{\psi m}{1+\psi m}, \end{aligned} \tag{B.2}$$

where $\psi := \frac{c(x^\star_{i^*})^{1/m}}{\sqrt{n}\alpha_{i^*}^{1/m}}(K)^{-\frac{1}{2m}}$ and the last step follows from Taylor's expansion: $(1+\psi)^m \geq 1 + m\psi$, for $\psi > 0$. Clearly, for large enough K, the expression in (B.2) can be made smaller than $\hat{\eta}$. Therefore, for large K we can write

$$\begin{aligned} E[\Delta W_t(\mathbf{q})] &\leq -|q_{i^*} - q^\star_{i^*}|\left(x^\star_{i^*}\frac{\psi m}{1+\psi m} - \frac{B}{|q_{i^*} - q^\star_{i^*}|}\right) \\ &\leq -|q_{i^*} - q^\star_{i^*}|\left(\frac{mc(x^\star_{i^*})^{1+\frac{1}{m}}}{\sqrt{n}\alpha_{i^*}^{1/m}(K)^{\frac{1}{2m}} + mc(x^\star_{i^*})^{\frac{1}{m}}} - \frac{B\sqrt{n}}{c(K)^{\frac{1}{2m}}}\right) \\ &\leq -\frac{|q_{i^*} - q^\star_{i^*}|}{(K)^{\frac{1}{2m}}}\left(\frac{mc(x^\star_{i^*})^{1+\frac{1}{m}}}{\sqrt{n}\alpha_{i^*}^{1/m} + mc(x^\star_{i^*})^{\frac{1}{m}}} - \frac{B\sqrt{n}}{c}\right) \end{aligned}$$

It is not difficult to see that the expression in the parentheses can be made strictly negative by choosing c sufficiently large, independent of K. Then the previous expression becomes $E[\Delta W_t(\mathbf{q})] \leq -\frac{\hat{\delta}}{(K)^{\frac{1}{2m}}}|q_{i^*} - q^\star_{i^*}|$, for some $\hat{\delta} > 0$. Using the fact that $\|\mathbf{q} - \mathbf{q}^\star\| \leq \sqrt{n}|q_{i^*} - q^\star_{i^*}|$, we can further write

$$E[\Delta W_t(\mathbf{q})] \leq -\frac{\delta}{(K)^{\frac{1}{2m}}}\|\mathbf{q} - \mathbf{q}^\star\|,$$

for all $\|\mathbf{q} - \mathbf{q}^\star\| \geq c(K)^{\frac{1}{2m}}$, for K large enough and where $\delta := \frac{\hat{\delta}}{\sqrt{n}}$.

When $\|\mathbf{q} - \mathbf{q}^\star\| < c(K)^{\frac{1}{2m}}$, it is not difficult to see that $E[\Delta W_t(\mathbf{q})] \leq \zeta$ for some $\zeta > 0$. Combining the previous two inequalities completes the proof. □

APPENDIX C

Some Proofs of Chapter 5

C.1 Proof of Proposition 5.3 - Strong Duality

Proof. Given any vector $\mathbf{b} = \{b_l\}_{l \in \mathcal{L}}$, we define the *primal value function* as

$$v(\mathbf{b}) = \max \left\{ \sum_{f \in \mathcal{F}} U_f(x_f) \text{ s.t. } y_l(\mathbf{x}) \leq \mu_l + b_l, \text{ and } \mu \in \Gamma \right\}.$$

The proof is complete due to [60, Corollary $4.3.6$], once we show that the value function is continuous at $\mathbf{0}$.

We claim that the value function is concave, which implies continuity. To show this, we consider any two vectors, $\mathbf{b}^{(1)}$ and $\mathbf{b}^{(2)}$ and let

$$\begin{aligned} (\mathbf{x}^{(i)}, \mu^{(i)}) \in \quad & \arg\max \quad \sum_{f \in \mathcal{F}} U_f(x_f) \\ & s.t. \qquad y_l(\mathbf{x}^{(i)}) \leq \mu_l^{(i)} + b_l^{(i)}, \ \forall l \in \mathcal{L}, \qquad \mu^{(i)} \in \Gamma, \end{aligned}$$

for $i = 1, 2$. For any $\theta \in [0, 1]$, we define $\mathbf{b}^\theta = \theta \mathbf{b}^{(1)} + (1-\theta)\mathbf{b}^{(2)}$, $\mathbf{x}^\theta = \theta \mathbf{x}^{(1)} + (1-\theta)\mathbf{x}^{(2)}$, and $\mu^\theta = \theta \mu^{(1)} + (1-\theta)\mu^{(2)}$.

Observe that

$$\begin{aligned} \theta v(\mathbf{b}^{(1)}) + (1-\theta) v(\mathbf{b}^{(2)}) &= \theta \sum_{f \in \mathcal{F}} U_f(x_f^{(1)}) + (1-\theta) \sum_{f \in \mathcal{F}} U_f(x_f^{(2)}) \\ &\leq \sum_{f \in \mathcal{F}} U_f(x_f^\theta), \end{aligned}$$

where the least inequality is due to the concavity of $\{U_f(\cdot)\}$. Also, note that $\mu^\theta \in \Gamma$ due to the convexity of the region Γ. And, finally $\mathbf{y}(\mathbf{x}^\theta) \leq \mu^\theta + \mathbf{b}^\theta$ by definition. Thus, we have

$$(\mathbf{x}^\theta, \mu^\theta) \in \{(\mathbf{x}, \mu) : y_l(\mathbf{x}) \leq \mu_l + b_l^\theta, \text{ and } \mu \in \Gamma\}.$$

Therefore,

$$\begin{aligned} v(\mathbf{b}^\theta) &\geq \sum_{f \in \mathcal{F}} U_f(x_f^\theta) \\ &\geq \theta v(\mathbf{b}^{(1)}) + (1-\theta) v(\mathbf{b}^{(2)}), \end{aligned}$$

which shows the concavity of the value function, and completes the proof.

□

C.2 Proof of Theorem 5.4

Proof. We start by considering the following $T-$step mean drift. For any $\mathbf{y} \geq \mathbf{0}$,

$$\begin{aligned} & E[V(\mathbf{q}[T]; \mathbf{q}^\star) | \mathbf{q}[0] = \mathbf{y}] - V(\mathbf{y}; \mathbf{q}^\star) \\ = & \sum_{t=0}^{T-1} E[V(\mathbf{q}[t+1]; \mathbf{q}^\star) - V(\mathbf{q}[t]; \mathbf{q}^\star) | \mathbf{q}[0] = \mathbf{y}] \\ = & \sum_{t=0}^{T-1} \sum_{\mathbf{q} \in \mathcal{Z}_+^N} P\left(\mathbf{q}[t] = \mathbf{q} | \mathbf{q}[0] = \mathbf{y}\right) E[V(\mathbf{q}[t+1]; \mathbf{q}^\star) - V(\mathbf{q}[t]; \mathbf{q}^\star) | \mathbf{q}[t] = \mathbf{q}] \qquad \text{(C.1)} \\ \leq & \zeta \sum_{\mathbf{q} \in \mathcal{D}} \sum_{t=0}^{T-1} P\left(\mathbf{q}[t] = \mathbf{q} | \mathbf{q}[0] = \mathbf{y}\right) - \sum_{\mathbf{q} \in \mathcal{D}^c} \frac{\delta \|\mathbf{q} - \mathbf{q}^\star\|}{(K)^\sigma} \sum_{t=0}^{T-1} P\left(\mathbf{q}[t] = \mathbf{q} | \mathbf{q}[0] = \mathbf{y}\right) \qquad \text{(C.2)} \end{aligned}$$

where $\mathcal{Z}_+^N$ denotes the set of all non-negative n dimensional integer valued vectors. In the above derivation, (C.1) follows from the fact that $\mathbf{q}[t]$ is a Markov chain, and we have used (4.8) to get the inequality in (C.2). We note that for any $\mathbf{q} \in \mathcal{Z}_+^N$,

$$\lim_{T \to \infty} \frac{1}{T} \sum_{t=0}^{T-1} P\left(\mathbf{q}[t-1] = \mathbf{q} | \mathbf{q}[0] = \mathbf{y}\right) = \pi_{\mathbf{q}}^\infty,$$

for all $\mathbf{y}$, where $\vec{\pi}^\infty$ denotes the stationary distribution of the Markov chain $\mathbf{q}[t]$. Next, we move $V(\mathbf{y})$ to the other side of the inequality in (C.2), divide both sides by T, and let T go to infinity.

This operation yields

$$0 \leq \zeta \sum_{\mathbf{q} \in \mathcal{D}} \pi^{\infty}_{\mathbf{q}} - \frac{\delta}{(K)^{\sigma}} \sum_{\mathbf{q} \in \mathcal{D}^c} \|\mathbf{q} - \mathbf{q}^{\star}\| \pi^{\infty}_{\mathbf{q}}.$$

Re-arranging the terms and with minor manipulations, this inequality can be written as

$$\frac{\delta}{(K)^{\sigma}} \sum_{\mathbf{q} \in \mathcal{Z}^N_+} \|\mathbf{q} - \mathbf{q}^{\star}\| \pi^{\infty}_{\mathbf{q}} \leq \sum_{\mathbf{q} \in \mathcal{D}} \left(\zeta + \frac{\delta}{(K)^{\sigma}} \|\mathbf{q} - \mathbf{q}^{\star}\| \right) \pi^{\infty}_{\mathbf{q}} \leq (\zeta + \delta c) \sum_{\mathbf{q} \in \mathcal{D}} \pi^{\infty}_{\mathbf{q}} \leq (\zeta + \delta c),$$

where the second inequality follows from the definition of $\mathcal{D}$. Here, the left-hand-side is nothing but $\frac{\delta E[\|\mathbf{q}^{\infty} - \mathbf{q}^{\star}\|]}{(K)^{\sigma}}$. So we multiply both sides with $\frac{(K)^{\sigma}}{\delta}$ to get

$$E[\|\mathbf{q}^{\infty} - \mathbf{q}^{\star}\|] \leq \left(c + \frac{\zeta}{\delta} \right) (K)^{\sigma},$$

which completes the proof for $\bar{c} := \left(c + \frac{\zeta}{\delta} \right)$. □

REFERENCES

[1] F. P. Kelly, A. Maulloo, and D. Tan, "Rate control in communication networks: shadow prices, proportional fairness and stability," *Journal of the Operational Research Society*, vol. 49, pp. 237–252, 1998.

[2] S. H. Low and D. E. Lapsley, "Optimization flow control, I: Basic algorithm and convergence," *IEEE/ACM Transactions on Networking*, pp. 861–875, December 1999.

[3] R. Srikant, *The Mathematics of Internet Congestion Control*. Birkhauser, 2004.

[4] S. Kunniyur and R. Srikant, "A time-scale decomposition approach to adaptive ECN marking," *IEEE Transactions on Automatic Control*, vol. 47, pp. 882–894, June 2002.

[5] D. P. Bertsekas and J. N. Tsitsiklis, *Parallel and Distributed Computation: Numerical Methods*. Belmont, MA: Athena Scientific, 1997.

[6] L. Tassiulas and A. Ephremides, "Stability properties of constrained queueing systems and scheduling policies for maximum throughput in multihop radio networks," *IEEE Transactions on Automatic Control*, pp. 1936–1948, December 1992.

[7] L. Tassiulas and A. Ephremides, "Dynamic server allocation to parallel queues with randomly varying connectivity," *IEEE Transactions on Information Theory*, vol. 39, pp. 466–478, March 1993.

[8] M. Andrews, K. Kumaran, K. Ramanan, A. Stolyar, R. Vijayakumar, and P. Whiting. "Scheduling in a queueing system with asynchronously varying service rates,", 2000. Bell Laboratories Technical Report.

[9] S. Shakkottai and A. Stolyar, "Scheduling for multiple flows sharing a time-varying channel: The exponential rule," *Translations of the AMS, Series 2,* A volume in memory of F. Karpelevich, vol. 207, 2002.

[10] S. Shakkottai, R. Srikant, and A. Stolyar, "Pathwise optimality of the exponential scheduling rule for wireless channels," in *Proceedings of ISIT*, Lausanne, Switzerland, July 2002. To appear in the *Advances in Applied Probability*, 2004.

[11] R. Leelahakriengkrai and R. Agrawal, "Scheduling in multimedia wireless networks," in *Proceedings of ITC*, Brazil, 2001.

[12] L. Tassiulas, "Scheduling and performance limits of networks with constantly varying topology," *IEEE Transactions on Information Theory*, pp. 1067–1073, May 1997.

[13] L. Tassiulas, "Linear complexity algorithms for maximum throughput in radio networks and input queued switches," in *Proceedings of IEEE Infocom*, 1998.

[14] P. Giaccone, B. Prabhakar, and D. Shah, "Towards simple, high-performance schedulers for high-aggregate bandwidth switches," in *Proceedings of IEEE Infocom*, 2002.

[15] P. Kumar and S. Meyn, "Stability of queueing networks and scheduling policies," *IEEE Transactions on Automatic Control*, vol. 40, pp. 251–260, February 1995.

[16] M. Armony and N. Bambos. "Queueing dynamics and maximal throughput scheduling in switched processing systems,". Technical Report Netlab-2001-09/01, Stanford University.

[17] K. Ross and N. Bambos. "Projective processing schedules in queueing structures: Applications to packet scheduling in communication network switches,". Technical Report Netlab-2002-05/01, Stanford University.

[18] D. Tse. "Forward link multiuser diversity through rate adaptation and scheduling,". In preparation.

[19] X. Liu, E. Chong, and N. Shroff, "Opportunistic transmission scheduling with resource-sharing constraints in wireless networks," *IEEE Journal on Selected Areas in Communications*, vol. 19, pp. 2053–2064, October 2001.

[20] P. Viswanath, D. Tse, and R. Laroia, "Opportunistic beamforming using dumb antennas," *IEEE Transactions on Information Theory*, vol. 48, pp. 1277–1294, June 2002.

[21] L. Li and A. J. Goldsmith, "Optimal resource allocation for fading broadcast channels-Part I: Ergodic capacity," *IEEE Transactions on Information Theory*, March 2001.

[22] D. Bertsekas, *Nonlinear Programming*. Belmont, MA: Athena Scientific, 1995.

[23] P. Billingsley, *Convergence of Probability Measures*. Wiley, 1968.

[24] D. Mitra and J. Morrison, "Multiple time scale regulation and worst case processes for ATM network control," in *Proceedings of the IEEE Conference on Decision and Control*, New Orleans, LA, 1995, pp. 353–358.

[25] S. Shakkottai and A. Stolyar, "Scheduling for multiple flows sharing a time-varying channel: The exponential rule," *Translations of the American Mathematical Society*, 2001. To appear.

[26] A. Eryilmaz, R. Srikant, and J. R. Perkins, "Stable scheduling policies for fading wireless channels," *IEEE/ACM Transactions on Networking*, vol. 13, pp. 411–425, April 2005.

[27] D. N. Tse. "Multi-user diversity and proportional fairness,". US Patent 6449490.

[28] Y. Liu and E. Knightly, "Opportunistic fair scheduling over multiple wireless channels," in *Proceedings of IEEE INFOCOM*, San Francisco, CA, April 2003.

[29] P. Bender, P. Black, M. Grob, R. Padovani, N. Sindhushayana, and A. Viterbi, "Cdma/hdr: A bandwidth efficient high speed wireless data service for nomadic users," *IEEE Communications Magazine*, pp. 70–77, July 2000.

[30] B. H. S. Sanghavi, "Adaptive induced fluctuations for multi-user diversity," in *Proceedings of ISIT*, Lausanne, Switzerland, July 2002.

[31] J. Padhye, V. Firoiu, D. Towsley, and J. Kurose, "Modeling TCP throughput: A simple model and its empirical validation," in *Proceedings of ACM SIGCOMM*, 1998.

[32] P. W. Glynn and W. Whitt, "Logarithmic asymptotics for steady-state tail probabilities in single-server queues," *Journal of Applied Probability*, vol. 31A, pp. 131–156, 1994.

[33] S. Shakkottai, "Effective capacity of the max-queue rule," in *Proceedings of the Allerton Conference on Control, Communications and Computing*, 2003, pp. 665–674.

[34] S. Shakkottai, "Modes of overflow, effective capacity and qos for wireless scheduling," in *ISIT*, 2003, p. 334.

[35] A. Eryilmaz, R. Srikant, and J. Perkins. "Stable scheduling policies for fading wireless channels,". Technical Report. Available at http://www.comm.csl.uiuc.edu/˜srikant.

[36] R. Buche and H. J. Kushner, "Control of mobile communication systems with time-varying channels via stability methods," *IEEE Transactions on Automatic Control*, 2004. To appear.

[37] M. Neely, E. Modiano, and C. Rohrs, "Dynamic power allocation and routing for time varying wireless networks," *Proceedings of IEEE Infocom*, April 2003.

[38] F. P. Kelly, "Charging and rate control for elastic traffic," *European Transactions on Telecommunications*, vol. 8, pp. 33–37, 1997.

[39] A. Jalali, R. Padavoni, and R. Pankaj, "Data throughput of CDMA-HDR: a high efficiency-high data rate personal communication system," in *Proceedings IEEE Vehicular Technology Conference*, pp. 1854–1858.

[40] V. Subramanian and R. Agrawal, "A stochastic approximation analysis of channel condition aware wireless scheduling algorithms," in *Proceedings of the INFORMS Telecommunications Conference*, 2002.

[41] H. J. Kushner and P. A. Whiting. "Convergence of proportional-fair sharing algorithms under general conditions,", February 2003. Preprint.

[42] R. Agrawal, A. Bedekar, R. J. La, and V. Subramanian, "Class and channel condition based weighted proportionally fair scheduler," in *Proceedings of the International teletraffic Congress*, 2001, pp. 553–65.

[43] S. Borst and P. Whiting, "Dynamic rate control algorithms for HDR throughput optimization," in *Proceedings of IEEE INFOCOM*, 2001, pp. 976–985.

[44] S. C. Borst, "User-level performance of channel-aware scheduling algorithms in wireless data networks," in *Proceedings of IEEE INFOCOM*, 2003.

[45] H. Yaiche, R. R. Mazumdar, and C. Rosenberg, "A game-theoretic framework for bandwidth allocation and pricing in broadband networks," *IEEE/ACM Transactions on Networking*, vol. 8, pp. 667–678, October 2000.

[46] F. Paganini, "A global stability result in network flow control," *Systems and Control Letters*, vol. 46, no. 3, pp. 153–163, 2002.

[47] J. Wen and M. Arcak, "A unifying passivity framework for network flow control," in *Proceedings of IEEE Infocom*, April 2003.

[48] T. Alpcan and T. Başar, "A utility-based congestion control scheme for internet-style networks with delay," in *Proceedings of IEEE Infocom*, San Francisco, California, March-April 2003.

[49] A. Stolyar. "Maximizing queueing network utility subject to stability: Greedy primal-dual algorithm,". Submitted.

[50] M. Neely, E. Modiano, and C. Li, "Fairness and optimal stochastic control for heterogeneous networks," *Proceedings of IEEE Infocom*, March 2005.

[51] H. Khalil, *Nonlinear Systems*. Upper Saddle River, NJ: 2nd edition, Prentice Hall, 1996.

[52] S. Asmussen, *Applied Probability and Queues*. Springer-Verlag, New York, 2003.

[53] A. G. Pakes, "Some conditions on the ergodicity and recurrence of Markov chains," *Operations Research*, vol. 17, 1969.

[54] D. Bertsekas and R. Gallager, *Data Networks*. Englewood Cliffs, NJ: Prentice Hall, 1987.

[55] R. J. Gibbens and F. P. Kelly, "Resource pricing and the evolution of congestion control," *Automatica*, vol. 35, pp. 1969–1985, 1999.

[56] S. Kunniyur and R. Srikant, "Analysis and design of an adaptive virtual queue algorithm for active queue management," in *Proceedings of ACM Sigcomm*, San Diego, CA, August 2001, pp. 123–134.

[57] A. Lakshmikantha, C. Beck, and R. Srikant, "Robustness of real and virtual queue based active queue management schemes," *IEEE/ACM Transactions on Networking*, 2004. To appear. An earlier version appeared in the *Proceedings of the American Control Conference*, June 2003.

[58] X. Lin and N. Shroff, "Joint rate control and scheduling in multihop wireless networks," in *Proceedings of IEEE Conference on Decision and Control*, Paradise Island, Bahamas, December 2004.

[59] J. Mo and J. Walrand, "Fair end-to-end window-based congestion control," *IEEE/ACM Transactions on Networking*, vol. 8, pp. 556–567, October 2000.

[60] J. M. Borwein and A. S. Lewis, *Convex Analysis and Nonlinear Optimization*. Canadian Mathematical Society, 2000.

[61] G. Sasaki and B. Hajek, "Link scheduling in polynomial time," *IEEE Transactions on Information Theory*, vol. 32, pp. 910–917, 1988.

[62] M. Kodialam and T. Nandagopal, "Characterizing achievable rates in multi-hop wireless networks: The joint routing and scheduling problem," in *Proceedings of ACM Mobicom*, San Diego, CA, September 2003.

[63] C. E. Shannon, "A theorem on coloring the lines of a network," *Journal of Mathematical Physics*, vol. 28, pp. 148–151, 1949.

[64] X. Lin and N. Shroff, "The impact of imperfect scheduling on cross-layer rate control in multihop wireless networks," in *Proceedings of IEEE Infocom*, Miami, FL, March 2005.

[65] X. Wu and R. Srikant, "Regulated maximal matching: A distributed scheduling algorithm for multi-hop wireless networks with node-exclusive spectrum sharing," 2005. Submitted to *IEEE Conference on Decision and Control*.

[66] H. Khalil, *Nonlinear Systems*. Upper Saddle River, NJ: 3nd edition, Prentice Hall, 2002.

[67] L. Ying, R. Srikant, A. Eryilmaz, and G. E. Dullerud, "A large deviations analysis of scheduling in wireless networks," in *INFORMS Applied Probability Conference*, Ottawa, CA, 2005. Available at http://www.comm.csl.uiuc.edu/~srikant.

[68] L. Bui, A. Eryilmaz, R. Srikant, and X. Wu. "Joint asynchronous congestion control and distributed scheduling for wireless networks,". Submitted to IEEE Infocom 2006.

AUTHOR'S BIOGRAPHY

Atilla Eryılmaz received his Bachelor of Science degree from Boğaziçi University, İstanbul, Turkey in 1999 and his Master of Science degree from the University of Illinois at Urbana-Champaign in 2001. He worked as a research assistant at the Coordinated Science Laboratory between 1999 and 2005. He also worked as an intern within the Wireless Communications Group of Bell Laboratories, Lucent Technologies in the summer of 2004. For the academic years 2004 and 2005, he was a recepient of the Vodafone Fellowship.

His research interests are in communication networks, queueing theory, routing and scheduling in wireless networks, stochastic control, network optimization, information theory, and network coding.